

INTRODUCTION TO HIGH-RESOLUTION NMR SPECTROSCOPY AND ITS
APPLICATION TO *IN VIVO* STUDIES OF AGRICULTURAL SYSTEMS

Philip E. Pfeffer and Walter V. Gerasimowicz

TABLE OF CONTENTS

I.	Introduction	4
II.	General Description of NMR Methodology	4
III.	Parameters of the <i>In Vivo</i> NMR Experiment	12
	A. Selecting a Nucleus (An Overview)	12
	B. Maintaining Viability	13
	C. Qualitative Aspects	15
	D. Quantitative Aspects	18
IV.	<i>In Vivo</i> NMR Applications	23
	A. ³¹ P Studies	23
	1. pH and Compartmentation	23
	2. Saturation Transfer	30
	3. Phosphate Uptake and Compartmentation	31
	4. Metal Ion Transport and Compartmentation	35
	5. Photosynthetic and Symbiotic Systems	39
	B. ¹³ C Studies	45
	1. ¹³ C Natural Abundance Studies	45
	2. ¹³ C Isotopic Enrichment Studies	47
	C. Other Nuclei	50
	1. ¹⁴ N and ¹⁵ N	50
	2. ¹ H and ¹⁹ F	53
	3. ²³ Na and ³⁹ K	59
	References	64

I. INTRODUCTION

Nuclear magnetic resonance (NMR) spectroscopy is a most powerful and versatile technique that continues to be applied to ever-increasing disciplines including physics, chemistry, biochemistry, physiology, and medicine. The development of modern high-speed computers coupled with the introduction of Fourier transform (FT) NMR methodology and high-field superconducting magnets has significantly increased the speed, sensitivity, and flexibility of this instrumentation. In addition, because NMR is nondestructive and noninvasive by design, it has developed into the method of choice for examining the molecular level chemistry of functioning biological systems.

Beginning with the early studies of Moon and Richards¹ in 1973, which demonstrated the correlation between intracellular pH in red blood cells and ³¹P NMR chemical shifts, *in vivo* NMR has rapidly expanded its application to the elucidation of biochemical pathways and bioenergetics of microorganisms,² cells,³ plant tissues,⁴ perfused organs,⁵ and organs in intact animals.⁶ Although these NMR experiments can measure the rates at which various reactions, e.g., those of the glycolytic pathway, take place *in vivo*, we would also like to understand how these rates are being controlled by the cells to provide the required fuel on demand. For this reason it is important to establish the level of metabolic activity in fully functioning systems by assessing simultaneously the *in vivo* concentration of metabolites such as ATP, ADP, etc. that play a key role in regulating the enzyme pools. Consequently, if we are to know the roles of these metabolites it is particularly important to relate their change in concentration to change in metabolic activity.

Little is known about the relationship between metabolism and physiological activity largely because of the experimental difficulties of examining a living system. NMR can give us a window for measuring metabolite levels, fluxes through metabolic pathways, rates of transport, or reactions under steady-state conditions and at the same time allow us to assess intracellular pH and compartmentation. Such an integrated approach can potentially create a bridge between how physiological and metabolic processes are controlled and integrated in a fully functioning system.

Although most of the early work has concentrated primarily on establishing the characteristic criteria associated with metabolic stability in living systems or verifying well-known biochemical pathways, a recent scrutiny of the literature indicates that the emerging work has begun to uncover novel findings that are making important contributions to our understanding of diverse biological systems in metabolically stressed and diseased states.⁷⁻⁹

In this chapter we will give a short, general description of the NMR methodology with emphasis on the basic resonance phenomena, design of the instrumentation, and instrumental parameters that influence the experimental results. This nonmathematical, descriptive approach is designed to acquaint the neophyte with some of the elementary principals of NMR. For a thorough and comprehensive treatment of modern high-resolution NMR spectroscopy, the reader is advised to consult three excellent texts by Becker,¹⁰ Shaw,¹¹ and Sanders and Hunter.¹²

The subsequent section of this chapter will give an overview of the application of *in vivo* NMR and a description of the kind of information that is obtained from such experiments utilizing a variety of nuclei and methodologies. The areas of investigation will be largely restricted to studies of microorganisms as well as plant and some animal tissues. Examples will be taken from work on agricultural systems whenever possible. Adaptation of the methods presented for characterizing nonagricultural systems should be obvious to the reader. ³¹P will be the nucleus of discussion for the majority of this portion although ¹³C, ¹⁴N, ¹⁵N, ¹H, ¹⁹F, ²³Na, and ⁴⁰K will also be considered to a minor extent.

II. GENERAL DESCRIPTION OF NMR METHODOLOGY

In general, spectroscopy deals with the interaction of electromagnetic energy (radiation) with

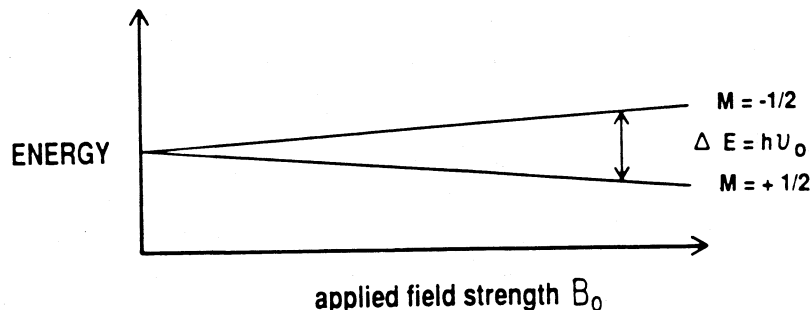


FIGURE 1. Energy of two orientations of a nucleus of spin one half as a function of magnetic field strength B_0 .

matter. The radiation that is absorbed or emitted by the material is then detected as a function of wavelength or frequency and is defined as the spectrum. This spectrum is then interpreted with regard to the atomic or molecular structure of the material under study. The frequencies associated with NMR are typically in the range of 100 to 600 MHz and are therefore associated with transitions between energy levels that are relatively closely spaced. These levels correspond to different magnetic states of the nuclei and are directly influenced by the strength of the applied magnetic field according to the equation (see Figure 1)

$$\Delta E = \hbar\gamma B_0 \quad (1)$$

where: ΔE = the difference in energy between the two states. B_0 = applied magnetic field. γ = magnetogyric ratio characteristic of each nucleus, and \hbar = Planck's constant.

In the NMR experiment the observation of a signal relies on the fact that the atomic nucleus with an odd atomic mass (i.e., sum to its neutrons and protons) has a net magnetic moment or spin, when placed in a magnetic field. This moment essentially turns the nucleus into a magnetic dipole or bar magnet. Unfortunately, these nuclear magnets interact very weakly with the applied field B_0 and separate into the two energy levels according to the Boltzmann distribution (population excess in the higher state of <1 part in 10^4). This small magnetic interaction accounts for the small energy separation ΔE and low frequency range of NMR (see Figure 1). In addition, the small population excess is also responsible for the inherent low signal intensity obtained which is characteristic of this methodology. Common nuclei that exhibit these magnetic properties are the highly abundant (100%) isotopes of ^1H , ^{31}P , and ^{19}F or low natural abundance isotopes ^{13}C (1.1%), ^{15}N (.37%), and ^{113}Cd (12.3%). These are the most widely utilized nuclei since they have only two quantized orientations (nuclear spin = $1/2$, quantum number $I = 1/2$) in the magnetic field which yield narrow line spectra. In contrast, those nuclei with higher quantum numbers such as the quadrupolar nuclei ^{23}Na , ^{14}N , ^2H with $I = 3/2$, 1, and 1, respectively, have many more orientations and correspondingly more complex and broadened spectral lineshapes and multiple transitions. Those nuclei with no net spin, i.e., the sum of their neutrons and protons = even number such as ^{16}O or ^{12}C , do not produce any resonance signal.

Two fields need to be used in order to observe an NMR spectrum. First, a strong static magnetic field designated B_0 is applied to the sample. This causes the nuclear dipoles to orient themselves with and against the magnetic field, i.e., into lower and higher energy states, respectively, as mentioned above (Figure 1). A second field, B_1 , is then generated in a coil perpendicular to the B_0 field via electromagnetic radiation in the radio frequency region of the spectrum. At every magnetic field B_0 , there is a specific frequency of electromagnetic radiation (Larmor frequency) that can induce an applied field B_1 . This B_1 field when applied can align or energetically flip the particular nucleus by way of the absorption of a discrete quantum of energy to a higher energy state. Thus, if a homogeneous B_0 field (superconducting magnetic field) is maintained, we can vary the radio-frequency rf-generated field B_1 until the characteristic Larmor

frequency of the nucleus under study is matched. The characteristic Larmor frequencies of each nucleus is determined by its individual shielding properties (magnetogyric ratio). For example, a static B_0 field of 9.3 Tesla (T) requires a B_1 -generated radio frequency or Larmor frequency, for example, of approximately 400 MHz to produce a resonance spectrum for ^1H , 100 MHz for ^{13}C , and 162 MHz for ^{31}P .

In addition to the static B_0 and applied B_1 field, there is a third small localized field, $B_0\sigma$, present around the nuclei which is produced by the electronic currents of the atoms and molecules. If it were not for $B_0\sigma$, where σ is designated as a shielding constant, all nuclei associated with a particular Larmor frequency, e.g., ^{13}C , would absorb energy at exactly the same frequency. However, because of σ , each nucleus within a molecule feels a slightly different effective magnetic field due to its chemical environment and absorbs energy at a slightly different frequency or resonance position. The separation of these resonance frequencies from an arbitrarily chosen reference is called the chemical shift (δ), a unitless number expressed in parts per million which is independent of field. In the spectrum each absorption is given a chemical shift value based on the relationship:

$$\delta_{\text{ppm}} = \frac{\nu_s - \nu_r}{\nu_r} \times 10^6 \quad (2)$$

where ν_s = resonance frequency of the sample peak and ν_r = resonance frequency of the reference peak.

For example, a chemical shift of 1 ppm observed for an ^1H CH_3 resonance relative to some internal reference peak obtained with an NMR spectrometer operating at 9.3T would also resonate at a 1-ppm chemical shift position in a spectrum taken at 2.3T. However, the difference in the two spectra would be that at 9.3T the separation of the CH_3 resonance from the reference would be 400 Hz, which corresponds to 1 ppm at this field while at a 2.3T field the separation would be only 100 Hz. Thus, higher static magnetic fields (B_0) yield greater chemical shift dispersion (resolution) in addition to increased sensitivity.

Tetramethylsilane (TMS) is commonly used as a reference compound (chemical shift $\delta=0.0$) for ^{13}C and ^1H spectra. Phosphoric acid (85%) is the most widely used reference for ^{31}P spectra, while others such as methylene diphosphonate (MDP),¹³ hexamethylphosphoramide (HMPA),¹⁴ or hexachlorocyclotriphosphazene (HCCTP)¹⁵ have also been used as either primary¹⁴ or secondary¹⁶ external references. Figure 2 shows the ^{31}P spectrum obtained from a perchloric acid extract of metabolites from soybean nodules. The chemical shift positions of the scale have been measured relative to an external reference peak of HMPA, whose shift has been established relative to 85% H_3PO_4 a primary reference whose ^{31}P resonance is assigned a value of 0.0 ppm. For most *in vitro* studies it is convenient to dissolve the reference compound in the solution except for those cases in which the reference compound may react with those compounds under study. However, for *in vivo* work, one must use an external standard such as a capillary or spherical cell containing the reference compound placed in the NMR tube. This kind of referencing sometimes presents problems in comparing chemical shifts because of the differences in susceptibility or chemical environment of the compartments, i.e., capillary vs. cells.¹⁷

The observed intensities (areas) of the resonances in the spectra are proportional to the number of nuclei they represent. However, as we will describe later, certain factors such as spin-lattice relaxation times, T_1 , and nuclear Overhauser enhancements can distort these intensities. In addition each resonance may be split or coupled into multiple lines as a result of its interaction with neighboring nuclei. This interaction, which is transmitted through bonds, is independent of magnetic field strength and is known as spin-spin scalar coupling. The splittings are often useful for identifying resonances of spin 1/2 nuclei because the $n + 1$ multiplicity of the splitting

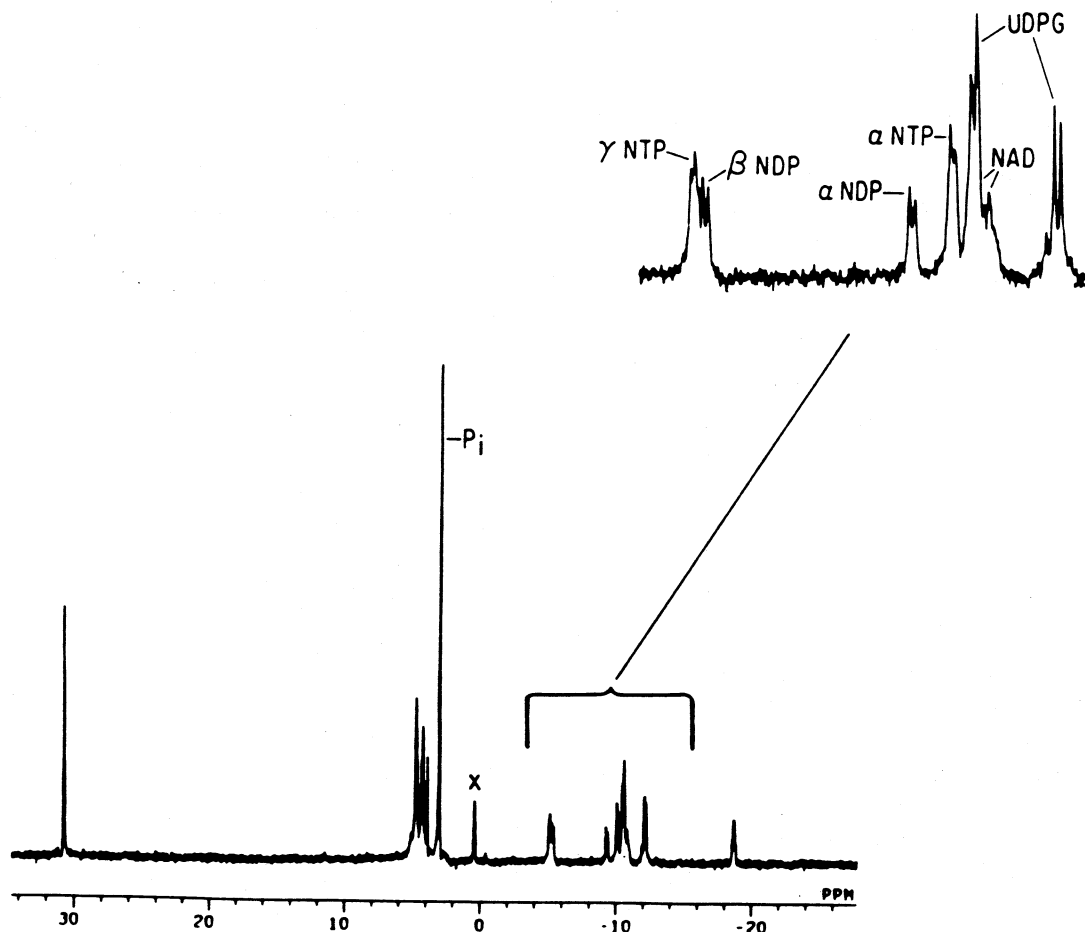


FIGURE 2. 161.7-MHz ^{31}P spectrum of phosphorus metabolites extracted with perchloric acid from soybean nodules. The HMPA reference peak at 30.73 ppm is assigned relative to 85% H_3PO_4 which is the primary reference peak assigned a value of 0.00 ppm.

pattern gives information about the number of adjacent bonded nuclei, and the magnitude of the coupling can be correlated with the dihedral angle between them. The insert in Figure 2 shows the mutual 16-Hz ^{31}P - ^{31}P doublet, homonuclear splitting in each of γ - and α -nucleotide triphosphate (NTP) and α - and β -nucleotide diphosphate (NDP) ^{31}P resonances due to the two (+1/2, -1/2) ^{31}P orientations of each nucleus in the magnetic field. The area of each resonance represents the molar concentration of the corresponding compound. The shift positions are reported relative to the external standard (HMPA) at 30.73 ppm (0.0 ppm being assigned to the H_3PO_4 resonance).

The line shapes of the NMR signals are largely determined by the spin-spin relaxation time T_2 , since the natural line width $\delta_{1/2}$ (width at half height) is given by:

$$1/T_2 = \pi\Delta\delta_{1/2} \quad (3)$$

In the case of large or immobilized molecules, broader line widths are observed and in principle these line widths can be used to assess molecular motion. However, one must be cautious in this interpretation since other factors such as chemical exchange and field inhomogeneity can also contribute to line widths. For the most part, high-resolution NMR is only used to study soluble molecules which are relatively mobile and whose correlation times, T_c , (a characteristic time scale of molecular motion or tumbling) are in the range of 10^{-8} to 10^{-12} s.

Early continuous wave NMR spectrometers used constant, continuously applied radio

frequency power in the presence of a slowly swept (because of spin population saturation) variable magnetic field. Because single slow field sweep was utilized, (although computer time averaging was later applied) only very highly concentrated samples could be examined. Each resonance signal was generated independently as the field was incremented. Modern spectrometers utilize high-power rf pulses and Fourier transformation to give much greater sensitivity. In the Fourier transform instruments, very strong and homogeneous B_0 fields (4.6 to 13.8T, 100 to 600 MHz) are produced by superconducting magnets and each spectrum is obtained by applying a short, high-power rf pulse to produce a B_1 radio frequency field. This pulse, which may only last for 15 to 25 μ s, can simultaneously excite the full spectrum of frequencies for each nucleus being examined (Figure 3A and B). The response obtained from this pulse, referred to as a time domain spectrum or free induction decay (FID), is stored in the computer memory and subsequently mathematically transformed into the conventional frequency domain (frequency vs. intensity) spectrum (Figure 4). In order to improve the signal/noise (S/N) ratio, the accumulated time domain spectra of many of these pulsed experiments are added together in the computer, and following the completion of the experiment they are retrieved and treated by Fourier transformation. The improvement in S/N for the resulting spectrum is proportional to the $\sqrt{\text{\#scans}}$ because the signal increases by a factor of the number of scans while the noise being random increases by the $\sqrt{\text{\#scans}}$. Thus, if a 10-fold increase in S/N is needed to give an acceptable spectrum, 100-fold more scans (pulsed spectra) should be required.

The sample is placed in the instrument probe, situated in the strong B_0 field (Figure 3A), and the transmitter sends radiation of the appropriate frequency through this compartment. Following the transmission of a specific amount of rf radiation corresponding to a 90° pulse applied in the xy plane, the magnetization is tipped 90° from its vertical Z axis alignment in the B_0 field to the xy plane (Figure 3B). The net magnetization (M_{xy}) then rotates coherently about, in the xy plane at the Larmor frequency ω_0 , and induces an electromagnetic force (emf) in the coil surrounding the sample. The rf-generated B_1 field is turned off and the nuclei undergo relaxation in the xy plane by T_2 (e^{-t/T_2}), and relaxation in the Z direction by T_1 (e^{-t/T_1}), (Figure 3C). The FID which results from the rf pulse corresponds to the T_2 decay of the induced signal, generated from the free precession of the nuclei in the B_0 field. This response is amplified and processed in the receiver of the spectrometer and stored in the computer. The same coil is normally used for transmitting the B_1 field as well as for detecting the resulting signal. Figure 5 shows a simple schematic representation of the basic FT NMR spectrometer.

In the NMR experiment, the value of the required interval between successive rf pulses is dependent on the magnitude of the spin-lattice relaxation time, T_1 , the time constant associated with the reestablishment of the equilibrium magnetization state in the Z direction (Figure 3A) according to the equation,

$$\frac{dM_z}{dt} = \frac{M_0 - M_z}{T_1} \quad (4)$$

where M_0 = the component of magnetization along the Z axis of equilibrium and M_z = the component of magnetization produced after a 90° rf pulse. To reestablish >99% of the initial magnetization along the Z axis, prior to the next successive pulse, requires an interval equal to $5 \times T_1$.

Spin-lattice relaxation is facilitated by dipole-dipole interactions of neighboring nuclei randomly tumbling in solution. This process is most efficient when the reciprocal of the molecular correlation time, T_c (see above), is equal to the resonance or Larmor frequency. At the same time magnetization is also decaying exponentially or spreading out in the xy plane (Figure 3C) with a time constant, T_2 , according to the relationship:

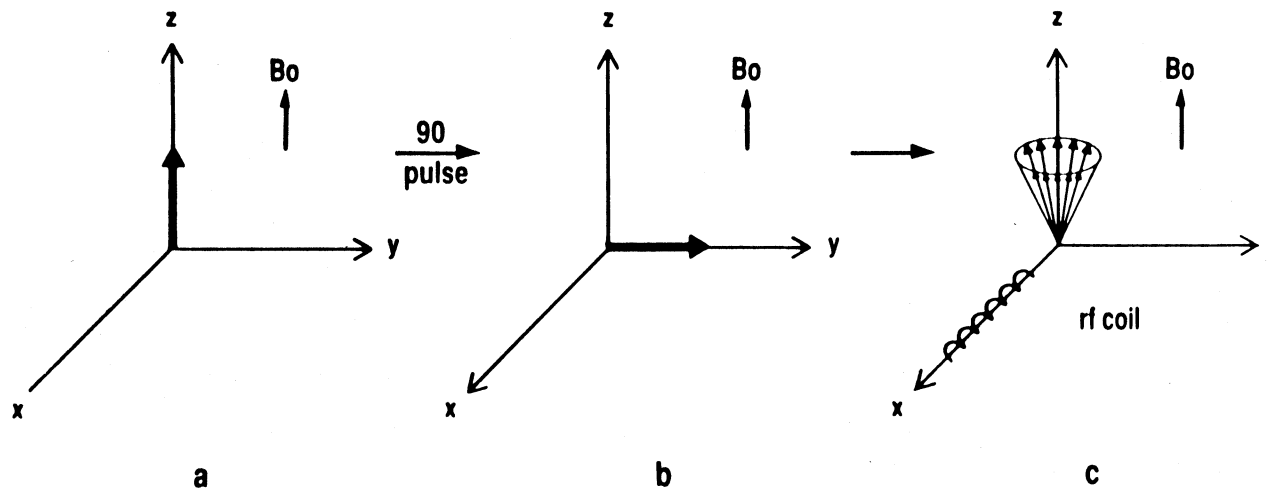


FIGURE 3. (a) Alignment of excess nuclei (Boltzman distribution) in the magnetic field prior to the rf pulse; (b) following a specific pulse of rf power the nuclei are tipped 90° in the xy plane; and (c) the B_1 field is turned off and the nuclei reestablish their orientation in the B_0 field via T_1 relaxation and dephase in the xy plane by the T_2 mechanism.

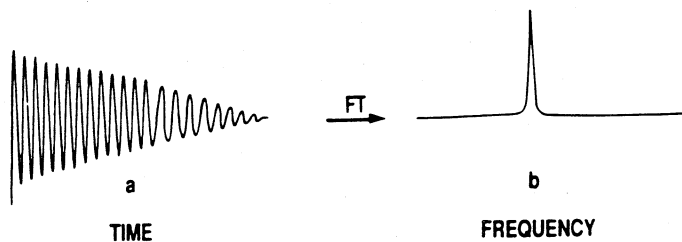


FIGURE 4. (a) Time domain response following a 90° rf pulse and (b) frequency vs. intensity spectrum resulting from Fourier transformation of a.

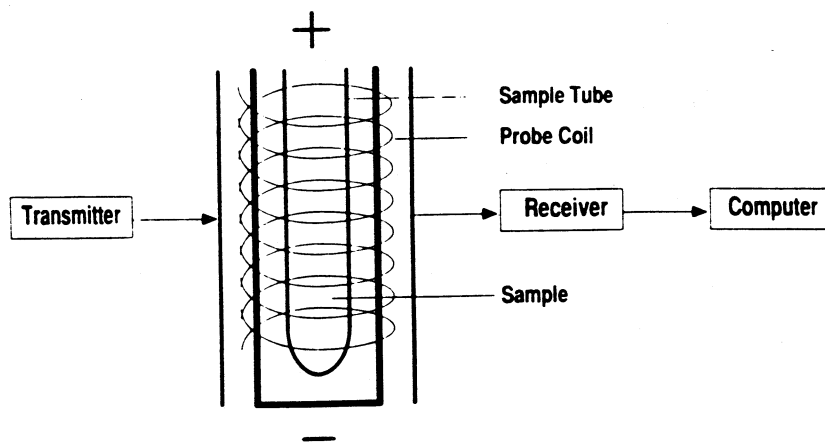


FIGURE 5. A simple schematic representation of an NMR spectrometer.

$$\frac{dM_{xy}}{dt} = -\frac{M_{xy}}{T_2} \quad (5)$$

where M_{xy} is the net magnetization in the xy plane.* As this dephasing process takes over, with a time constant of T_2 , the observed resonance lines experience broadening according to Equation 3. Both spin-lattice T_1 , and spin-spin T_2 relaxation processes are governed by fluctuating magnetic fields associated with molecular motion. However, the time scales for these two relaxation processes differ. Slow motions in the kilohertz range contribute only to spin-spin relaxation, whereas components of motion at the resonance frequency level (MHz) contribute to both spin-spin and spin-lattice relaxation. Figure 6 shows how molecular correlation times in the resonance frequency range give rise to the shortest T_1 values, while those at 10^{-6} s promote rapid T_2 relaxation. Note that those molecules having T_c values less than 10^{-9} s are generally high molecular weight macromolecules, viscous liquids, or solids, whose wide line widths are a result of the rapid loss of phase coherence in the xy plane. For small freely tumbling molecules with $T_c < 10^{-9}$, $T_2 = T_1$. Over the whole range of correlation times T_2 can never be longer than T_1 . With NMR frequencies in the range of 100 to 300 MHz, the minimum in the T_1 curve will occur in

* Actually, the line broadening of the NMR signal is due to T_2^* , which is a time constant that takes into account other relaxation processes, such as B_0 field inhomogeneities. Thus, the decay of the M_{xy} magnetization is always more rapid than would be anticipated, based on a value of T_2 resulting from spin-spin interactions alone. For this reason, it is essential to maintain a relatively homogeneous B_0 field for high-resolution NMR. Unfortunately, because of the inherent inhomogeneity of tissue used in *in vivo* studies, the control of line narrowing by careful attention to B_0 homogeneity is minimal.

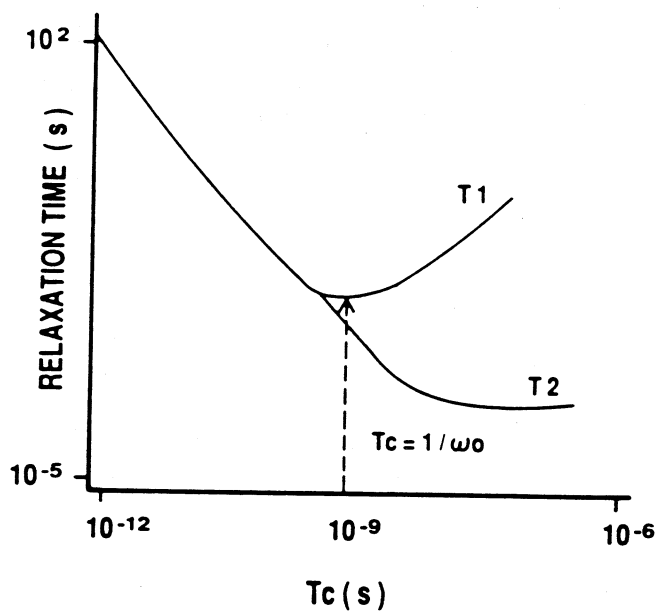


FIGURE 6. Efficiency of T_1 and T_2 relaxation processes as a function of molecular correlation times, T_c .

the vicinity of 5×10^{-10} to 2×10^{-7} s. In non-viscous solution, small molecules with molecular weights of less than 200 almost always have correlation times and relaxation times to the left of the minimum (Figure 6). Polymers such as small proteins of molecular weights in the range of 10,000 to 25,000 Da may have relaxation times on either side of the minimum depending on the Larmor frequency of the experiment.

A number of methods for making relaxation time measurements, i.e., inversion recovery, saturation recovery, and progressive saturation, have been amply discussed in the literature.^{8,10,12} Suffice it to say that one must pay careful attention to relaxation parameters in any NMR experiment if a quantitative assessment of the resulting spectrum is to be made. Failure to implement the proper recycle time following each pulsed spectrum can lead to incorrect conclusions regarding the ratio of various resonance intensities. Examples of these problems and their solutions will be mentioned in the following section.

In the final analysis there are three essential features in an NMR experiment that can be utilized to give information about a living system. These considerations are (1) chemical shifts, which ultimately allow us to identify and quantitate the concentration of compound(s) in question, as well to probe (in some instances) the intracellular pH of the cells, (2) the resonance splitting patterns which are diagnostic for determining the geometric relationships between chemically bonded species, and (3) the two different relaxation processes, T_1 and T_2 , that can be used to simplify spectra and probe molecular motion and interaction in two distinct frequency ranges. In the chapters to follow we will elaborate on the exploration of such parameters to help define the chemical state of living systems.

Clearly, modern NMR methodology can solve problems in ways that could barely be imagined 10 years ago, but many of these new methods have only been successfully employed by a relatively small number of agricultural scientists, i.e., animal and plant physiologists, food scientists, and nutritionists. How do these scientists decide whether *in vivo* NMR or any other NMR approach is appropriate for solving their problems? We hope after digesting the material in this and the other chapters in this book the readers will have better insights into the selection of those NMR experiments that would benefit their research.

Ultimately, one must gain access to an NMR spectrometer or spectroscopist with whom to collaborate.

Table 1
RELATIVE SENSITIVITIES AND CONCENTRATION
THRESHOLDS OF COMMON NUCLEI REQUIRED FOR
COMPARABLE SPECTRA

Nucleus	Sensitivity	Concentration threshold* (mM)
^1H	1.0	$\ll 1$
^{23}Na	9.25×10^{-2}	5
^{31}P	6.64×10^{-2}	1
^{14}N	1.01×10^{-1}	10^b
^{39}K	4.7×10^{-4}	20
^{13}C	1.76×10^{-4}	$\gg 20$
^{15}N	3.85×10^{-6}	$\gg 20$

* This concentration threshold takes into account the difference in relaxation properties. Concentrations are averaged over the total volume of the sample in the detecting coil, corresponding to 1 g fresh weight of sample and a spectral accumulation time of 20 min (see Reference 18).

^b This threshold is considered for molecules with local fields that are tetrahedrally symmetrical around the nitrogen atom, e.g., NH_4^+ , NO_3^- .

From Ratcliffe, R. G., *Inorg. Biochem.*, 28, 347, 1986. With permission.

III. PARAMETERS OF THE *IN VIVO* NMR EXPERIMENT

A. Selecting a Nucleus (An Overview)

The choosing of an appropriate nucleus to study a particular biological system must be based on a number of considerations. First and foremost, one must consider the quality and quantity of information that is required. For example, what is the concentration of the active metabolites in the cells, and at what level of abundance is the magnetically active nucleus present? Can one use isotopically enriched compounds where the natural level is too low to detect these molecules? What is the spin state of the naturally abundant isotopes vs. the enriched nonabundant one? In some instances it may be useful to enrich a tissue with an isotopically labeled nucleus (spin 1/2), e.g., ^{15}N (natural abundance 2.24×10^{-2}) in favor of examining the more highly abundance (5.7%) nucleus ^{14}N which is quadrupolar and would generally, except in certain circumstances, give poorly interpretable, broadened spectra. Some examples demonstrating the advantages, disadvantages, and methods of circumventing these problems will be discussed in subsequent sections.

Ratcliffe¹⁸ has compiled a list of nuclei and their inherent sensitivities as they relate to the S/N ratio of resulting spectra. In addition, he has compared this to the threshold concentration of each nucleus needed to produce comparable spectra in a period of 15 to 20 min. Table 1 contains a listing of this information for quick reference. To date, the most commonly used nucleus for *in vivo* NMR work is ^{31}P because of its spin 1/2, relatively simple interpretable spectra, and the key metabolic significance of the compounds it represents. Although ^{23}Na and ^1H have lower concentration thresholds, sodium is quadrupolar and has a smaller chemical shift range (~10 ppm) while *in vivo* proton NMR requires special spectrometer techniques because of the dominance of the water resonance in the spectra. ^{13}C has a very meager level of natural abundance (1.1%), but is useful in studies of tissues that accumulate carbon-containing storage compounds; however, most *in vivo* investigations require ^{13}C -labeled compound precursors to examine metabolic sequences in functioning tissues and cells. The latter methodology is an excellent alternative to radio tracer experiments since ^{13}C NMR allows the direct observation of specific metabolic pathways and distributions of label within metabolites without the need for

complex degradation procedures. On a one-to-one concentration basis ^{13}C is actually two to three times more sensitive than ^{31}P . This greater sensitivity is primarily a result of its narrow line widths and signal enhancement gained from broad-band proton decoupling (nuclear Overhauser enhancement, NOE). As you will see, the extremely large chemical shift range of ^{13}C makes this nucleus ideal to utilize when resolving a large assortment of cellular metabolites. As with ^{13}C , the natural abundance of ^{15}N is very low; in fact, it is only 1/50th as sensitive as ^{13}C . Therefore, ^{15}N NMR can only be examined with labeled substrates *in vivo*. However, the ^{15}N chemical shift range is 50% larger than ^{13}C making ^{15}N more sensitive to structural changes associated with the nitrogen environment. Potassium has similar problems to sodium in that it is quadrupolar in nature in addition to being a less sensitive nucleus than sodium. Consequently, ^{39}K is rarely used for *in vivo* investigations even though it is a physiologically important nucleus. The ^{19}F nucleus is close to ^1H in sensitivity and its chemical shift range far outstretches that of ^{13}C . Thus, one would expect this nucleus to be the perfect probe for biological studies. Unfortunately, naturally occurring ^{19}F -containing compounds are rarely found in biological systems. To take advantage of the excellent spectroscopic properties of fluorine, many researchers have incorporated this nucleus into compounds that could be diffused into cells. These spy molecules can then be examined to probe intracellular pH and the binding of other NMR invisible ions. The various NMR nuclei used to detect inorganic ions are summarized in Table 2, adapted from Ratcliffe.¹⁸ These studies will be discussed under the heading of each nucleus that follows.

B. Maintaining Viability

In vivo applications put additional experimental demands on NMR spectroscopy. One must pay careful attention to the condition and maintenance of the living system being examined. How well is it being perfused? What are the optimum conditions necessary for sustaining it for extended periods of time? How does one prevent bacterial contamination? In addition, we must also consider the conditions of the spectrometer. We must have a leakproof perfusion system to prevent damage to the probe and shim coils. Figure 7 shows the configuration of the perfusion apparatus commonly used in *in vivo* tissue studies. Often multiple connected reservoirs are used so perfusates with different reagents may be perfused and switched without having to stop ongoing experiments.¹⁴ NMR tubes from 10 to 75 mm in diameter have typically been used for studies of small excised plant tissues,¹⁹ cells,²⁰ organs,⁸ and intact anesthetized small animals;⁸ however, a recent study reported a more sophisticated system that can use a 5-mm tube.²¹ In a circulating system it is convenient to bubble the required gas such as O_2 , air, N_2 , He, etc. into the reservoir containing the perfusing liquid. This technique prevents problems associated with the loss of field homogeneity when gas bubbles are passed directly into the NMR tube containing the sample. In some instances microbubbling techniques or enzymatic generation of oxygen have been employed to circumvent possible homogeneity problems.²² Figure 8 shows a typical NMR assembly used for the perfusion of plant tissue.¹⁴ Note the two failsafe features: pressure-sensitive connections positioned close to the peristaltic pump and the spinner housing overflow vacuum line. Observe also that the flow in the tube is downward, i.e., the liquid is drawn out from the bottom of the tube. This arrangement is utilized to prevent any trapped gas in the lines from accumulating in the interstitial space between the tissue.²³ This assembly is quite convenient for examining most small or excised tissues and cultured cells (plant and mammalian). The ^{31}P spectra shown to the right in Figure 8 demonstrate the maintenance of a consistently healthy physiological state of excised maize root tips during 34 h of perfusion. To study small cells with continual perfusion requires a somewhat more elaborate design since these small organisms must be kept from flowing along with the perfusing liquid. To circumvent this problem, researchers have devised a dialysis microfiber arrangement that allows liquid to flow through and evenly bathe the cells.²³ Figure 9 shows three ^{31}P NMR spectra of maize root tips at different levels of viability as a function of perfusion condition.

In Figure 9A, we see a spectrum representing a highly energized state, i.e., high levels of NTP

Table 2
NMR DETECTION OF INORGANIC IONS IN PLANT TISSUES

Ion	NMR nucleus	Comments
H ⁺	¹ H	pH-dependent chemical shifts and line widths (¹⁵ N) for metabolites containing ionizable groups can be used to estimate intracellular pH;
	¹³ C(*)	³¹ P NMR is of only limited use for measuring the pH of the acidic vacuolar compartment ([H ⁺] ≥ 1 μM)
	¹⁵ N(*)	
	³¹ P	
Carbonate	¹³ C(*)	Detectable in tissues labeled with ¹³ CO ₂
NH ₄ ⁺	¹⁴ N	The naturally abundant ¹⁴ N is quadrupolar (I = 1) and most ¹⁴ N resonances are unacceptably broad; NH ₄ ⁺ and NO ₃ ⁻ give narrow lines, but to follow their metabolic transformation by NMR it is necessary to use ¹⁵ N NMR in isotopically labeled tissues
	¹⁵ N(*)	
NO ₃ ⁻	¹⁴ N	
	¹⁵ N(*)	
Na ⁺	²³ Na	Potentially complicated, but informative, line shapes for this nucleus (I = 3/2)
Mg ²⁺	³¹ P	The ³¹ P resonances of ATP are Mg ²⁺ dependent
Ortho-phosphate (P _i)	³¹ P	The most commonly observed nucleus <i>in vivo</i>
SO ₄ ²⁻	³³ S(*)	³³ S is a difficult NMR nucleus, and even in a fully labeled system it is unlikely to be of any use for the detection of intracellular SO ₄ ²⁻
Cl ⁻	³⁵ Cl	Potentially complicated, but informative line shapes for the nucleus (I = 3/2)
K ⁺	³⁹ K	Similar to ²³ Na, but the sensitivity is much less (I = 3/2)
Ca ²⁺	¹⁹ F	An indirect method requiring infiltration of a ¹⁹ F labeled probe; problems in infiltrating the related fluorescent probes into plant cells suggest that this NMR method is inapplicable to plant tissues
Mn ²⁺	¹ H	Extensive literature on chloroplast suspensions (with confusing differences in interpretation between the two groups involved)
Mn ²⁺	³¹ P	Mn-induced line-broadening effects in ³¹ P spectra can be interpreted in terms of the intracellular distribution of Mn ²⁺
Al ³⁺	³¹ P	Estimates the effect of this ion on energetics of the cells, ATP levels, intracellular pH, and Pi depletion

Adapted from Ratcliffe, R. G., *Inorg. Biochem.*, 28, 347, 1986.

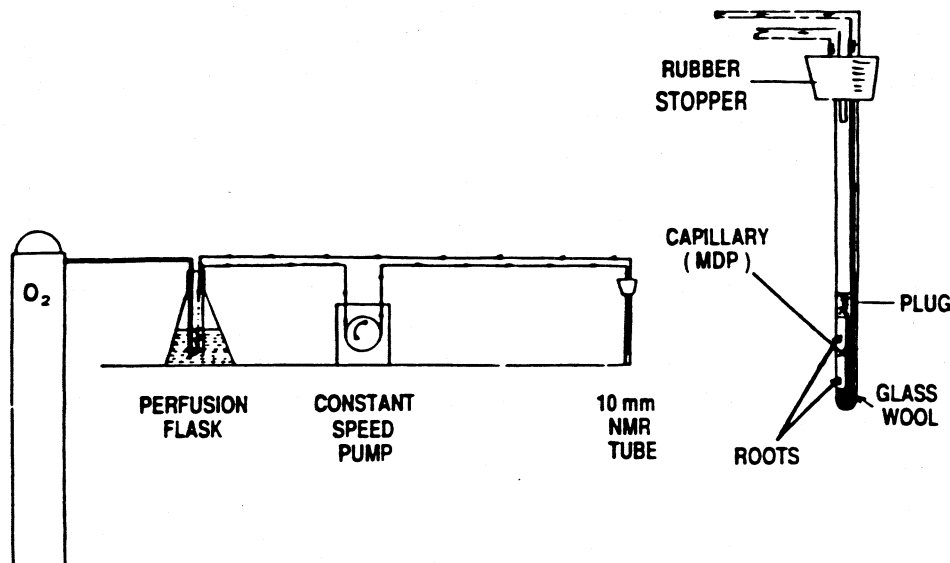


FIGURE 7. Schematic representation of tissue perfusion system.

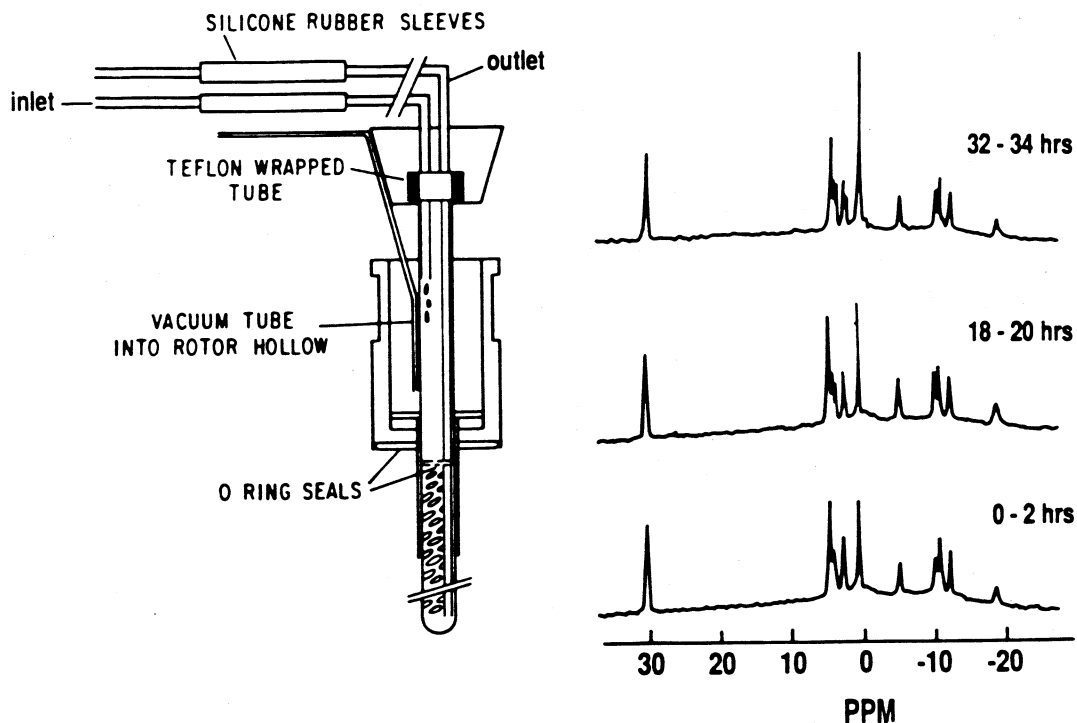


FIGURE 8. NMR tube perfusion device with overflow prevention tube and breakaway sleeves and 161.7-MHz ^{31}P spectra of perfused maize root tips after 34 h.

and glucose-6-phosphate. In Figure 9B, these levels have dropped significantly due to only trace amounts of oxygen (hypoxia) perfusing through the tissue; however, the tissue still remains viable. With no perfusion, Figure 9C, anoxia is complete within 20 min following a concomitant buildup of localized CO_2 and membrane destruction. More details concerning these experiments will follow in this chapter and Chapter 3. Whole organs such as hearts, kidneys, and livers are generally perfused with a cannula and often the pumping of the fluid is gated or timed to the pulsing of the spectrometer so as not to obtain spectral artifacts from the movement of the flowing liquid.²⁴ Studies of organs of small intact animals only require that the animal be properly anesthetized.²⁵ Whole limb, NMR spectroscopy, usually of a leg or arm muscle, is performed with a wide-bore (25 cm or greater) horizontal magnet. Spectra from such experiments are used for clinical examinations for diagnosing diseased muscle function or exercising physiology studies.²⁶

C. Qualitative Aspects

Identification of the resonances in an *in vivo* NMR spectrum is not always a simple matter. Often the observed resonances are broadened and overlap badly in the spectrum, making it difficult to resolve and quantify each peak. This resonance overlap is a particular problem for ^{31}P and ^1H NMR. For ^{31}P NMR a simple comparison of shifts of known compounds in solution whose ionic strength and pH are close to those of the cell can help eliminate some compounds as contributors to the *in vivo* spectrum. Following this procedure, careful cold perchloric acid extraction²⁰ of the tissue, lyophilization, and subsequent inspection of the extract in a solution containing CDTA or other paramagnetic metal ion sequesterant will yield a relatively narrow line spectrum of metabolites. Figure 10 shows the downfield portion of the ^{31}P NMR spectrum of a perchloric acid extract of soybean nodules with small amounts of suspected nucleotides added to verify the identity of each resonance. To the left of the extract spectra (Figure 10) is the *in vivo* ^{31}P spectrum of the intact nodules from which the extract was prepared. Note that the two resonances labeled Pi cyt and Pi vac in the *in vivo* spectrum have become one Pi resonance at

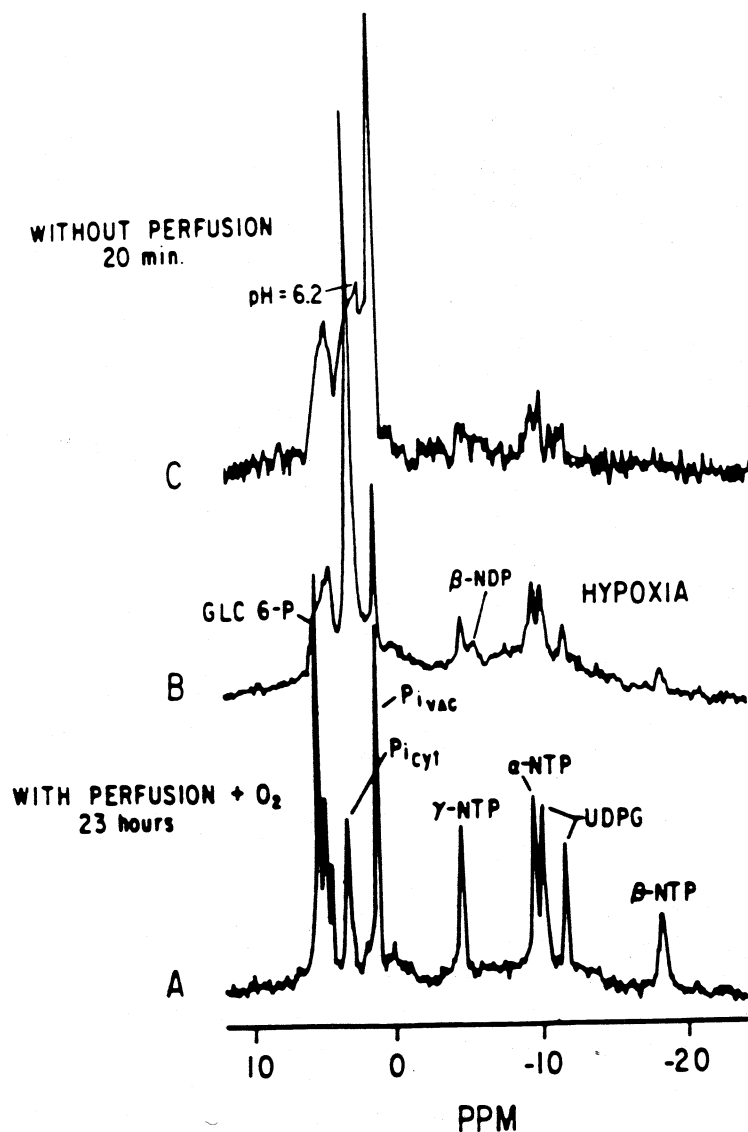


FIGURE 9. 161.7-MHz ^{31}P spectra of maize root tips, 10,000 scans each (27-min accumulation). (A) after 23 h of perfusion with an oxygen saturated perfusate (B) following 1 1/2 h of perfusion with a nitrogen-saturated perfusate and (C) without perfusion for 20 min.

23.1 ppm in the extract spectra ($\text{pH} = 7.8$). Thus, the extract spectra helps to identify the resonances representing P_i in two different chemical environments (membrane separated) within the cell and distinguishes them from other nucleotides whose resonances may be in close proximity. If one suspects that there is more than one P_i peak present in the *in vivo* spectrum due to different compartmentation, the extract spectra will clarify this point, since only one P_i resonance will appear. Another check on the identity of each resonance can be made by titration of the extracts of phosphorus metabolites since most of these ^{31}P compounds exhibit characteristic titration curves that correlate with chemical shift in the vicinity of their respective pK_a s. This topic will be discussed in more detail in the section on ^{31}P studies. Additionally, extracts can be treated with various specific enzymes, e.g., a phosphodiesterase or mutase, to establish the identity of individual compounds.²⁷

The identification of ^{13}C resonances is somewhat more complex because of the large number of observable metabolites. Also with some exceptions that we will mention later, ^{13}C resonances do not always exhibit the broad titration/chemical shift range of ^{31}P , especially at physiological pH . For this reason one must often rely primarily on resonance peak matching. This method is

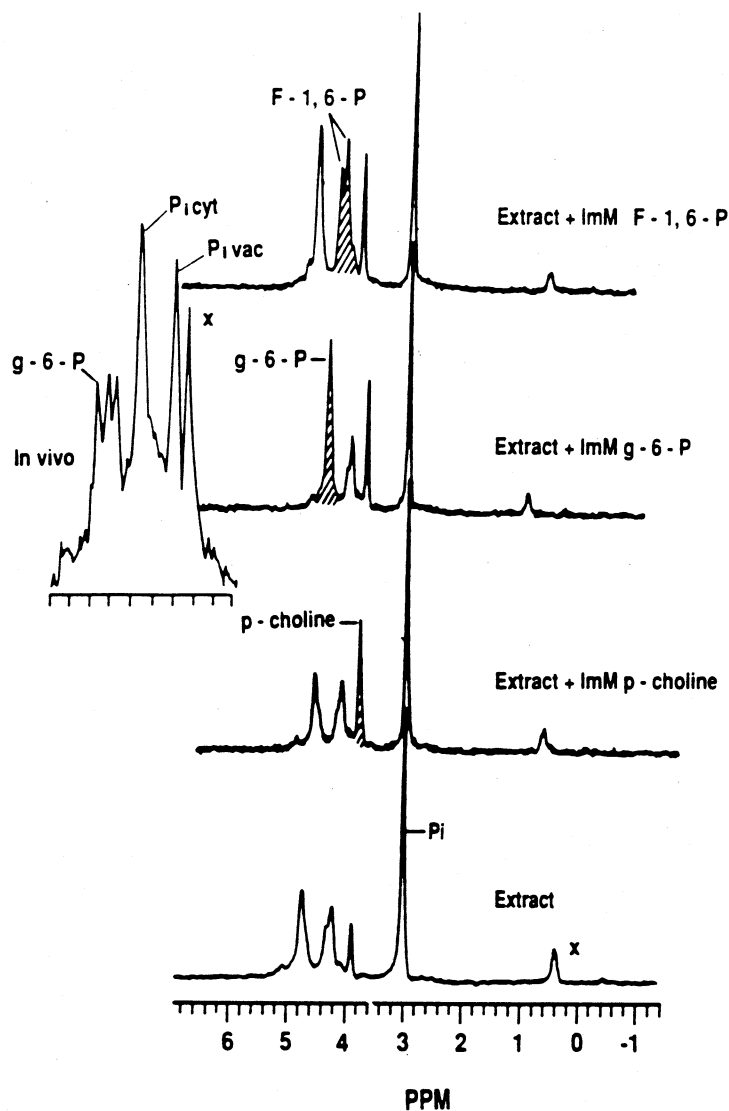


FIGURE 10. Low-field section of 161.7-MHz ^{31}P spectra of the *in vivo* and perchloric acid extracts of soybean nodules. Each resonance is identified by the successive addition of a known metabolite. Each spectrum required 1000 scans with a 3-s pulse delay.

usually quite reliable since resonance patterns for ^{13}C spectra are well established and reproducible.²⁸ Additionally, the identity of a carbon resonance, i.e., a CH, CH_2 , CH_3 or quaternary carbon, can be verified by examining the proton-coupled ^{13}C spectrum of an extract. In such spectra the CH carbon resonances are doublets, CH_2 s are triplets, CH_3 s quartets, and quaternary Cs are seen as singlets ($n + 1$ lines), due to the coupling to n magnetically equivalent protons.²⁹ This analysis may also be accomplished using recently devised NMR pulse sequences (INEPT, DEPT, etc.) to obtain the multiplicity of each resonance.³⁰

^{13}C , which is a spin 1/2 nucleus, shows ^{13}C - ^{13}C $n + 1$ line splitting in labeled metabolites. This splitting can be diagnostic for evaluating biosynthetic and metabolic labeling patterns. The splitting attributed to ^{13}C - ^{13}C coupling between neighboring carbons gives direct insight into pathways for the incorporation of ^{13}C -labeled precursors.³¹ When ^{13}C is next to an unlabeled natural abundance ^{12}C (~99%), the former gives rise to a singlet resonance, indicating that only one carbon of the ^{13}C -labeled precursor was incorporated at that site in the metabolite.³² This method is useful for establishing intermediate steps in biosynthetic pathways.³¹ A new double quantum coherent 2D NMR pulse sequence³⁰ (INADEQUATE) has recently become useful for

detecting ^{13}C - ^{13}C bonds in biosynthetic intermediates.³³ However, this method can only be used if relatively large amounts of the labeled metabolites are available.³⁰

Identification of ^{15}N resonances generally offers no problem because each represents a unique isolated nucleus associated with a specific compound. For example, when enriched ^{15}N -labeled NH_4Cl was used as a nutrient source for fungi, the resulting ^{15}N spectra of the labeled amino acids gave a clear profile of the sequence of nitrogen incorporation.³⁴ ^{14}N on the other hand, because of its quadrupolar nature, is not a practical nucleus for evaluating compounds other than those that are tetrahedrally symmetrical such as NO_3 or NH_4 .³⁵ All other natural abundance ^{14}N compounds within a tissue are not readily visible by NMR because of their broad lines (100 to 1000 Hz), whereas ^{14}N line widths of cellular $^{14}\text{NH}_4$ and $^{14}\text{NO}_3$ are only 10 Hz.³⁶

Proton, with the most sensitive nucleus natural abundance levels, offers the most complex spectra to analyze largely because of its limited chemical shift range (10 ppm) and complex homonuclear spin-spin coupling pattern and strong dipole-dipole interactions. Typically, the ^1H signals derived from large macromolecules such as proteins *in vivo* are very broad due to short T_2 (slow motion), whereas, the signal from the small rapidly tumbling metabolites are sharp (longer T_2). Taking advantage of this difference in T_2 values, Brown et al.³⁷ were able to "edit" the ^1H spectrum of human erythrocytes with a spin echo pulse sequence and suppress the broad overlapping resonances due to the relatively immobile proteins. Identification of the remaining metabolite resonances could then be made by spectral comparison with authentic compounds or titration of selected residues associated with specific chemical shifts.³⁷ Fan and co-workers²¹ have utilized homonuclear correlated two-dimensional NMR both *in vivo* and *in vitro* in addition to gas chromatography-mass spectrometry to identify sugars, organic acids, amino acids, and ethanol in carrot roots, maize roots, and rice shoots. Figure 11 and the corresponding Table 3 show an impressive number of metabolites that may be identified using this methodology.³⁰

Other nuclei such as ^{23}Na and ^{39}K do not present any resonance identification problems since these peaks are not associated with any particular compound *in vivo*, but can reflect the chemical environment characteristic of a cell compartment. The ^{19}F nucleus is generally used as a label on compounds to probe pH or metal ion concentrations and as such does not represent a problem in terms of chemical shift assignment.

D. Quantitative Aspects

As mentioned earlier, the spin-lattice relaxation time (T_1) is the most important factor contributing to quantitation of the NMR spectral responses for spin 1/2 nuclei, such as ^{31}P , ^{13}C , ^{15}N , and ^1H . To obtain full resonance responses, one should initiate each pulse after a waiting period of five times that required for the resonance having the longest T_1 . However, this waiting is not always convenient since T_1 can often be >5 s. Also, because of the constraints of time resolution, the metabolic process one follows may be past history by the time the final spectrum has been acquired. Furthermore, it is sometimes advantageous to recycle the scans faster and excite the frequencies with a smaller than 90° pulse angle to emphasize certain features of the spectrum. Figure 12 illustrates ^{31}P spectra of maize root tips which were acquired under (A) nonquantitative and (B) quantitative conditions.^{14,38} Clearly, one observes an obvious difference in the ratio of the resonances in each of the spectra due to the differences in the acquisition conditions used. If we look at Table 4 we can immediately see what has occurred. Those resonances whose T_1 values are very long, i.e., Pi vac, Pi cyt, and sugar phosphates are seriously suppressed during rapid recycling and those with short T_1 s, e.g., NTP and uridine diphosphoglucose (UDPG), are more strongly emphasized under these conditions. Although spectrum A is distorted in terms of the true ratios of resonances representing each component, it offers the advantage that one can readily quantify changes taking place at the concentration level of the nucleotides over shorter periods of time.¹⁴ However, if one wants to compare the ratios, for example, of nucleotides to phosphomonoesters and Pi under the fast acquisition conditions, one would necessarily have to first perform the long acquisition time experiments, to establish the true relative intensities. After performing this experiment the fast acquisition data can be

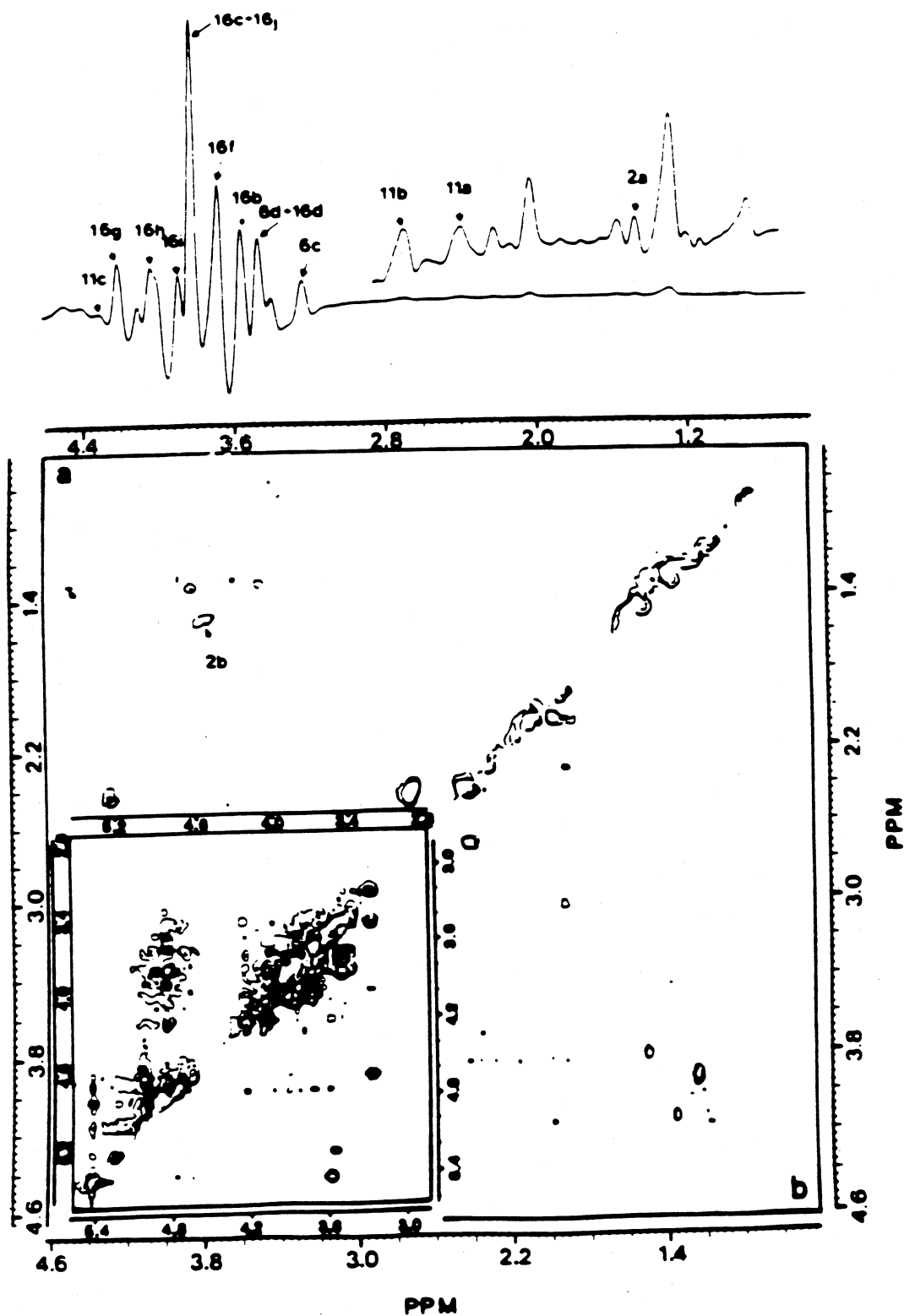


FIGURE 11. *In vivo* COSY spectrum of a carrot root under superfusion. The *in vivo* COSY part is displayed in the upper triangle (a) as contour plots along with the 1-D spectrum while the COSY spectrum of the PCA extract of the same tissue is shown in the lower triangle (b). The inset represents the sugar region and was plotted at higher contour levels than the 0.6- to 4.6-ppm region. These two regions were presented separately because of the much greater peak intensities in the sugar region than in the 0.6- to 4.6-ppm region, which would obscure the cross-peaks in the latter if they were plotted at the same contour levels. The peaks are numbered according to Table 3. (From Fan, W.-M., Higashi, R. M., and Lane, A., *Arch. Biochem. Biophys.*, 251, 674, 1986. With permission.)

Table 3
**IN VIVO ¹H NMR ASSIGNMENT OF RESONANCES IN CARROT ROOT,
MAIZE ROOT, AND RICE SHOOT TISSUES**

Peak number	Assignment	δ <i>in vivo</i>	δ <i>in vivo</i>	Tissues in which <i>in vivo</i> resonances were observed
1	<i>t</i> -Acon- α CH	6.80	6.58	Maize root
2a	Ala- β CH ₂	1.48	1.47	Carrot, maize root, rice shoot
2b	Ala- α CH	3.77	3.76	Carrot
3a	Asn- β CH	2.86	2.84	Maize root, rice shoot
3b	Asn- β CH	2.95	2.94	Carrot, maize root, rice shoot
3c	Asn- α CH	4.03	4.00	Maize root
4	EToch- β CH ₂	1.18	1.16	Maize root, rice shoot
5a	GAB- β CH ₂	1.89	1.89	Maize root, rice shoot
5b	GAB- α CH ₂	2.29	2.29	Carrot, maize root, rice shoot
5c	GAB- γ CH ₂	3.00	3.01	Carrot, maize root, rice shoot
6a	Glc-C ₁ β	5.24	5.23	Carrot, maize root, rice shoot
6b	Glc-C ₁ α	4.65	4.64	Carrot
6c	Glc-C ₂ β	3.24	3.24	Carrot, maize root, rice shoot
6d	Glc-C ₂ β	3.47	3.47	Carrot
7a	Gln- β CH ₂	2.13	2.13	Carrot, maize root, rice shoot
7b	Gln- γ CH ₂	2.45	2.44	Carrot, maize root, rice shoot
8a	Glu- β CH ₂	2.07	2.06	Maize root, rice shoot
8b	Gln- γ CH ₂	2.36	2.34	Carrot, maize root, rice shoot
9	His-C ₁ H	8.66	7.86	Maize root
10	Ile- δ CH ₂	0.96	0.93	Carrot, maize root
11a	Malate- β CH	2.43	2.40	Carrot
11b	Malate- β' CH	2.72-2.68	2.67	Carrot, maize root, rice shoot
11c	Malate- α CH	4.32-4.30	4.30	Carrot, maize root
12a	Lactate- β CH ₂	1.32	1.32	Carrot, maize root, rice shoot
12b	Lactate- α CH	4.11	4.11	Carrot, maize root
13	Leu- δ CH ₂	0.96	0.94	Carrot, maize root, rice shoot
	Leu- δ CH ₂	0.96	0.96	Carrot, maize root, rice shoot
14	OAc- α CH ₂	2.01	1.91	Maize root, rice shoot
15	Succ- α and - β CH	2.38	2.39	Maize root, rice shoot
16a	Sucrose-G ₁	5.42	5.41	Carrot, maize root, rice shoot
16b	Sucrose-G ₂	3.56	3.56	Carrot
16c	Sucrose-G ₃	3.81	3.75	Carrot
16d	Sucrose-G ₃	3.47	3.47	Carrot
16e	Sucrose-G ₄	3.81	3.83	Carrot
16f	Sucrose-F ₁	3.70	3.68	Carrot
16g	Sucrose-F ₁	4.20	4.20	Carrot, maize root
16h	Sucrose-F ₂	4.03	4.04	Carrot, maize root
16i	Sucrose-F ₃	3.89	3.88	Carrot
16j	Sucrose-F ₄	3.81	3.88	Carrot
17	Thr- γ CH ₂	1.32	1.32	Carrot, maize root, rice shoot
18	Val- γ CH ₂	0.96	0.98	Carrot, maize root, rice shoot

Adapted from Fan, W.-M. T., Higashi, R. M., and Lane, A., *Arch. Biochem. Biophys.* 251, 674, 1986.

modified by the appropriate response factors to yield reliable ratios.^{16,39} It should be emphasized that interconversion of metabolites can be continually occurring during these experiments, which means that a resonance representing a particular component with a specific relaxation time may be converted into another component whose resonance relaxation time is different. For example, γ -NTP \rightarrow Pi represents a relaxation change of the corresponding resonances of 0.35 to 2.78 s, respectively. To account for this difference, under fast acquisition conditions one must compensate for the disparity in magnetization of the two resonances, because after the γ -NTP phosphate is hydrolyzed to Pi *in vivo* the γ -NTP contributes less of a response (area) to the Pi

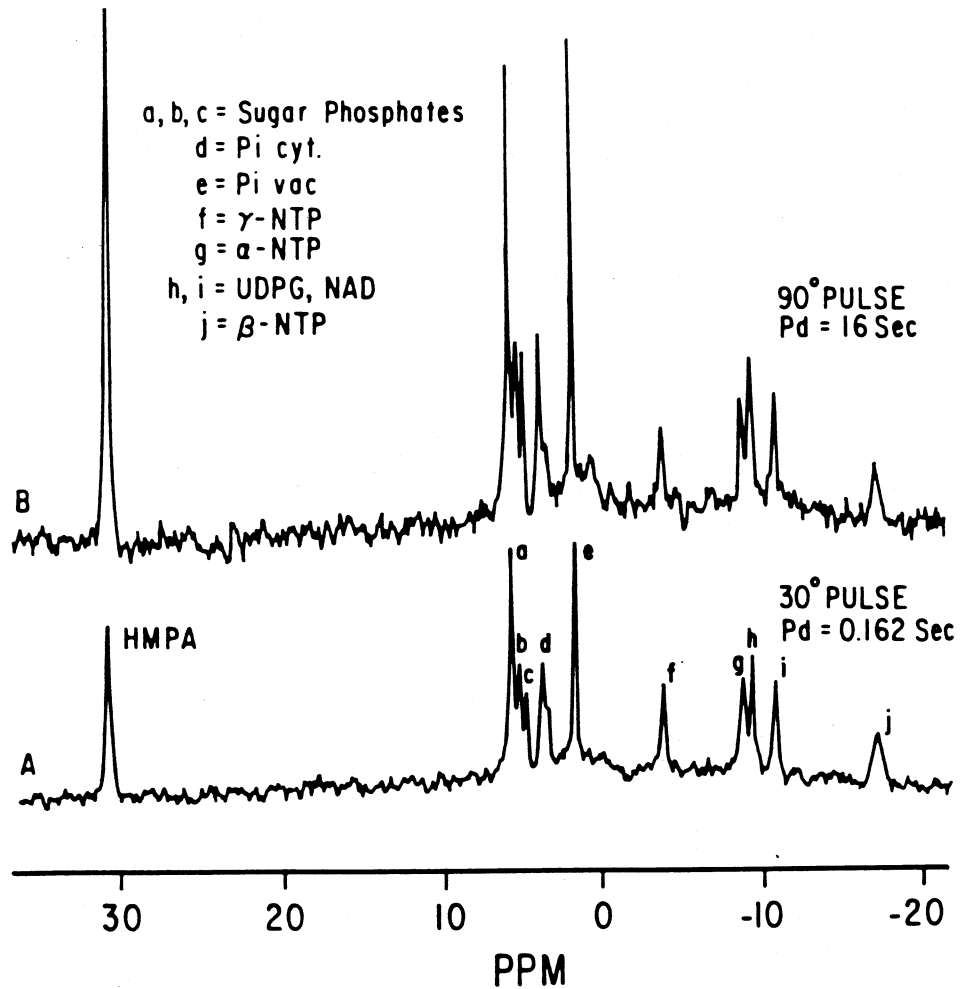


FIGURE 12. Intensity distortion due to rapid acquisition. (A) 161.7-MHz ^{31}P spectrum of approximately 900 excised root tips (5 to 7 mm) taken under fast acquisition accumulation parameters. 30° pulse (12 μs) 2000 data points zero filled to 16,000 recycling time of 0.162 s. 10,000 transients, frequency of 16 KHz. 15-Hz line broadening, and total time for acquisition of spectrum 27 min. (B) Slow recycling time full 90° pulse-generated spectrum obtained with a 16-s recycling time. 1000 scans. 16,000-Hz frequency, 15-Hz line broadening, and total time for acquisition of spectrum 3.5 h. (See Reference 14.)

resonance than it did when it was observed as a γ -NTP resonance.¹⁶ This kind of treatment allows one to assess the material balance of mobile phosphorus metabolites in tissues and thereby account for any generation or leakage of material during the study.¹⁶

Under quantitative acquisition conditions, the ^{31}P line intensities correspond to the concentration of each particular compound contained in the collection of cells or tissue residing in the volume of the detection coil of the probe. Each of these resonances can be measured against the reference peak area which has previously been calibrated with standard solutions of the various compounds being examined. In essence, the spectrum displays changes in the overall concentration of components within the enclosed coil volume. However, a knowledge of the cell volume as well as the cytoplasmic and vacuolar compartment volumes is necessary to provide a meaningful estimate of intracellular concentrations.^{40,41}

^{13}C and ^{15}N T_1 relaxation is largely dependent on molecular motion as it modulates the dipolar interaction of these nuclei with their directly bonded protons. In addition to the spin-lattice relaxation phenomenon discussed above, the resonance intensity of ^{13}C and ^{15}N is also subject to another phenomenon associated with relaxation known as the nuclear Overhauser effect.¹¹ When we observe the spectra of both ^{13}C or ^{15}N the full frequency range of the corresponding

Table 4
³¹P NMR SPIN-LATTICE
RELAXATION TIMES (T₁) OF
INTRACELLULAR
COMPONENTS OF MAIZE
ROOT TIPS

Compound	T ₁ (s)
G-6-P	2.89 ± 0.24
Pi vacuolar	3.58 ± 0.5
Pi cytoplasmic	2.78 ± 0.31
NTP	
γ	0.35 ± 0.06
α	0.39 ± 0.05
β	0.21 ± 0.02
UDPG	0.63 ± 0.06

Adapted from Pfeffer, P. E., Tu, S. I., Gerasimowicz, W. V., and Cavanaugh, J. R., *Plant Physiol.*, 80, 77, 1986.

proton spectrum is routinely broad-band noise decoupled to remove spin-spin scalar splitting.¹¹ During the saturation of all the proton lines, a secondary effect produces a rearrangement of energy level populations resulting in a modification of the ¹³C or ¹⁵N line intensities. ¹³C resonances always experience an enhancement of signal from 0 to 3 depending on the number of directly bonded protons, and molecular motion. The greater the number of bonded protons, the greater is the enhancement for ¹³C, while the efficiency of the NOE as molecular motion slows, becomes impaired.¹¹ Under the conditions where T_c ≅ 1/ω₀, the NOE shows a magnetic field dependence which can be used to calculate molecular motion.⁴² Because of its negative magnetogyric ratio, the NOEs for the ¹⁵N resonance have a range of 0 to -5 and in some instances may not be visible or are observed as negative peaks in the spectrum under complete proton decoupling conditions.⁴³ Typically NOE for ³¹P is much smaller because the magnetogyric ratio for ³¹P is larger relative to that of protons and also because it is rare to find ³¹P directly bonded to protons (NOE is dependent on internuclear distance and proportional to 1/r⁶ where r is the internuclear distance between ¹H and ³¹P). Also the ³¹P-¹H couplings are usually very small. Consequently, proton decoupling yields little change in the ³¹P spectrum but may generate some rf heating that can be detrimental to biological samples. To achieve quantitative responses for both ¹³C or ¹⁵N resonances, one must not only pay attention to T₁-dependent recycling times but Overhauser effects as well. The former is easily accomplished as described above, while the latter can be corrected by decoupling the proton spectrum only during the time the rf pulse is being applied.¹¹ This method of gated decoupling removes the scalar ¹H splitting from the ¹³C or ¹⁵N spectra without transmitting the proton polarization effects responsible for the distorted intensities. Of course, one must recognize that in these experiments it can take up to three times longer to obtain ¹³C spectra and up to five times longer to obtain ¹⁵N spectra* under these conditions.

Quadrupolar nuclei such as ²³Na, ³⁹K, or ¹⁴N present no problem as far as spin-lattice relaxation is concerned, that is, because their relaxation mechanism is dominated by efficient quadrupolar interactions with neighboring nuclei (T₁ ~ millisecond range). In spite of the relatively low sensitivity of ¹⁴N, one can pulse its spectrum and recycle rapidly without being concerned with saturation. Rapid scanning enables the accumulation of a large number of transients in a relatively short period of time.

^{23}Na and ^{39}K have problems which make them difficult nuclei to quantify. In particular spin 3/2 quadrupolar nuclear interactions within living cells and tissues can give rise to two different T_2 values. One has a T_2 so short that its corresponding resonance is not detectable.^{44,45} This translates into a resonance "visibility" of only 40% because the transition corresponding to the longer T_2 represents two fifths of the total signal.^{45,46} Recently, a study has revealed that these "invisible" populations may be "unmasked" using a sophisticated two-dimensional double-quantum NMR method.⁴⁷

IV. *IN VIVO* NMR APPLICATIONS

A. ^{31}P Studies

^{31}P NMR spectroscopy is the most widely used technique for examining biological systems. The most recent review describing some NMR studies of plant tissue including the use of ^{31}P has been given by Ratcliffe.⁴⁸ This nucleus combines the advantages of 100% natural abundance, relatively high sensitivity, and a chemical shift range for metabolic compounds of 30+ ppm to make it most attractive for the examinations of microorganisms, plants, and animal tissues. This spectrum contains only 8 to 12 resonances representing, for example, 3 to 4 different phospho-monoesters, orthophosphate (Pi), NTP, in some instances NDP, uridine diphosphoglucose UDPG and nicotinamide adenine dinucleotide (NAD), as seen in Figure 12. However, the spectrum provides valuable information concerning many critical cell functions.*. For example, the Pi resonance can provide valuable information concerning Pi utilization which modulates glycolysis,⁵² respiration,⁵³ photosynthesis,⁵⁴ and starch breakdown.⁵⁵ The bioenergetics of the cell can also be examined by the assessment of the NTP/NDP ratio,⁸ the intracellular pH,⁸ and intracellular metabolic fluxes of Pi.⁵⁵ While spectral analysis is often relatively straightforward, one must bear in mind that we can only examine mobile, low molecular weight compounds with standard high-resolution instrumentation. Thus, a large fraction of the larger phosphorus-containing materials such as membrane phospholipids, nucleic acids, and phosphoproteins are NMR invisible. In some rare situations, this NMR invisibility can present a problem if, for example, one wants to follow the pathway of the production of polymeric materials in which fluxes are rapid through low steady-state concentrations of mobile metabolites.⁵⁶ Methods such as saturation transfer, which shall be discussed in this section, can give quantitative information concerning the interconversion of key metabolites under various cell-stressing conditions. Obviously, high resolution *in vivo* ^{31}P NMR cannot give the complete picture of the functioning cell. However, in conjunction with other methods, *in vivo* NMR can strengthen conclusions concerning various mechanisms affecting metabolic processes.

1. pH and Compartmentation

^{31}P NMR has gained the reputation of being an "expensive" pH meter. However, it may be worth the price,** since the NMR can perform this task continuously and simultaneously on different intracellular compartments as it monitors other metabolic functions. In addition, one can also correlate the levels of high- and low-energy phosphates, membrane integrity, and intracellular pH in a single experiment.

The measurement of intracellular pH is most often made utilizing the Pi resonance as a spy or probe molecular within the cellular compartments, although the resonances of other phosphorus compounds such as glucose-6-phosphate (G-6-P),³⁸ 2-deoxy-glucose-6-phosphate

* In animal tissues phosphocreatin and phosphodiester resonances are also observed; while fungi and yeast exhibit resonances associated with stored polyphosphates** and phosphodiester** such as phosphorylserine (PS), phosphorylethanolamine (PE), and phosphorylinositol (PI); in algae, ** glycerol 1,2-cyclic phosphate has been observed and fast-growing *Rhizobium* exhibit glycerophosphorylated cyclic β -1,2-glucans.

** The price of a basic broad-banded high-resolution NMR instrument is generally \$1,000/MHz, so a 400-MHz instrument would cost approximately \$400,000

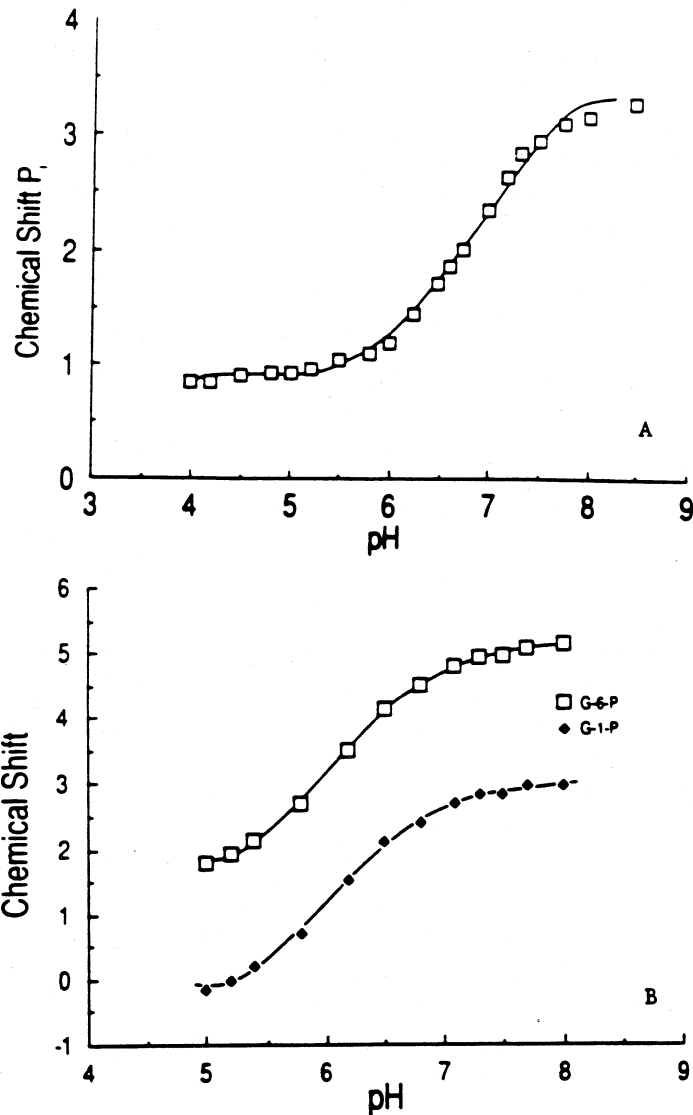


FIGURE 13. pH vs. ^{31}P chemical shift at 22°C. Solutions contained 5.0 mM K_2HPO_4 , 2.0 mM MgCl_2 , and 100 mM KCl for the P_i titration curve and 2.5 mM G-6-P and 2.5 G-1-P plus 2.0 mM MgCl_2 and 100 mM KCl for the sugar phosphate titration curve. The shift positions are given relative to HMPA which is assigned a value of 30.73 ppm (relative to 85% $\text{H}_3\text{PO}_4 = 0.00$).

(2DG-6-P),¹³ methylphosphonate (MP),⁵⁷ and inosine monophosphate (IMP)⁵⁸ have also been used. The application relies on the fact that P_i exists as an equilibrium mixture of HPO_4^{2-} and H_2PO_4^- under physiological conditions ($\sim\text{pH } 7$). Since the equilibrium between these two ions is rapid on the NMR time scale, we only see a single resonance representing the concentration of P_i at any particular pH. The observed δ_o or chemical shift of this P_i resonance is the weighted average shift of $\delta^{\text{HPO}_4^{2-}}$ and $\delta^{\text{H}_2\text{PO}_4^-}$ given by the relationship:

$$\text{pH} = \text{pk} + \log \frac{\delta^{\text{HPO}_4^{2-}} - \delta_o}{\delta_o - \delta^{\text{H}_2\text{PO}_4^-}} \quad (6)$$

By plotting the change in chemical shift δ_o of P_i vs. the known pH of standard solutions we obtain a titration curve as shown in Figure 13. The resonance position of two other metabolites within a cell can also be used to establish if they are in the same pH environment. For example,

the chemical shift position of G-6-P or G-1-P should correspond to the same pH as reported by the Pi resonance if they are contained in the same cellular compartment (Figure 13). Since the pKas of these compounds are in the range of 6.2 to 6.8, they can report intracellular pH in the range of 5.5 to 7.8 ± 0.1 most accurately. Unfortunately, one cannot monitor pH changes for compartments with pHs below 5.5 or above 7.8 with any accuracy using the compounds shown in Figure 13 because of the flattened slope of the pH curve in these regions. However, in certain tissues, it is possible to introduce a nontoxic compound such as MP (pKa = 7.5) to report pH changes in the range of 8.⁵⁷ When constructing the pH vs. chemical shift plots, one must take into account the ionic strength, metal ion concentration, and interaction of other metabolites. Roberts⁵⁹ has thoroughly investigated the effects of a number of factors on the titration curves and pKas of Pi and G-6-P.

Once the ability to evaluate cellular pH was realized,¹ the method was exploited to evaluate subcellular compartmentation. The question was whether NMR would be able to provide information concerning the distribution of metabolites between the cell cytoplasm and mitochondria. Ogawa et al.⁶⁰ used the resonances of ATP, ADP, and Pi to monitor two environments (intra- and extramitochondrial) in suspensions of rat liver mitochondria. The two sets of observed Pi resonances were attributed to the difference in pH between the external and internal environments. The downfield shift of resonances corresponding to internal ATP and ADP was ascribed to their binding to divalent metal ions within the mitochondria. Metal ion binding, particularly that of magnesium, causes predictable chemical shift changes on the resonances of nucleotides such as ATP. These shifts give a direct measure of the ratio of ATP/Mg²⁺ *in vivo*.^{38,61,62} As seen in Figure 12A, the γ -, α -, and β -NTP resonances show no ³¹P-³¹P coupling, but rather are broad and featureless. This is due primarily to the intracellular Mg²⁺ ion exchange broadening which provides an efficient mechanism for rapid spin-spin relaxation ($T_2 \sim 50$ ms).

Cohen et al.⁶³ studied suspensions of hepatocytes in the presence of valinomycin and observed a split in the Pi resonance corresponding to cytoplasmic and mitochondrial pHs. The cytoplasmic Pi resonance assignment was confirmed when fructose was added to the cells and produced a fructose-6-phosphate resonance whose chemical shift corresponded to the pH given by the upfield Pi resonance.

Roberts¹³ and Kime et al.³⁸ examined the compartmentation of excised maize root tips. The resonances reported in Figure 12 corresponding to vacuolar Pi and cytoplasmic Pi have been assigned based on three criteria: (1) morphology, (2) pH, and (3) phosphorylation of glucose. In one of the first plant tissue NMR experiments, Roberts¹³ demonstrated that upper root sections containing large vacuoles exhibited ³¹P spectra in which the upfield Pi peak dominated, whereas, 1- to 2-mm root tip sections that are known to contain cells with small vacuoles gave spectra in which the lower field Pi resonance was very large. Kime et al.³⁸ showed that G-6-P generated from perfusion of maize root tips with 50 mM glucose exhibited a peak whose shift corresponded to a pH of 7.5, the same as the low-field Pi resonance. The upfield Pi had a shift corresponding to a pH of approximately 5.5, characteristic of an acidic vacuolar compartment.

The addition of 2-deoxyglucose to maize root tips can be useful as a pH marker for intracellular and metabolite compartmentation. Because of the large buildup of 2DG-6-P (see Figure 14), we can also observe the appearance of 2-deoxyglucose-1-phosphate which is not normally visible because of the high cellular ratio of G-6-P/G-1-P of approximately 19.⁶⁴ We also note that although 2DG-6-P cannot be metabolized through the normal glycolytic pathway, this compound can be incorporated via 2-deoxyglucose-1-phosphate into a new uridine derivative carrying the deoxysugars, whose chemical shifts are slightly downfield from UDPG.⁶⁵

Kime et al.³⁸ examined the excised portions of potato tissue, i.e., the pith, parenchyma, cortex, radial pith, and a collection of potato buds. The pith tissue from the center of the potato gave a ³¹P spectrum corresponding to phytic acid, whereas the parenchyma and cortex only showed a Pi resonance corresponding to an acidic vacuolar compartment. The radial pith tissue which links the central pith tissue to the potato bud gave a spectrum of phytic acid. The bud, however,

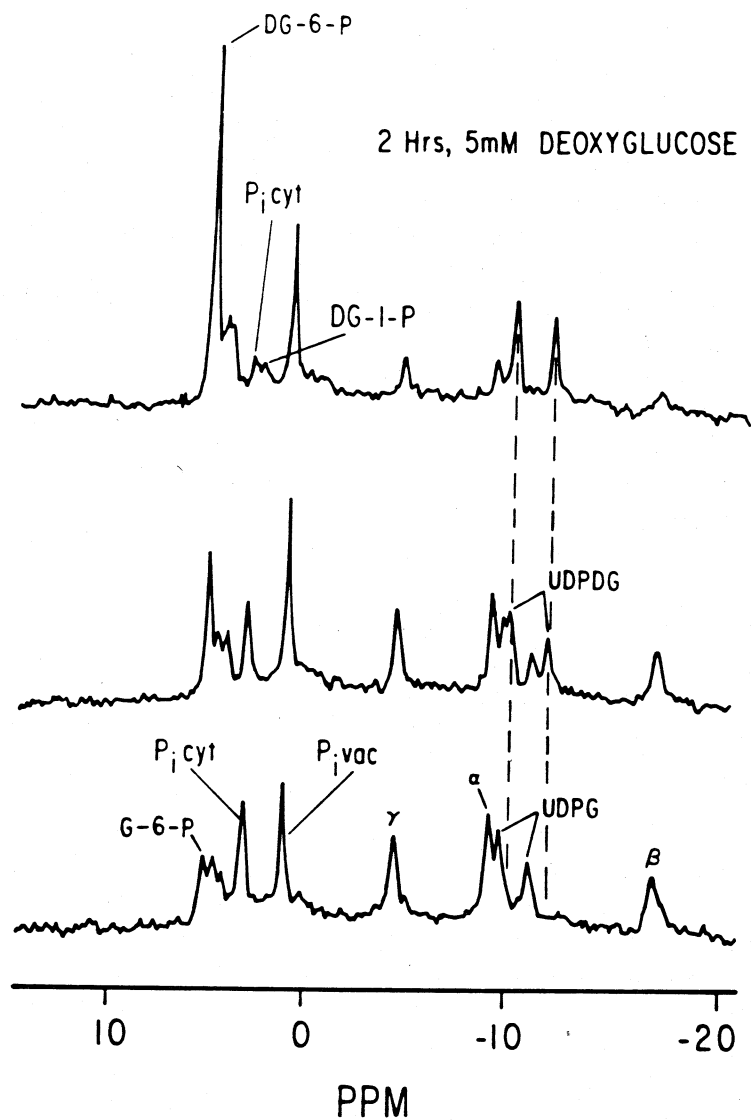


FIGURE 14. Incubation with 2-deoxyglucose 161.7-MHz ³¹P spectra of maize root tips: lower spectrum before addition of 5 mM 2-deoxyglucose; middle spectrum, following 30-min treatment with 5 mM 2-deoxyglucose; and upper spectrum, after 2-h treatment with 5 mM 2-deoxyglucose. (See Reference 65.)

displayed a typical spectrum characteristic of meristematic tissue, exhibiting a cytoplasmic and vacuolar Pi as well as monophosphate esters. Earlier reports had suggested that phytic acid was distributed uniformly throughout potato tubers.⁶⁵ This study emphasizes the fact that certain key metabolites may be compartmented within a diverse differentiated tissue. However, to establish such differentiation, one must physically separate the parts of a tissue before examining them by ³¹P NMR. If the whole tissue including the bud were examined intact, no spectral resolution or interpretation of the spectra could have been achieved. These authors³⁸ have also demonstrated in a similar experiment the differentiation and compartmentation of immobilized phytic acid in a seed, mobile, vacuolar Pi in a proximal root section, and mobile monophosphate esters and vacuolar and cytoplasmic Pi in a root tip from the same maize seedlings. This tissue differentiation is clearly illustrated in the ³¹P NMR spectra shown in Figure 15. Others have also examined the ³¹P spectra of developing turnip,⁶⁷ lettuce,⁶⁸ and cotton seeds.⁶⁹ In the spectra of the turnip and lettuce seeds, compartmented metabolites were visualized following approximately 20 h of imbibition.

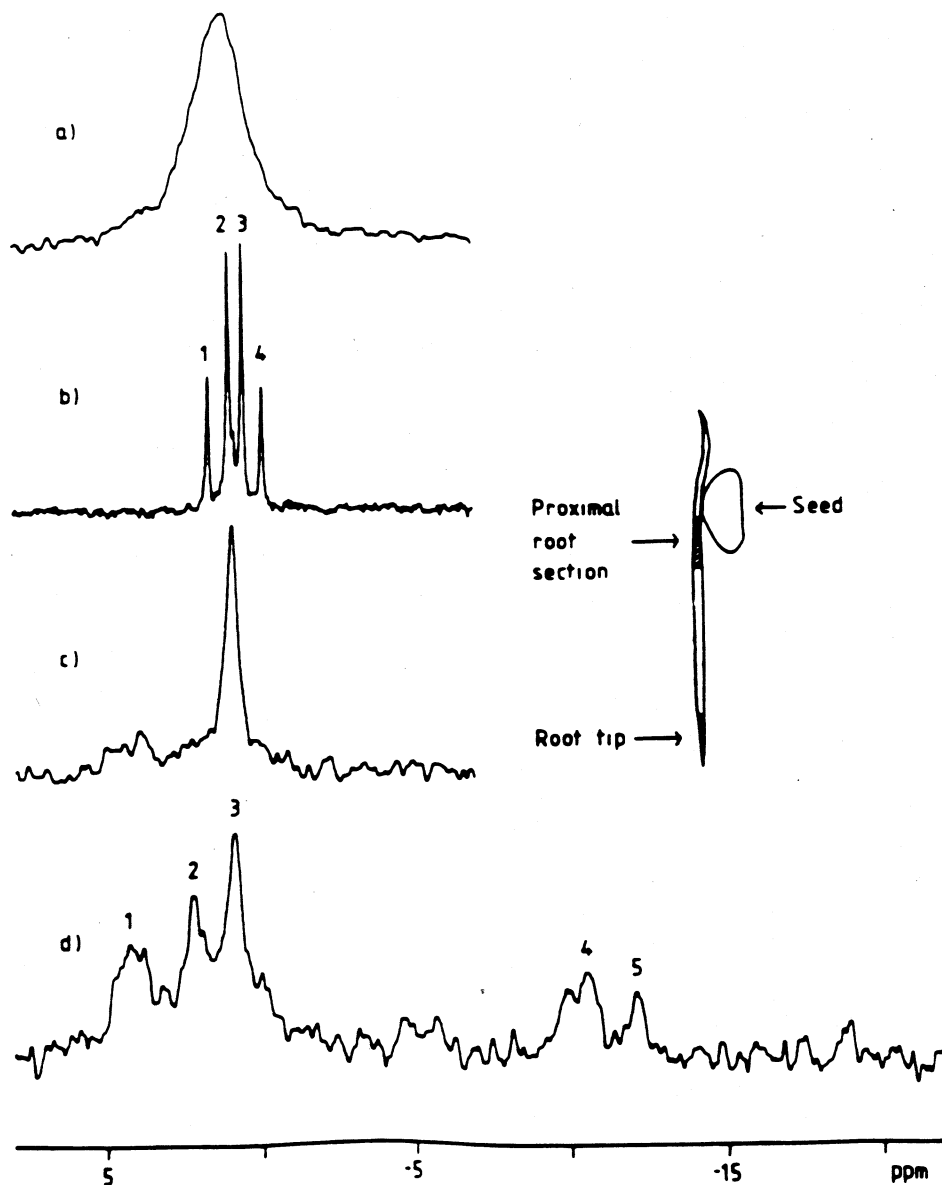


FIGURE 15. 121.49-MHz ^{31}P spectra of sections of 2-d-old maize seedlings (*Zea mays*, L. var. Aurelia): (a) 3 half seeds; (b) an aqueous extract from the same seeds at pH 5.2; (c) 100, 5.0-mm proximal section 2 s from the 4.0-cm primary roots of the Aurelia plants; and (d) 100, 3.0-mm root tips from the 4.0-cm primary roots of the Aurelia plants. The schematic diagram in the inset defines the different regions of the tissue. All the spectra are the result of 4000 scans with the slow acquisition cycle, using the coaxial 8 in 10 tube system. In the extract spectrum (b), the phytic acid resonances are labeled 1 to 4 and the small P_i resonance is visible as a shoulder to peak 2. In the root tip spectrum (d), the assignments are peak 1, monophosphate esters; peak 2, cytoplasmic P_i ; peak 3, vacuolar P_i ; and peaks 4 and 5, UDPG. (From Kime, M. J., Ratcliffe, R. G., and Williams, R. J. P., *J. Exp. Bot.*, 33, 656, 1982. With permission.)

^{31}P studies of dormant *Artemia* embryo spores showed that, as these spores develop following perfusion with O_2 , their interior changed from pH 6.3 to 7.9 as reported by their P_i shift.⁷⁰ Moreover, nucleotide resonances appeared and an additional P_i resonance was seen and tentatively identified as a nonviable fraction of the cysts (~35%). This rather large and reversible shift in interior pH is very remarkable; however, the source of the proton equivalents generated during the induction of anaerobic dormancy of these spores is unknown.

Many workers have attempted to evaluate the effect of external environment on intracellular

pH in different plant tissues and cells. An early study⁷¹ of the temperature dependence of the cytoplasm of maize root tips indicated that the pH of the cytoplasm dropped approximately 0.5 pH units when the temperature was raised from 4 to 28°C. The poor quality of these spectra due possibly to the bubbling of air without perfusion make it unclear whether the upfield shift (acidification) of the cytoplasmic Pi resonance was due to mild hypoxia rather than a temperature-dependent pH change associated with an alteration in metabolism. Agents such as K₂SO₄ which induce the extrusion of four to five microequivalents of H⁺ per gram per hour from maize root tips do not produce any measurable change in the cytoplasmic or vacuolar pH.⁷² However, hypoxia, a subject that will be covered in Chapter 2, does cause a significant acidification of the cytoplasm. Dilute NH₄OH, on the other hand, induced a pH rise in the vacuolar compartment more rapidly and to a greater extent than the cytoplasm. This difference is presumed to be due to tighter pH regulation in the cytoplasm than in the vacuole, or possibly may be attributed to the fact that the vacuole is a better, more acidic trap for NH₄OH. That the cytoplasm was found to return more rapidly to the initial pH after treatment suggests that the former explanation is correct. This study points to the fact that cytoplasmic and vacuolar pHs are regulated for the most part by separate mechanisms in meristematic cells. Reid et al.⁷³ measured the cytoplasmic pH change caused by sodium azide treatment and anaerobiosis of maize root tips. Their findings suggest that when respiration was inhibited by azide, H⁺ influx was the dominant effect in the acidification of the cytoplasm, whereas during anoxia, lactate formation was the main source of protons. Butyrate at a concentration of 1 mM had no effect but fusicoicin caused a 0.1 to 0.2 pH rise in barley root tips.⁷⁴ The effects of external acidity have been examined in both maize root tips¹⁴ and barley shoot tissue⁷⁵ to simulate the effects of acid soil and acid rain, respectively, on intracellular pH, metabolism, and growth. While excised maize root tips show almost no change in cytoplasmic or vacuolar pH, as revealed by the pH-dependent Pi signal after perfusion at pH 4.0 for 20 h, barley shoot tissue exhibited a small measurable pH lowering of vacuolar pH following 2 d of spraying with acidic (pH 3 to 4) solutions. Although no growth reduction was noted in the barley tissue, the changes in vacuolar pH and plastidic sulfate content may have an energetic cost to the plant that could translate into reductions in growth.⁷⁵

At high concentrations ($5 \times 10^{-4} M$) and pH 6.0, 2,4-dinitrophenol (DNP) caused a loss of the pH gradient across the tonoplast of maize root tips.³⁸ Membrane integrity was restored, however, following continuous washing of the tissue. In contrast, at $1 \times 10^{-5} M$ and pH 5 or 7, no ATP uncoupling or loss of tonoplast gradient was observed in barley root tips.⁷⁶ These workers⁷⁶ indicate that the collapse of the pH tonoplast gradient and loss of ATP previously reported³⁸ for maize root tips was caused by a large increase in permeability resulting from the high concentration of protonated DNP ($5 \mu M$ at pH 6) and was not a result of uncoupling per se. Treatment of maize root tips with uncoupler carbonyl cyanide p-trifluoro-methoxy-phenylhydrazone (FCCP) at $10^{-5} M$ in 2% DMSO₄ (used for solubilization) caused a full collapse of the tonoplast gradient as well as the plasmalemma within $3 \frac{1}{2}$ h (see Figure 16). This effect could not be reversed by tissue washing (unpublished results). Similar results have been reported for *Acer pseudoplatanus* cells.²⁷ Intracellular pH and K⁺ ion concentration have been evaluated in mung bean roots following treatment with Ca²⁺ ionophores.⁷⁷ These experiments demonstrated that the Ca²⁺ ionophore A23187 increased [K⁺] and decreased cytoplasmic pH from 7.2 to 6.6 (pH 6.6 is near the optimum pH for K⁺-ATPase). This activation of K⁺ uptake by Ca²⁺ makes a convincing argument that Ca²⁺ enhances the K⁺-ATPase activity through acidification of the cytoplasm.

Martin and co-workers²⁷ have made a thorough evaluation of different factors (e.g., O₂, hypoxia, anoxia, Mn²⁺, PO₄²⁻ content, temperature, and FCCP) affecting the viability and ³¹P NMR spectra of three varieties of cultured plant cells (*A. pseudoplatanus*, *Catharanthus roseus*, and *Glycine max*), in an unperfused state. This paper is an excellent introduction into the use of *in vivo* ³¹P NMR with cultured plant cells. Following this work Hughes et al.⁷⁸ reported an

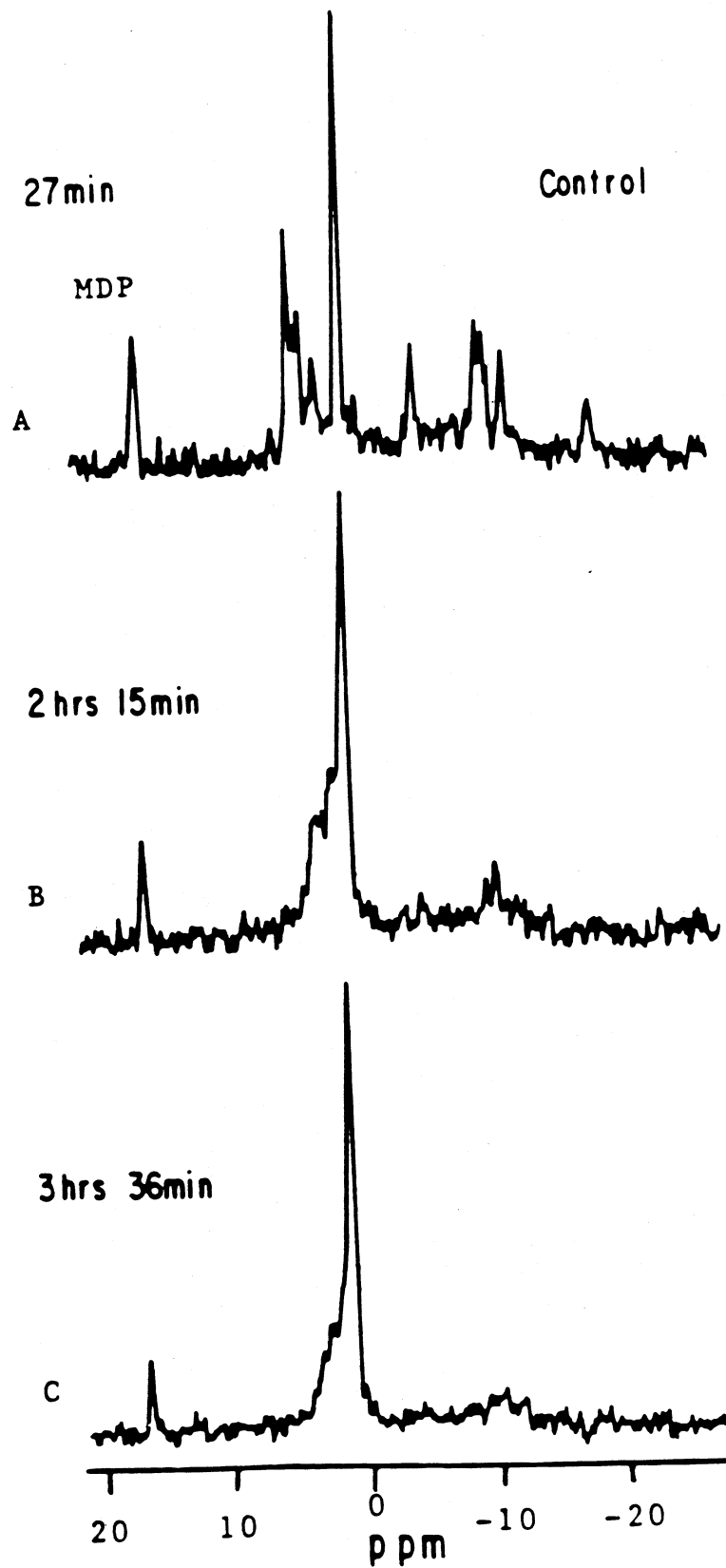


FIGURE 16. Uncoupling and loss of pH gradient. 161.7-MHz ^{31}P spectra of maize root tips (A) prior to treatment and (B) after 2 h, 15 min of treatment with 10^{-4} M FCCP and 2% DMSO in the circulating perfusion system saturated with O_2 . (C) same as B after 3 h, 36 min.

improved method for obtaining extraordinarily good ^{31}P spectra of cell suspensions of *Elaeis guineensis* during perfusion. This paper demonstrates that the spectra can be utilized to probe the action of the uncoupling behavior of the auxin analogue, 2,4-dichlorophenoxy acetic acid (2,4-D). The effects of acid loading and cytoplasmic pH regulation in *A. pseudoplatanus* have been evaluated by Guern et al.⁷⁹ Acid loading of cultured plant cells stimulates the plasmalemma proton pump and can be used to study the relationship between cytoplasmic pH and growth. Their findings show that cultured cells can regulate their cytoplasmic pH during acid loading and, on the alkaline side, after removal of acid. That there is a strong pH regulatory mechanism in plant cells is indicated by the rapid recovery of the cytoplasmic pH.⁷⁹ ^{31}P studies of *Phaseolus vulgaris* cells under nonperfusion conditions (oxygen bubbling only) have demonstrated four changes following the addition of the elicitor phaseollin.⁸⁰ These are decreases in the vacuolar pH, cytoplasmic pH, ATP, and cytoplasmic Pi. Although the authors claim to observe a drop in vacuolar pH from 5.3 to 4.8, a change possibly associated with a metabolic process leading to phytoalexin formation, it seems doubtful that such a small pH drop could be accurately noted from the Pi shift in this acidic environment.⁸⁰ In addition, the loss of ATP, which was not found to be equated with any increase in Pi, was attributed to its utilization by the cells in phosphorylation reactions required for the synthesis of mRNA, which is NMR invisible. The slow recovery of the cell suspension to its original metabolic state took 48 h, indicating that enzyme degradation of the elicitor was complete after this time period.

Other kinds of plant materials that have been examined by ^{31}P NMR include an intact stem segment from sunflower⁸¹ and pollen grains from flower buds of tobacco.⁸¹ Spectra of these tissues exhibit evidence of cytoplasmic and vacuolar compartmentation. In addition, the spectrum of the pollen grain extract showed a large quantity of a phosphodiester, tentatively identified as glycerophosphorylcholine (GPC). GPC as well as glycerophosphorylethanolamine has also been recently reported in rice shoots.⁸² These metabolites are both presumed to be present in the cytoplasm but only the GPC is modulated by the environmental oxygen level, i.e., GPC is produced in large quantities over long periods of anoxia. The authors hypothesized that GPC is produced to maintain cell membrane functionally under environmental stress, since GPC is a known inhibitor of lysolecithinase.

2. Saturation Transfer

By simply measuring the equilibrium levels of metabolites, e.g., NTP from the ^{31}P NMR spectrum of different tissues under a variety of stressing conditions, we cannot assess whether the rate of synthesis of NTP is increasing, decreasing, or remaining unchanged. We cannot assess the real change in these metabolite concentrations because the concentration of nucleotides and products of nucleotide breakdown do not bear a simple relationship to variations in the rate of nucleotide turnover.⁸³ To gain insight into true rates of production or consumption of a nucleotide such as ATP, one must be able to evaluate the rate constant for ATP interconversion. Saturation transfer is an NMR technique whereby low-power rf field saturation of a spin on a nucleus will transmit that saturation to any other nucleus with which it is exchanging. The rate of appearance of the nonequilibrium spin magnetization of the second resonance is monitored to determine the reaction rate. In order to measure these unidirectional reaction rates, the system must be in a steady state; the exchanging partners, e.g., γ -ATP and Pi must have separate and detectable NMR signals and the rate constants for both the forward and reverse reactions must be of the magnitude of the spin-lattice relaxation rate of each of the exchanging nuclei. In general, processes that are occurring with rate constants of roughly 10 s^{-2} to 10 s^{-1} may be probed by saturation transfer. A review covering the application of saturation transfer to the *in vivo* study of animal tissues and microorganisms has recently been published.⁸⁴ Using oxygen tension measurements in conjunction with saturation transfer experiments, Roberts and co-workers⁸⁵ have demonstrated that the P/O ratio, which is 3 in normal metabolizing root tips drops to 2 when succinate is substituted for glucose. This observation indicates that a secondary pathway in the

electron transport system has been activated in which FADH_2 is the principal electron donor. Addition of cyanide with succinate suppresses the rate of ATP synthesis completely while cyanide and glucose still gave a P/O ratio of 1. These results indicated that this plant tissue contains a cyanide-resistant respiration pathway in which electrons travel to a terminal oxidase from a point between the first and second-coupling sites of the mitochondrial electron transfer chain and, therefore, only the first coupling site of the electron transfer chain is used.

Although comparable experiments have not been reported in agricultural systems, *in vivo* unidirectional fluxes between creatin phosphate and γ -ATP have been determined by an alternate two-dimensional exchange experiment (2D-NOESY) in the head and leg of an anesthetized rat.²⁵ The 2D-NOESY experiment monitored an exchange process by taking advantage of a transient frequency label that is imposed on each of the exchanging species, e.g., ATP and creatin phosphate during some specific mixing time. The resulting two-dimensional spectrum is then plotted along two frequency axes, F_1 and F_2 . F_1 is the precessional frequency of the nucleus before mixing with the second nucleus and F_2 is the frequency obtained following the mixing time. Nuclei that have not undergone exchange during the mixing time should show resonance signals only along the diagonal since they have the same precessional frequency in F_1 and F_2 . Those nuclei that have undergone exchange will have two different frequencies, one on the diagonal corresponding to F_1 and a new position in F_2 corresponding to a change in chemical shift due to the dipolar interaction with the second nucleus during the mixing time. These second peaks representing the interaction frequencies are visualized as cross or off-diagonal peaks as illustrated in Figure 17. The unidirectional flux of creatin phosphate to γ -ATP was found to be $13 \mu\text{mol/s/gwt}$ (gram-weight) in the leg and $2 \mu\text{mol/s/gwt}$ in the head of the rat. These values are in good agreement with the standard saturation transfer measurements.⁸⁶ No unidirectional flux between γ -ATP and Pi was noted because it was assumed to be too slow ($<0.1 \mu\text{mol/s/gwt}$) to measure.²⁵ Some discrepancy exists between these results and those reported for the saturation transfer experiment,⁸⁶ since magnetization transfer was observed between γ -ATP and Pi in the latter. The authors suggest that the disparity in the results could come from the fact that some of the "bound" substrate pools which exchange with the observed free pools may have been saturated in the saturation transfer experiment.

3. Phosphate Uptake and Compartmentation

As mentioned earlier, phosphate is a key nutrient that is involved in a variety of life functions, which include muscle contraction in mammalian tissue,⁸ regulation of glycogen⁸⁷ and starch breakdown in animal and plant cells,⁵⁴ glycolysis,⁵¹ and mitochondrial function.⁸⁸ Thus, in order to understand these regulatory functions we must understand (1) how phosphate is distributed in the cell, (2) in what form is it stored, and (3) how Pi uptake and distribution in the cell is affected by different stresses.

Pi uptake has been extensively studied by ^{31}P NMR in various plant tissues, cells, and microorganisms. Kime et al.³⁸ carried out the first ^{31}P NMR experiments on aged potato parenchyma tissue that demonstrated uptake of Pi into the vacuole compartment. Pea root tips, under aerobic conditions show the same selective accumulation of Pi in the vacuole.⁴⁰ By measuring the relative areas of the vacuole and cytoplasmic Pi resonances under quantitative conditions, these workers were able to establish the ratio of Pi in the two compartments. Following the wet chemical determination of total Pi per unit fresh weight and an estimation of the size of the cytoplasmic and vacuolar volumes, the actual concentrations of vacuolar and cytoplasmic Pi were calculated. Vacuolar Pi concentration varied significantly as a function of the concentration of Pi supplied, yet the cytoplasmic Pi concentration remained remarkably constant over the entire range of Pi nutrition. The cytoplasmic Pi concentration was estimated to be approximately 18 mM while the vacuolar Pi concentration varied from 3 to 14 mM .⁴⁰ These studies assumed any Pi which could be taken up in the mitochondria would only represent approximately 6% of the total Pi in the cytoplasm and, therefore, not contribute to any serious

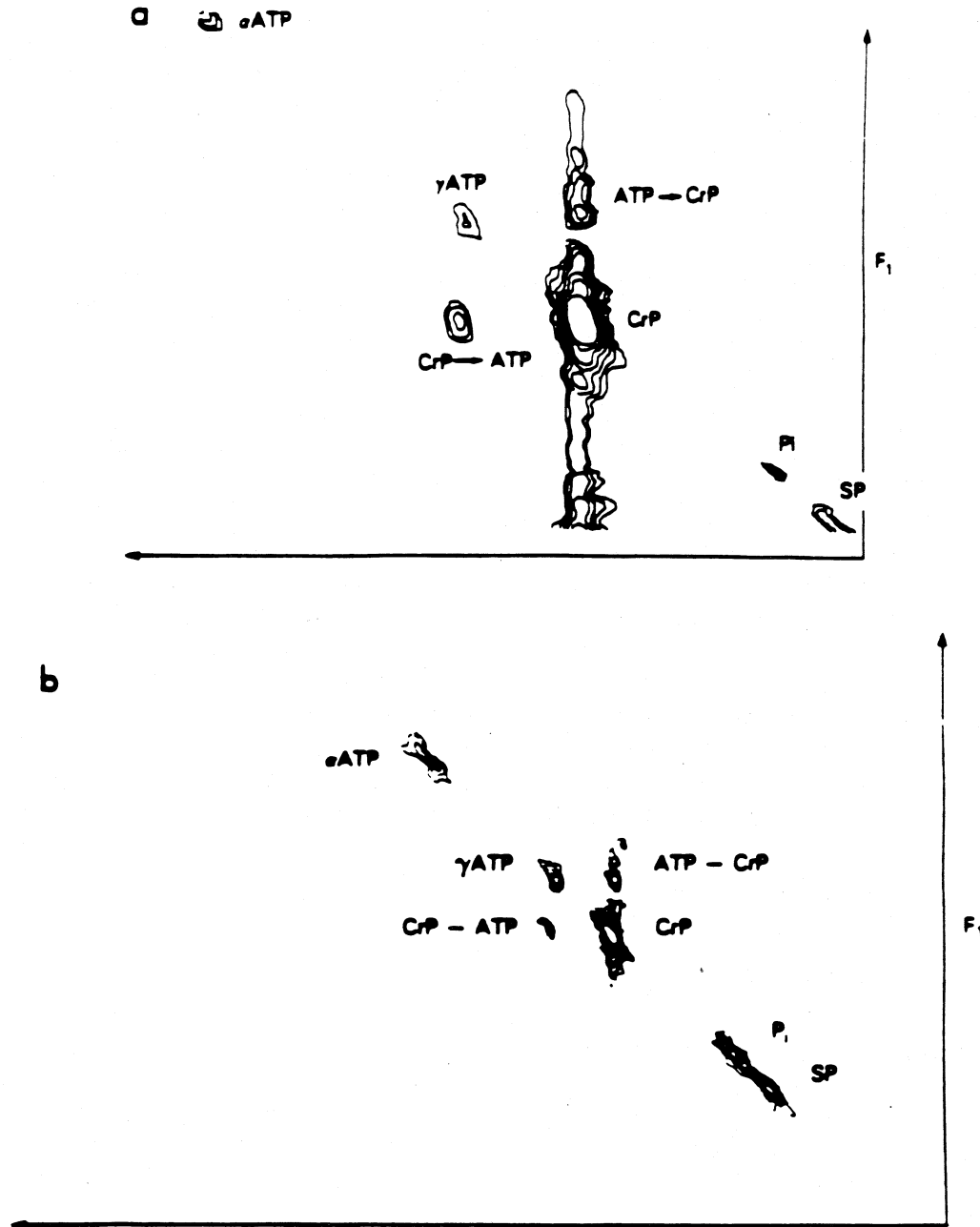


FIGURE 17. Two-dimensional contour plots of the (a) rat leg and (b) head. Diagonal peaks represent chemical species which have not undergone exchange. The lack of symmetry in the cross-peaks is caused by the added noise in the F_1 axis produced by pulse synchronization distortion. Contour *a* was collected with a t_{mix} of 0.6 s without quadrature detection with 16 scans per spectrum, and a sweep width of 2000 Hz. Contour *b* was with a t_{mix} of 0.4 s with 32 scans per spectrum with a 4000-Hz sweep width. (From Balaban, R. S., Kantor, H. L., and Ferretti, J. A., *Biol. Chem.*, 21, 12787, 1983. With permission.)

error in these calculations.⁴⁰ Rebeillé et al.⁵⁵ carried out a similar study of P_i uptake in *A. pseudoplatanus* cells and obtained comparable results as far as relative uptake of P_i in the vacuole and cytoplasm was concerned. When the cells were starved of P_i , the intracellular P_i concentration fell from 3 to 0.1 mM and the concentration of phosphate esters dropped from 8 to 2 mM. However, following starvation, uptake of P_i was stimulated, indicating that P_i uptake depends on the intracellular P_i and/or cytoplasmic ester-phosphate pool. These data suggested that P_i and/or ester-phosphates might act as modifiers of the transport system to alter its affinity

or as a competitive inhibitor. Low extracellular pH fostered the uptake of Pi which the authors attribute to an H⁺ symport mechanism. Further studies⁸⁹ of this system under sucrose starvation showed a slow down in metabolism, as evidenced by lowered NTP levels and a replacement of sucrose breakdown with starch hydrolysis. During this time the intracellular Pi concentration increased and ³¹P NMR indicated that the majority of Pi was accumulated in the vacuole. Introduction of sucrose, following starvation led to the disappearance of the cytoplasmic Pi resonance and a significant increase in the G-6-P resonance.⁹⁰ However, the vacuolar Pi concentration was not depleted to replace the utilized cytoplasmic Pi. During sucrose deprivation a resonance corresponding to the choline phosphate (P-choline) was noted. These authors suggest that this compound is a good marker for membrane breakdown under stressing conditions.^{90,91} Subsequently, Brodelius and Vogel⁹² studied the Pi uptake and storage of *C. roseus* and *Daucus carota* cells in a perfused state. These workers noted that in *C. roseus* Pi was the first stored in the vacuoles. One part of this pool was subsequently used to maintain a constant cytoplasmic Pi level, while loss of additional Pi signal was attributed to the accumulation of Pi in an NMR-invisible state (immobile or bound state) in another cell organelle. *D. carota* did not accumulate Pi in its vacuoles and took up Pi from the medium only as it was required during growth.⁹¹ Yeast (*Candida utilis*) vacuolar-stored Pi as well as polyphosphates (PPs) were mobilized to replenish cytoplasmic Pi when glucose was metabolized.⁹³ Following glucose depletion, resynthesis of vacuolar PP takes place under aerobic conditions. However, under anaerobic conditions these yeast continue to hydrolyze PP.⁹³ This hydrolysis is probably due to the lower level of ATP present during this time. Figure 18 shows the sequence of events following glucose addition relating to PP breakdown, movement of vacuolar Pi to the cytoplasm, synthesis of sugar phosphates, and resynthesis of vacuolar PP following depletion of glucose under aerobic conditions. When ethanol was used as a substitute, only PP synthesis was noted. These results suggest that PP may have a dual role as a store of Pi as well as an energy source.⁹³ Nitrogen-starved yeast cells (*Saccharomyces cerevisiae*) respond to treatment with ammonium salts at pH 8.0 with a rapid hydrolysis of intravacuolar PP to tripolyphosphate (TPP) and Pi, followed by movement of the Pi to the cytoplasm.⁹⁴ This sequential process could be examined by ³¹P NMR since the intermediate PP breakdown products, i.e., TPPs and tetrapolyphosphates, and the decrease in the ratio of the central to terminal phosphate resonances could be observed throughout the time course of treatment. The authors⁹⁴ hypothesize that the ammonium-initiated PP breakdown provides another mechanism of maintaining pH homeostasis in the vacuoles of energy-depleted cells when they are stressed with a highly basic metabolite. A fungal pathogen *C. albicans* was examined in its transition from yeast-form cells to germ tubes and hyphae by ³¹P NMR.⁹⁵ In the exponentially growing yeast-form cells, the PP resonance was high but progressively declined in the stationary phase and became very low and finally undetectable in the germ tube and hyphae stages, respectively. At the same time, cytoplasmic Pi grew in intensity. Thus, PP appears to accumulate early during growth and is disposed of when the organism shows its growth due to limitations of its carbon source. When the organism was grown with a surplus of phosphate, both the PP and vacuolar Pi signals increased in intensity relative to the cytoplasmic Pi signal, indicating that there is probably a metabolic interchange between PP and free Pi in the vacuole,⁹⁵ similar to that mentioned above.⁹³ Maize root tips exposed to high concentrations of NaCl (100 mM) took up twice as much Pi from a 10-mM KH₂PO₄ solution.⁹⁶ This stimulated uptake of Pi was associated with an increase in the concentration of cytoplasmic Pi. Following the Pi uptake, Pi was transferred to the vacuole. The NaCl appeared to increase the permeability of the plasmalemma to Pi, which resulted in a large influx of Pi from the external solution. In contrast, the movement of Pi from the cytoplasm to the vacuole depended on the ratio of Pi to total phosphate (Pi + G-6-P + NTP + UDPG) in the cytoplasm.

Ben-Hayyim and Navon⁹⁷ examined the uptake of Pi under salt stress for wild-type and NaCl-tolerant citrus cultured cells. The wild type was found to accumulate higher amounts of Pi than the NaCl-tolerant variety when exposed to equal external concentrations of Pi. As observed in

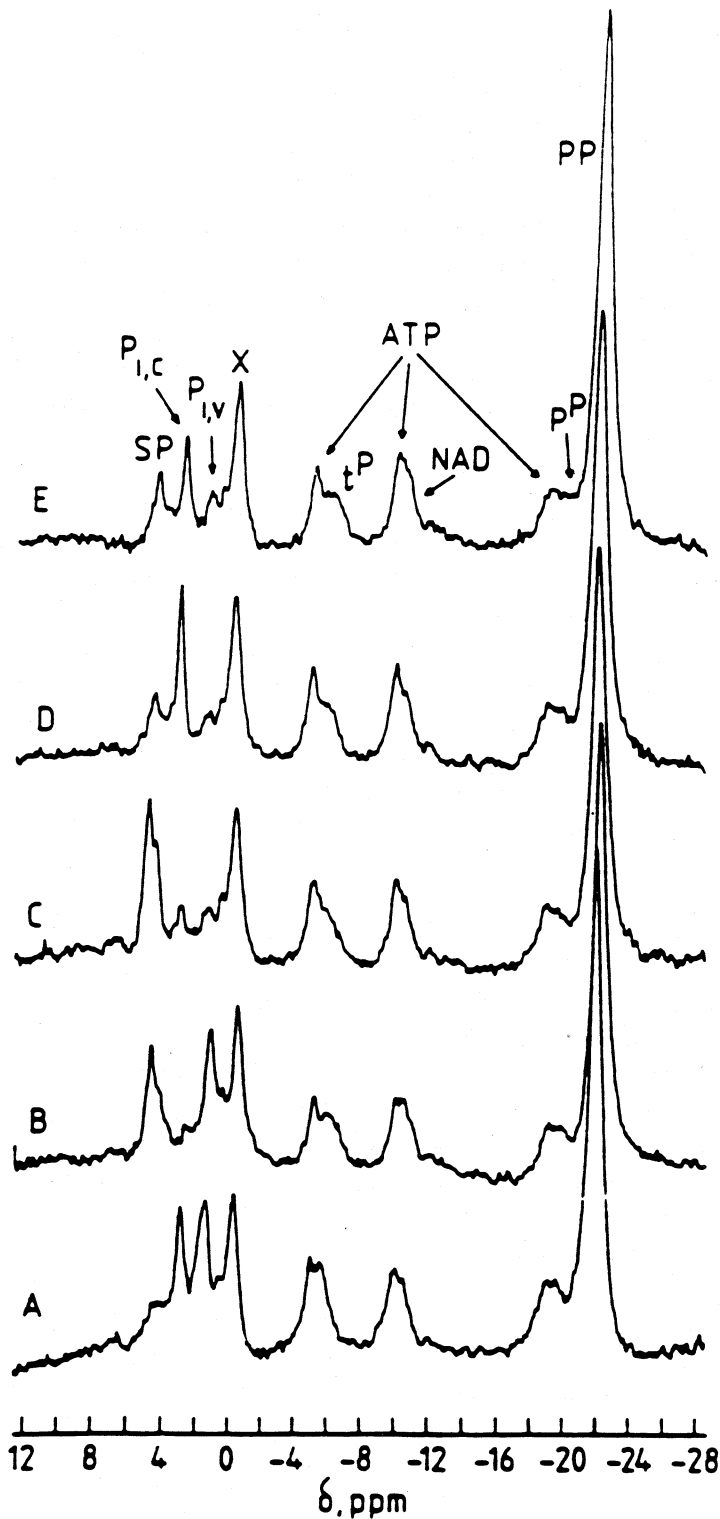


FIGURE 18. A to E. ^{31}P NMR spectra of an aerobic suspension of *C. utilis*. The temperature of the sample was maintained at 8°C . Each spectrum represents the sum of 2 consecutive blocks of 250 scans. A spectrum accumulated immediately before introduction of 100 mM glucose into the cell suspension; B, C, D, and E spectra taken 1.4, 22.7, 68.0, and 99.2 min after glucose addition, respectively. Assignments are SP, sugar phosphates; $\text{P}_{1,c}$, cytoplasmic P_i ; $\text{P}_{1,v}$, vacuolar P_i ; X, unassigned; ATP, adenosine triphosphate; NAD, nicotinamide adenine dinucleotides (reduced plus oxidized); and t^{P} , P^{P} , and PP , terminal, penultimate, and middle phosphate groups of polyphosphates, respectively. Resonance t^{P} includes inorganic pyrophosphate. (From Nicolay, K., Scheffers, W. A., Bruinenberg, P. M., and Kaptein, R., *Arch. Microbiol.*, 134, 270, 1983. With permission.)

the previous study,⁹⁶ the additional Pi finally moved to the vacuole. The cytoplasmic Pi concentration reached saturation at a relatively low external Pi concentration whereas the vacuolar Pi showed an increase many times its original.

4. Metal Ion Transport and Compartmentation

Both soil acidity and its effects on the liberation of toxic metals such as Al, Mn, and Cd can produce adverse conditions for the growth and production of plants.⁹⁸ Although much work has gone into the development of new strains of metal-tolerant plants to combat such problems, little is known concerning the physiological mechanisms responsible for stress tolerance or susceptibility in plants.⁹⁹

Low pH (<4.5) conditions in the soil can perturb the overall functioning of a plant and its ability to assimilate adequate levels of organic and inorganic nutrients. However, the exact effect of hydrogen ion concentrations on this phenomenon is often difficult to determine because of the occurrence of solubilized forms of toxic metals that are present under these conditions.⁹⁸ With regard to the plant root system, it is thought that acid conditions are responsible for greater membrane permeability,⁹⁸ impaired cation transport,¹⁰⁰ metal displacement, and inhibition of metal uptake.¹⁰¹ A paper reviewing general ion absorption studies in maize and potato tissue with ³¹P NMR has recently appeared.¹⁰²

Al³⁺ is among the most studied metals in terms of its toxic effects on plant function.⁹⁸ The specific action of this metal has been attributed to interactions with nucleotides, nucleic acids, and membrane lipids, as well as important calcium-regulating ATPase and phosphorylating enzymes.¹⁰³

Another metal which poses a problem for plant development and production is divalent manganese. In general, Mn²⁺ is not as toxic to such a wide variety of plants as Al³⁺, yet its ease of transport across the cell membrane is well known.⁹⁸ In some instances healthy roots have been shown to reduce Mn²⁺ toxicity by precipitating oxidized Mn²⁺ as MnO₂ on root surfaces.⁹⁸ Plants such as maize, however, may avoid Mn²⁺ toxicity by entrapment of relatively high concentrations of the metal in nonmetabolic centers such as the vacuole.¹⁰⁴

Although many of the biologically important metals have isotopes that are directly detectable by NMR, often they have too low a natural abundance level, are paramagnetic, quadrupolar, and/or are too low in concentration in the biological system to be observed. A way around this problem is to examine the indirect consequences of a particular invading metal ion on the metabolism, bioenergetics, intracellular pH, and, when the metal ion is paramagnetic, the line broadening of metabolite resonances associated with the metal ion following its entry into the cell.

Prior to characterizing the effects of mobile metal ions in acid soils on the function of maize root tissue, Pfeffer et al.^{14,16} studied the role of the acid environment on the viability of these cells. The presence of an acid medium on excised maize root tips after 20 h of perfusion fostered the production of significant amounts of excess (>75% over the initial amount) mobile Pi residing in the vacuole (see Figure 19). Based on a quantitative treatment of the ³¹P NMR data and calculated resonance response factors for each hydrolyzable metabolite, we concluded that the excess phosphate was not generated from mobile metabolites.¹⁶ The significant increase of the choline phosphate resonance at approximately 4.0 ppm gave a strong indication that membrane breakdown was responsible for the additional phosphorus signal^{90,91} (see Figure 19B). In contrast, treatment of the same tissue at pH 4.0 with 0.5 mM Al³⁺ for 20 h resulted in a loss of 50% of Pi content of the cells (Figure 20) with little effect on the nucleotide levels. This Pi loss was principally attributed to cell wall precipitation of Al₂(PO₄)₃ and acid phosphatase inhibition by Al³⁺.¹⁶ The presence of Ca²⁺ did not suppress the effects of Al³⁺ and when used alone Ca²⁺ also showed a similar but less intense modulation of Pi generation. Over a growing period these effects could be manifested in phosphate deficiency resulting in diminished plant production.

Under conditions of lowered metabolism induced by the deprivation of a carbohydrate source

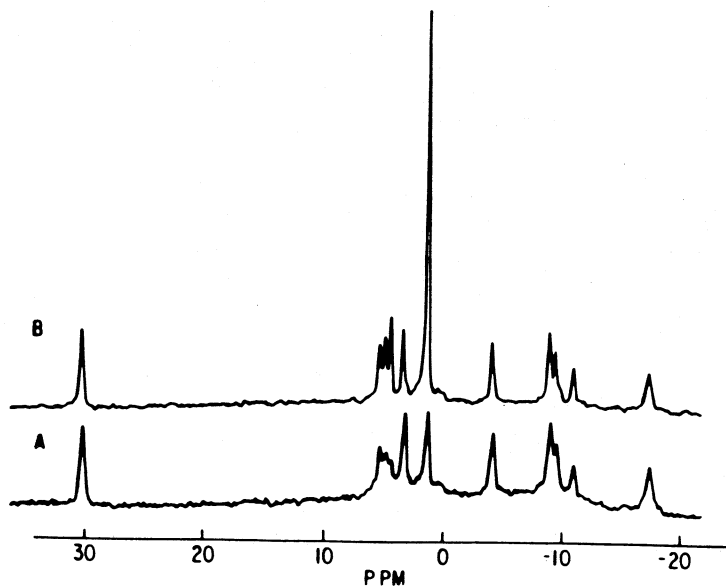


FIGURE 19. (A) 161.7-MHz ^{31}P spectrum of approximately 900 excised root tips (5 to 7 min) taken under the fast acquisition conditions following 2 h in the NMR perfusion system. pH = 4.0, 0.1 mM CaSO_4 , 50 mM glucose, 4000 transients. (B) Same as (A) after 20 h of perfusion. (See Reference 14.)

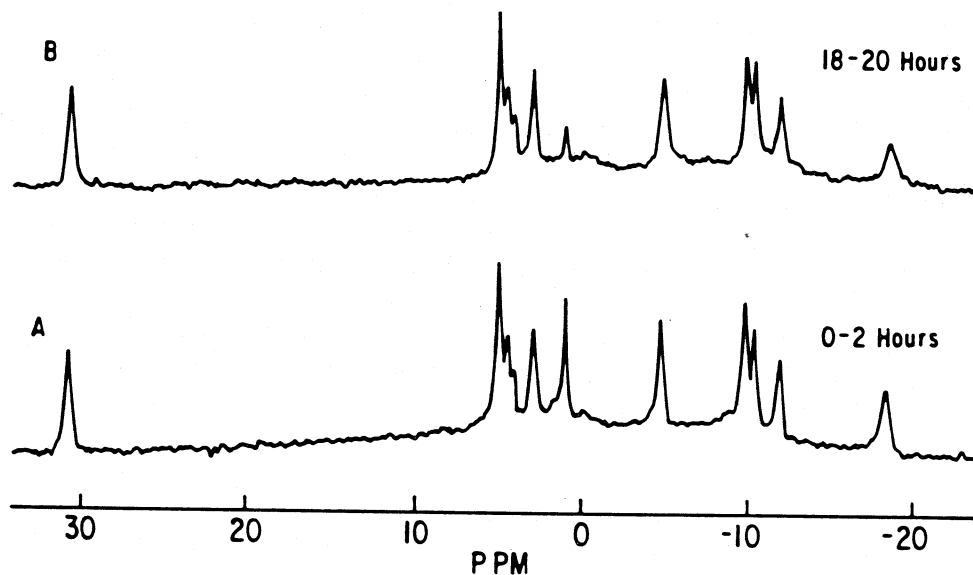


FIGURE 20. 161.7-MHz ^{31}P spectra of 3-d-old, 3 to 5 mm corn root tips perfused with a solution containing 50 mM glucose, 0.1 mM CaSO_4 , and 2.5 mM $\text{Al}_2(\text{SO}_4)_3$, pH 4.0 for (A) 0 to 2 h and (B) 18 to 20 h. (See Reference 16.)

(glucose). the maize root tips underwent a drop in respiration and a drop in nucleotide levels when challenged with Al^{3+} . A similar loss of nucleotides and membrane integrity was noted in the ^{31}P spectrum of aluminum-treated tips under hypoxia.¹⁶ Thus, cells already under a metabolic stress such as carbohydrate deficiency or hypoxia are much less able to maintain their energetic status to exclude toxic metal ions such as Al^{3+} .

Mn^{2+} is a useful paramagnetic metal ion for exploring metal interactions with NMR-active nuclei.¹⁰⁵ The presence of manganese in a cellular compartment is noted by the occurrence of broadened resonances (resulting from shortened T_1 and T_2 relaxation times) associated with the

ites of metal binding. Several groups^{14,65,105} have examined the sequential movement of Mn^{2+} into maize root tips by ^{31}P NMR to assess its metabolic fate. Under aerobic conditions, a slow entry of the metal ion into the cytoplasm was observed as evidenced by the gradual broadening of the cytoplasmic nucleotides and Pi resonances (Figure 21). Both the UDPG and phosphate monoesters were only broadened slightly because of their lower binding constant for Mn^{2+} , whereas NTP, which has a strong binding constant for Mn^{2+} , underwent extreme resonance broadening within 81 min. Final entry of Mn^{2+} into the vacuole compartment was verified by complete broadening of the vacuolar Pi resonance after 135 min. Following a thorough washing of the tissue with Mn^{2+} -free buffer, we observed that the vacuolar Pi resonance could not be regenerated,^{14,65,106} whereas the cytoplasmic resonances were restored. Thus, Mn^{2+} was irreversibly trapped in the vacuolar compartment. Omission of glucose from the perfusion medium slowed the migration of Mn^{2+} into the vacuole, while rapid movement into the cytoplasm was still evident. A complete inhibition of the glycolytic pathway by incubation of the tissue with 5 mM 2-deoxyglucose depleted the cells of cytoplasmic Pi and nucleotides⁶⁵ (Figure 14). Subsequent treatment with Mn^{2+} followed by washing of the tissue showed the full restoration of the vacuole Pi resonance, indicating that Mn^{2+} had not traversed the tonoplast.⁶⁵

During hypoxia, maize root tips can be sustained by an anaerobic metabolism with much reduced levels of NTP.¹⁰⁷ In this state, Mn^{2+} was slowly taken up in the cytoplasm in trace quantities; however, following a washing of the tissue with Mn^{2+} -free buffer, no sequestering of the metal was noted in the vacuole^{14,65} (see Figure 22). A full description of the proposed mechanism responsible for the metal ion entrapment under aerobic conditions and nontransport under hypoxia are given in this report.⁶⁵ Ca^{2+} is known to protect plants from the invasion of toxic metals; however, whether this is a direct consequence of Ca^{2+} competing more favorably than other metal ions for movement across the plasmalemma is unknown. In competitive experiments with 10:1 Ca^{2+} : Mn^{2+} , it was demonstrated that a much-diminished level of Mn^{2+} buildup in the cytoplasm was observed while only minimal vacuole sequestering was noted.⁶⁵ Cd^{2+} toxicity, as observed by interference in the metabolic functioning of intact heart cells, by ^{31}P NMR has been reported by Kopp et al.¹⁰⁸ A similar effect has also been observed in plant tissues.⁶⁵ Ca^{2+} can effectively compete with toxic Cd^{2+} entry into these cells. Figure 23A and B show the ^{31}P spectra depicting the effect of 1 mM Cd^{2+} /0.1 mM Ca^{2+} on the metabolism of corn root tips following 3 1/2 h of perfusion. Note the rapid loss of cytoplasmic Pi and drop of the cytoplasmic pH from 7.6 to 7.0. In contrast, treatment of the tissue with a perfusate containing 10 mM Ca^{2+} /1 mM Cd^{2+} showed only marginal cytoplasmic "poisoning" after 3 1/2 h of perfusion (see Figure 23C and D).

The data obtained in these studies demonstrated that the uptake of metal ions (e.g., Mn^{2+}) in maize root tips is regulated by the energetic status (O_2 + exogenous glucose > O_2 > O_2 + 2-deoxyglucose > N_2 + glucose). Furthermore, different divalent cations may compete for the same root tip membrane transport apparatus. Based on the accepted general concepts¹⁰⁹ of ion transport developed mainly from research in nonplant systems, a detailed mechanism was proposed by the authors to account for the observations of these studies.⁶⁵

Subsequent work describing a comparative study of facilitated transport of Mn^{2+} in *A. pseudoplatanus* (sycamore cells) and excised maize root tips by ^{31}P NMR has uncovered an important difference between the dicotyledon and monocotyledon cells, respectively.¹¹⁰ Although passage of Mn^{2+} across the tonoplast of both sycamore cells and maize root tip cells was comparable, the entry through the plasmalemma was found to be much faster in the root tips. The slower movement across the sycamore cell plasmalemma was attributed to the occurrence of a high content of acidic polysaccharides in the cell walls of sycamore cells relative to the cell walls of root tissue. In the former, the high protonation of a plasma membrane carrier resulted in a lower affinity for metal ion binding and consequently a slower rate of Mn^{2+} movement. In addition, the greater ion exchange properties of these cell walls lowered the effective free metal ion concentrations in proximity to the membrane surface.¹¹⁰

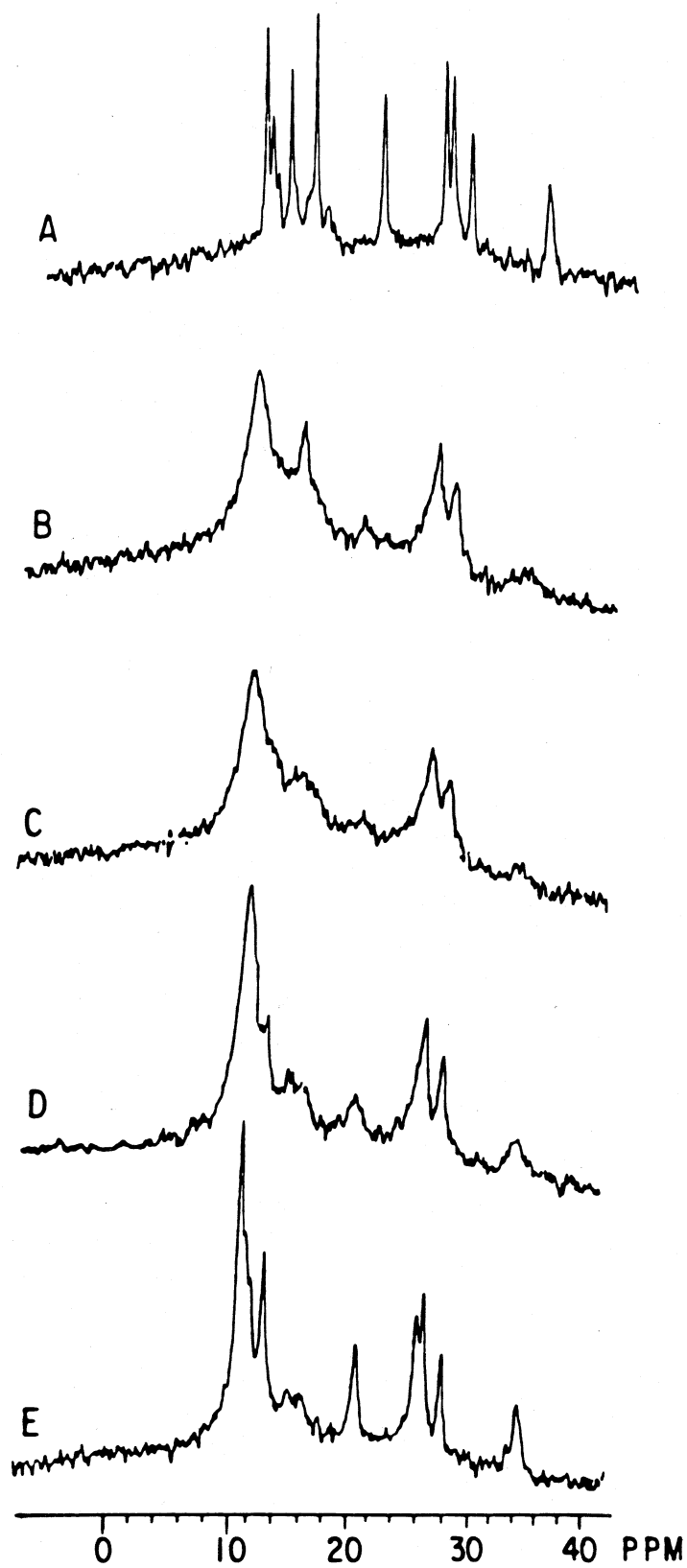


FIGURE 21. (A) ^{31}P spectrum (10,000 transients) taken in Figure 20 after 3 h of perfusion with a solution of 0.1 mM CaSO_4 , 50 mM glucose, 10 mM Mes buffer (pH 6.0) O_2 . (B) Same as above except for the addition of 1.0 mM MnCl_2 and exposure for 54 to 81 min. (C) Same as (B), exposure 108 to 135 min. (D) Sample perfused with buffer as in (A) for 0 to 27 min. (E) Same as (D) for 81 to 108 min. (See Reference 14.)

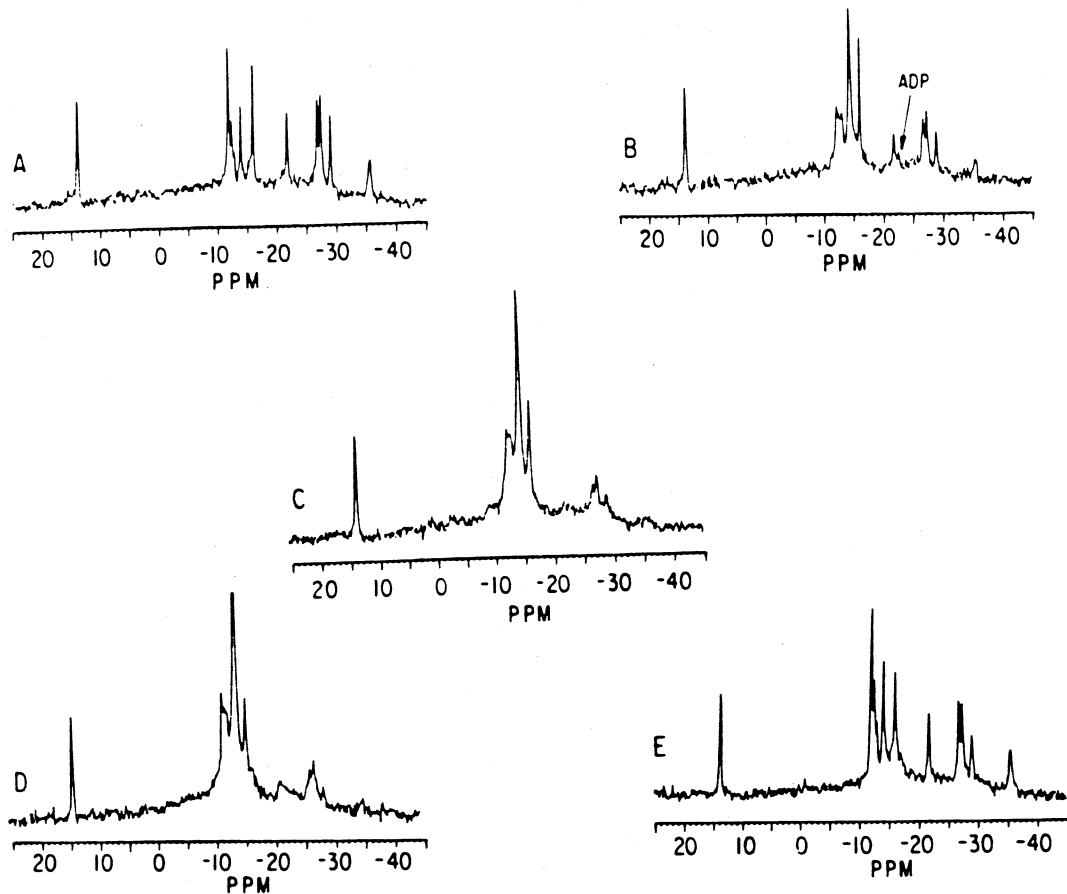


FIGURE 22. (A) ^{31}P spectrum (100,000 transients) taken as in Figure 21 above and perfused with a solution containing 0.1 mM CaSO_4 , 50.0 mM glucose, 10.0 mM MES buffer (pH 6.0) O_2 . (B) Same as (A) except perfusate is saturated with N_2 , 54 to 81 min. (C) Hypoxic state 189 to 216 min, treatment with perfusate containing 1.0 mM MnCl_2 for 108 to 135 min. (D) Hypoxic state 297 to 324 min after being washed out with non-Mn-containing buffer for 81 to 108 min. (E) Washout as in (D) with O_2 after 81 to 108 min. (See Reference 14.)

5. Photosynthetic and Symbiotic Systems

Kallas and Dahlquist¹¹¹ demonstrated the first application of ^{31}P NMR to an active photosynthesizing system. They examined the ^{31}P spectra of actively photosynthesizing and darkened suspensions of *Cyanobacterium synechococcus*. These photosynthesizing microorganisms exhibited a single intracellular P_i resonance corresponding to the cytoplasmic compartment, but the second photosynthetic intrathylakoidal compartment was not resolved. The failure to resolve this compartment was presumably partly a result of the low S/N of the low-field instrument used and the small volume of the intrathylakoidal space (7 to 10%) in the bacteria.¹¹¹ In general, the pH of the cytoplasm was maintained at a higher level than the external pH when the external pH was in the range of 6.3 to 6.7. Exposure to light caused an increase in intracellular pH of 0.4 of a pH unit. The addition of CCCP destroyed the internal pH control in both light and darkness. Following this work, Foyer et al.¹¹² studied compartmentation from ^{31}P NMR spectra of intact cells, protoplasts, and chloroplasts from photosynthetic tissues. These workers observed individual pools (vacuolar and extravacuolar compartments) of P_i in the dark from asparagus cells and spinach protoplasts. The spectra from whole leaves of spinach, wheat, and rye grass were found to be difficult to interpret because of the broadening of the ^{31}P signals due to the large air spaces that occur between the mesophyll cells and the presence of intracellular paramagnetic metal ion.¹¹² However, the intact cells, protoplasts, and chloroplasts gave better defined spectra. Unlike previously examined bacteria,¹¹¹ the intracellular pH was not tightly controlled in these cells, but determined by the pH of the suspending medium. Waterton et al.¹¹³ have been able to

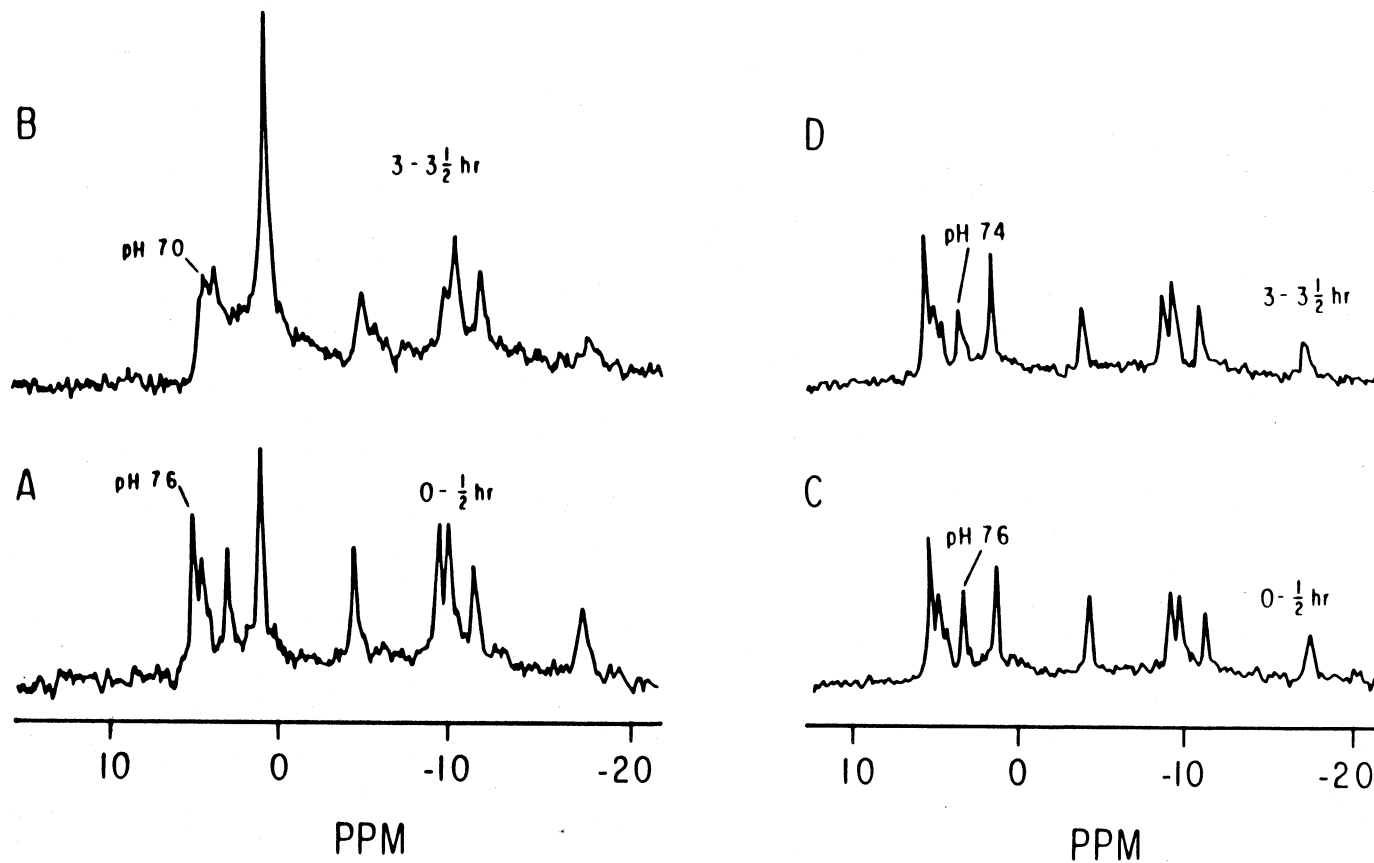


FIGURE 23. 161.7-MHz spectra of maize root tips (A) perfused with 50 mM glucose, 10 mM MES buffer, pH 6.0, 0.1 mM CaSO_4 for 1/2 h; (B) 3 1/2 h after the addition of 1 mM CdCl_2 ; (C) same as A except 10 mM CaSO_4 was used for 1/2 h; and (D) 3 1/2 h after the addition 1 mM CdCl_2 .

establish the nature of the line broadening in the ^{31}P spectra of intact leaf tissue. Using wheat leaf disks, they measured the line width of the ^{31}P (in hertz) and showed that they were linearly dependent on the size of the external magnetic field. Thus, the line broadening observed in the previous study¹¹² was found to be a function of the leaf tissue air spaces. This effect arises because of the difference in the magnetic susceptibilities of the tissue water and intracellular air. Furthermore, these workers verified the phenomenon by elimination of the broadening with high-speed magic angle spinning (see Chapter 9 for details of this technique). Vacuum infiltration with buffered sorbitol was also found to be useful for improving the line width and resolution.^{113,114} Two peaks, an extracellular P_i resonance corresponding to pH ~ 7.0 and vacuolar P_i (below pH 6.0) were detected in the dark with the ratio of 1:4, respectively.¹¹³ Under illumination the extracellular P_i signal moved to lower field, indicating a more alkaline environment consistent with the extrusion of protons from the chloroplast stroma. Incubation with mannose produced mannose-6-phosphate outside of the vacuole, while the vacuolar P_i was depleted to maintain a constant level of P_i in the cytoplasm.

To obtain useful spectra from pea or spinach leaves, Foyer and Spencer¹¹⁵ utilized ATP in the infiltrating medium as a chelating agent to distinguish between the acidic and neutral P_i pools. Barley tissue did not require the ATP treatment to distinguish the vacuolar and cytoplasmic P_i pools. Barley, soybean, and spinach leaf tissue showed a uniform response to P_i deficiency by increasing starch synthesis relative to sucrose, but the limitation under these conditions on photosynthetic capacity showed great variation among these plants.¹¹⁵

Unicellular algae such as *Chlorella* are ideal models for studying plant cell biology since they are simple systems (one cell and one chloroplast) and their extracellular growth conditions can be easily controlled. Also, because *Chlorella* can be treated as homogeneous cell suspensions, they are very amenable to examination by *in vivo* NMR methodology. Mitsumori and Osamu¹¹⁶ were the first to simultaneously observe two compartments corresponding to the stroma of chloroplasts and cytoplasm in *Chlorella* by ^{31}P NMR. The two P_i signals from these compartments were assigned based on their responses to light and dark cycles and treatment with 3(3,4-dichlorophenyl)-1,1 dimethylurea. In the light, the chloroplastic pH became more alkaline, while the cytoplasmic pH became nonacidic. An increase in ATP was also observed upon illumination (see Figure 24). However, a more recent investigation of this organism using 2DG-6-P as a pH marker has reassigned the light-dependent resonance to the cytoplasmic P_i and not the stromal fraction.¹¹⁶ Additional studies of *C. vulgaris* 11-h cells showed that no acidic compartment was detectable by ^{31}P NMR when the cells were treated with NH_4OH .¹¹⁷ The vacuolar pH was also lowered by anaerobic treatment in the presence of glucose, but was not affected by external pH during preincubation in medium with pHs ranging from 3 to 10. These results suggest that acid fermentation takes place in *Chlorella* cells in the presence of glucose under anaerobic conditions, and therefore vacuoles may play a role as lysosomes as well as "metabolic buffer" in the cytoplasm.¹¹⁷ A ^{31}P NMR study of unicellular alga acidophilic *Cyanidium caldarium* revealed a change in intracellular pH (acidification in darkness), but did not detect the vacuolar compartment in this species.¹¹⁸ Illumination conditions maintained the intracellular pH from 6.8 to 7.0 even in environments with pH ranges from 1.2 to 8.4. These authors¹¹⁸ contend that *Cyanidium* cells must have light to maintain their intracellular pH at a constant physiological level against passive H^+ leakage. The halotolerant alga *Dunaliella parva* studied by Ginzburg et al.¹¹⁸ showed only a single pool of intracellular P_i . The intracellular pH was also found to be sensitive to changes in illumination as well as oxygenation. Spectra of the extract from these alga demonstrated the presence of a relatively rare metabolite, glycerophosphorylglycerol, whose function is not understood.

For the study of mycorrhizal systems, ^{31}P NMR affords the opportunity to examine an intact symbiotic assembly and evaluate the nature and distribution of phosphate compounds between the fungi and plant cell partners. Some preliminary studies of mycorrhizal root tips of beech (*Fagus sylvatica*) have shown the presence of a PP resonance (fungal) in addition to the normal

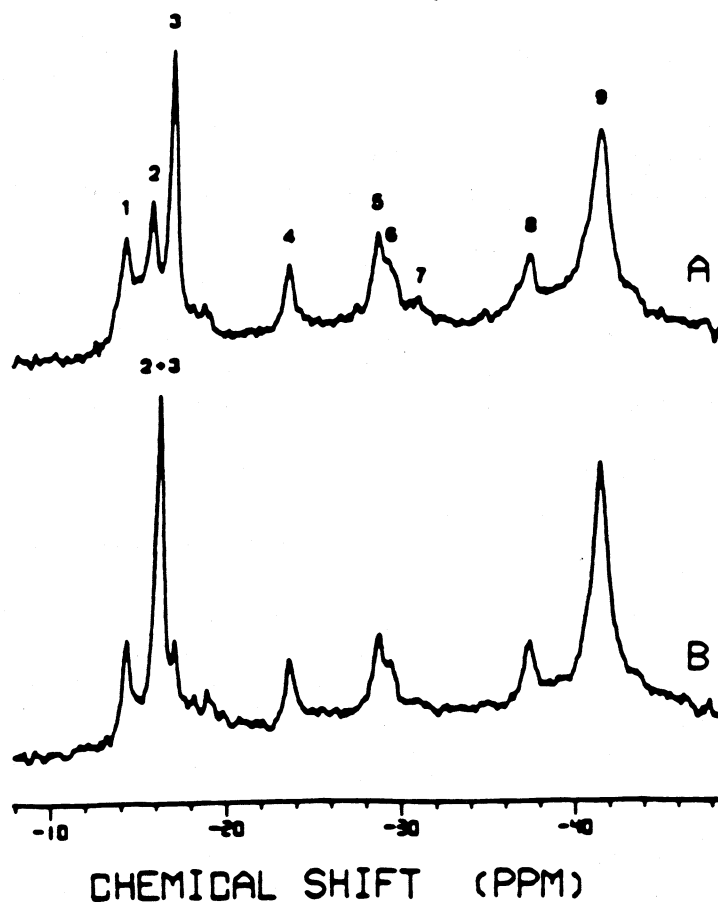


FIGURE 24. 161.8-MHz ^{31}P NMR spectra of intact autotrophically grown *Chlorella* cells measured in the dark (A) 27 min and (B) 137 min after light was turned off. Spectral assignments are 1, sugar phosphates; 2, chloroplastic P_i ; 3, cytoplasmic P_i ; 4, $\text{ATP}\gamma$; 5 $\text{ATP}\alpha$; 6, $\text{NAD} + \text{UDP-glucose}$; 7, UDP-glucose ; 8, $\text{ATP}\beta$; and 9, polyphosphate. Chemical shift values are in ppm from external MDP . Packed *Chlorella* cells (1.0 ml) were suspended in the equal volume of medium containing KCl (100 mM), several mineral nutrients, Hepes (20 mM), and D_2O (10%). The initial pH of the cell suspension was adjusted to 7.0. External P, had been removed by washing cells with P_i -free medium three times. The 2500 transients were accumulated with the recycle time of 0.22 s at 25°C. O_2 bubbling (10 ml/min) was performed to maintain aerobic conditions during NMR measurements. (From Mitsumori, F. and Osamu, I., *FEBS Lett.*, 174, 248, 1984. With permission.)

peaks of P_i .⁴ Rapid hydrolysis of the PP following homogenation of the tissue suggested to the authors that the PP and polyphosphatase were located in different cellular compartments in the intact matrix.⁴ Martin¹¹⁹ has analyzed intact ectomycorrhizal fungi grown in pure and batch culture by ^{31}P NMR and has found them to contain a surprisingly low level (17% of total P) of PPs. However, the bulk of this polymer is observable by high-resolution ^{31}P NMR. Estimates of the chain lengths (average = 12) of soluble PP were made by evaluating the fungal extract spectra in terms of the ratio of the ^{31}P resonances associated with the inner and penultimate positions of the polymer. The observed relatively low concentration of short-chain PP is consistent with the fact that PPs are not normal metabolites of microorganisms, but are only rapidly accumulated by them under conditions of nutritional imbalance in older cultures.¹¹⁹ Further studies of the two strains of ectomycorrhizal fungi, *Cenococcum graniforme* (CG) and *Hebeloma cylindroporum* (HC), verified that the PP content was highest in the older and nitrogen-starved cultures and lowest in the rapidly growing mycelia.¹²⁰ The two varieties showed a difference in their

Table 5
LONGITUDINAL RELAXATION TIMES (T_1)
AND LINE WIDTHS ($\Delta\nu_{1/2}$) OF ^{31}P NUCLEI OF
INTRACELLULAR PI AND POLYP IN
ECTOMYCORRHIZAL FUNGI COMPARED TO
THOSE OF THE COMPOUNDS IN MODEL
SYSTEMS

Phosphorylated compounds	$\Delta\nu^{1/2}$ (Hz)	T_1 (ms)
Pi		
Growth medium Intracellular	40 ± 0.3	650
<i>H. crustuliniforme</i>	14 ± 4	150 ± 44
<i>C. graniforme</i>	22 ± 11	141 ± 27
PolyP		
Growth medium	21 ± 2	790 ± 85
Growth medium + glycerol Intracellular	—	960 ± 100
<i>H. crustuliniforme</i>	109 ± 21	290 ± 3.0
<i>C. graniforme</i>	187 ± 33	4.4 ± 2.2

Note: All measurements were obtained at 36.4 MHz with a sample temperature of 4°C. The pH is 5.6 in all model systems as well in the growth medium. The line widths given represent the average of 3 measurements for model systems and at least 10 measurements for living mycelia. T_1 values were the average of three measurements (\pm SD).

Adapted from Martin, F., Marchal, J.-P., Timinska, A., and Canet, D., *New Phytol.*, 101, 275, 1985.

respective rates of PP degradation which appeared to be related to difference in the intracellular state of the PP. ^{31}P line width and spin-lattice relaxation measurements for Pi and PP in both intact strains and in culture medium (*in vitro* solution) demonstrated that the intracellular relaxation times were significantly shorter (see Table 5). This is attributed to a combination of factors such as partial immobilization of the polymer by cellular components and/or possible interaction with paramagnetic metal ions such as Mn^{2+} . The greater mobility (longer T_1) of the PP in *HC* compared with *CG* seems to explain the more rapid degradation of PP in the former.

Symbiotic nodules produced from the infection of soybean seeds (*Glycine max*) with rhizobium can be readily examined in a detached state with ^{31}P NMR.^{81,121} In this condition the nodules fix little nitrogen. However, the respiration of the assembly is maintained. Because nodules contain a mixture of uninfected plant and cortical cells which contain vacuoles, in addition to the infected cells that contain no vacuole, one would anticipate that the ^{31}P spectra would be more complex than those obtained from a single plant or organism. In fact, even at magnetic fields as high as 161.7 MHz, the ^{31}P spectra show considerable overlap of the resonance associated with the plant and micro-organism cells. Continuous perfusion of the nodules¹²¹ with an oxygen-saturated solution of 50 mM glucose, pH 7.5, does however improve the resolution of the spectrum over those obtained previously⁸¹ in an unperfused state. Figure 25 shows the clear separation of the three phosphate monoesters, centered at approximately 4.4 δ and an unknown phosphate diester at approximately 0.40 δ that were not resolvable without perfusion. The latter resonance appears to represent a marker compound associated with the encapsulated

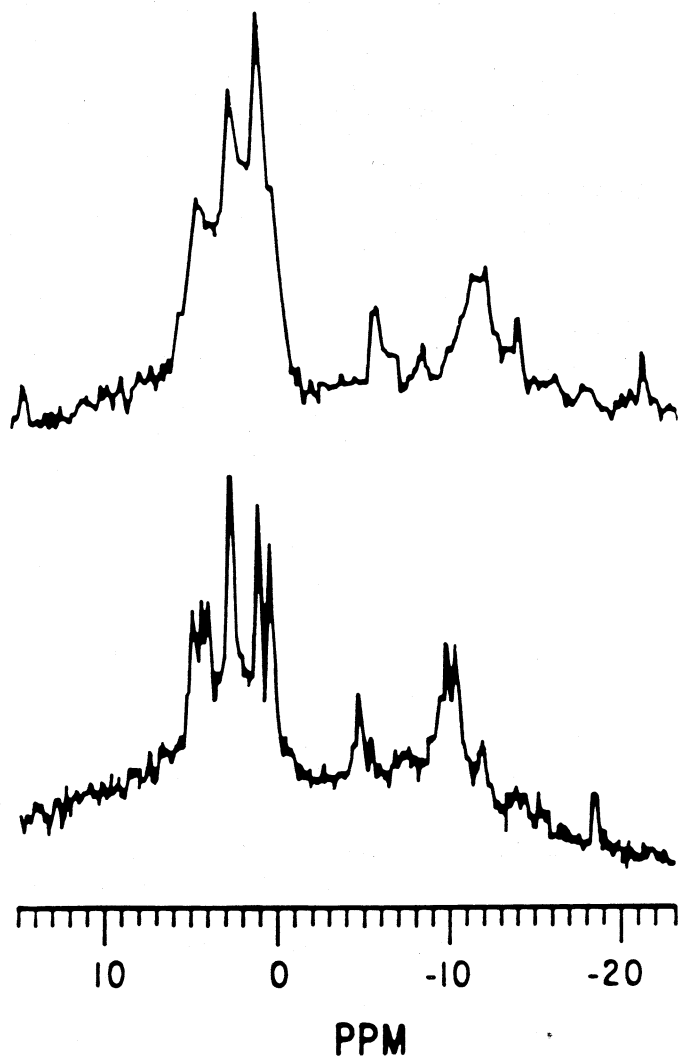


FIGURE 25. 161.7 MHz ^{31}P spectra of detached soybean root nodules: upper spectrum, 20,000 scans, no perfusion only bubbling with O_2 . (From Mitsumori, F., Yoneyama, T., and Ito, O., *Plant Sci.*, 38, 87, 1985. With permission.) Lower spectrum, 20,000 scans with perfusion (unpublished results).

bacterioids, since it has also been observed in the spectra of extracts of the free-living rhizobia.¹²¹ This compound does not correspond to any of the known phosphate diesters in any previously described *in vivo* plant or microorganism study.

^{31}P spectra of the perchloric acid extracts of the freshly detached nodules (Figure 2) showed an unusually low ratio of NTP/NDP (1.5), reflecting the anaerobic environment of the intracellular bacterioids.¹²¹ These values are consistent with those obtained by wet chemical luciferase analysis (1 to 1.5) of the same nodule tissue.¹²¹ With the exception of hypoxic conditions, all plant tissues and plant cells that have been examined by ^{31}P NMR in an aerobic state have shown NTP/NDP ratios approaching 25.⁸³

The near coalescence of the P_i resonances at approximately 0.89 and 3.0 δ following treatment with 200 μM CCCP verified the presence of two membrane- and gradient-separated compartments with pHs of approximately 7.1 and 5.9.⁸¹ Application of 1 mM Mn^{2+} to the perfusion medium caused a preferential broadening of the P_i resonance at 0.89 δ representing the presumed acidic plant vacuole compartment (unpublished results) as observed previously in the spectra of maize root tips.¹⁴ Steam girdling treatment of the stem of the host soybean plants

cut off the supply of carbohydrate to the root system as demonstrated in the ^{31}P spectra of the nodules which showed diminished levels of sugar phosphates and NTP.⁸¹

B. ^{13}C Studies

This section will cover the application of *in vivo* ^{13}C NMR, primarily to plants and microorganisms in both natural abundance (1.1%) and isotopic enrichment studies. A more comprehensive review of the use of ^{13}C , ^{14}N , and ^{15}N NMR for monitoring plant metabolism has been published by Martin.²⁹ For this reason we will try to cover the more recent developments in this area and highlight only some of the older studies that have already been reviewed. The same will be true for the sections on ^{14}N and ^{15}N NMR applications.

1. ^{13}C Natural Abundance Studies

Natural abundance (1.1%) in *in vivo* ^{13}C NMR spectroscopy, because of its inherent insensitivity, is only a practical technique for examining high concentrations of small, mobile, storage compounds that are metabolized over long periods of time. In principle this methodology is well suited to the study of certain microorganisms, fruits, storage roots, and seeds. The analysis of intact seeds will be covered in Chapter 4.

Martin et al.¹²² have examined the natural abundance ^{13}C spectrum of intact ectomycorrhizal fungi mycelia and observed a large quantity of the storage carbohydrates, trehalose and mannitol, as well as triacylglycerols and glycogen. The concentration of the stored carbohydrates was shown to change as the fungi aged. In this way the NMR was able to examine the interchange of carbohydrates and lipids and the biochemical relationship between them.¹²² ^{13}C has also been useful for studying the role of organic solutes in controlling cell osmolarity. Glucosyl glycerol, for example, was found to be produced in response to osmotic stress in cyanobacteria,¹²³ while glycerol was observed to be accumulating in the ^{13}C spectrum of halophilic alga (*Duwaliella salina*) under similar conditions.¹²⁴ However, only about 60% of the total glycerol in *D. salina* was NMR visible in the intact cells.¹²⁴ This may be a consequence of a slow exchange between free and cell-bound glycerol or an interaction with paramagnetic metal ions within the chloroplast.¹²⁴ ^{13}C T_1 measurements can be used to estimate the intracellular viscosity in mycelia and other intact organisms. Martin et al.¹²⁵ measured the T_1 values for fatty acid acyl chain carbon resonances in ectomycorrhizal fungi and found them to reflect a high degree of molecular motion, comparable to that found in mammalian tissue. However, a highly viscous environment characterized by a shortened T_1 of intracellular mannitol was observed in the fungi *Penicillium janczewskii*.¹²⁶

Kainosho and Konishi¹²⁷ examined the ^{13}C spectrum of the intact pericarp of star anise and found it to contain anethole, an essential oil. Upon crushing the pericarp, the ^{13}C spectrum became broadened and highly degraded, indicating that the free motional state of the molecule was highly restricted. This change was attributed to the fact that the anethole existed as a neat, freely mobile liquid in the parenchyma of the intact pericarp prior to crushing. However, following crushing, the oil leaked from the cells and was absorbed on the woody tissue where it became motionally restricted.¹²⁷

^{13}C spectra of intact white potatoes only showed the resonances corresponding to the mobile sugars, glucose, sucrose, and fructose, and fatty acids which represent about 1% of the potato tissue.¹²⁸ Boiling the potato, however, suppressed the spectrum of the low molecular weight species and revealed the intense spectrum of starch. These studies indicate that the large molecules of starch in the potato tend to break down into small units when exposed to boiling water. We have examined the ^{13}C spectrum of intact nonboiled potatoes to evaluate changes in glucose and sucrose storage and interconversion following different genetic manipulations and periods of storage.¹²⁹ In addition, the chemical shift of the citrate resonance was useful for evaluating the intracellular pH.¹²⁹ This methodology was used to follow the composition changes in malate, tartrate, glucose, and fructose in developing unpicked and picked grapes.¹³⁰ The changes were then correlated with known changes in berry deformability. Thomas and

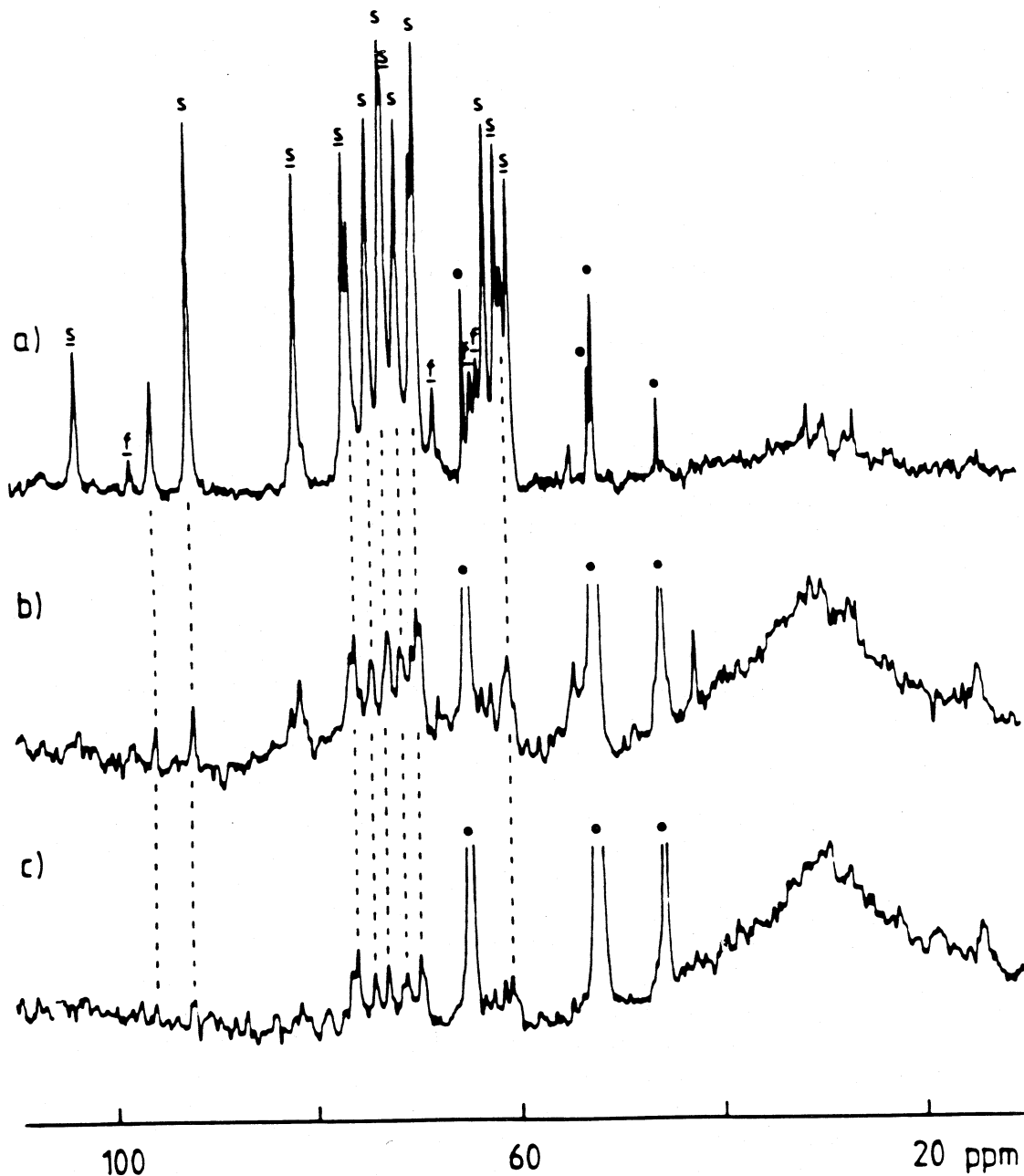


FIGURE 26. Natural abundance ^1H -decoupled 75.46 MHz ^{13}C NMR spectra of root tissues from carrot plants grown in nutrient culture: (a) a single tap root (FW = 1.7 g) from a 12-week-old plant, 4,000 transients, total acquisition time 153 min; (b) six tap root (total FW = 0.79 g) from 8-week-old plants, 16,000 transients, total acquisition time 613 min, and (c) the fibrous root system (FW = 0.65 g) from a 12 week old plant, 16,000 transients, total acquisition time 61.3 min. A line broadening of either (a) 8 Hz or (b) and (c) 16 Hz was applied before Fourier transformation. The spectra can be assigned by comparison with the characteristic spectra of sucrose, glucose, and fructose. The 12 sucrose resonances are labeled in (a) as either \underline{s} or \underline{s} , where the underlining indicates that sucrose is the only contributor to the observed peak. The eight glucose resonances are indicated by the vertical dotted lines. Several of the fructose resonances are overlapped by the sucrose and glucose, but four clearly resolved resonances are labeled in (a) as \underline{f} . The MES buffer contributed the four peaks labeled \underline{o} : these resonances were truncated when plotting (b) and (c). The broad hump centered at 30 ppm was caused by the plastic tubing in the system used to circulate the aerated buffer through the NMR tube. (From Thomas, T. H. and Ratcliffe, R. G., *Physiol. Plant.* 63, 284, 1985. With permission.)

Ratcliffe¹³¹ examined the ^{13}C spectrum of detached fibrous and storage roots of carrots (see Figure 26). The relative amounts of sucrose, glucose, and fructose in the storage roots of two ages and in fibrous roots were found to be similar to those detected by the standard, destructive

enzymatic procedures. In tap roots, all three sugars were present, while in fibrous roots glucose was the major sugar. The organic acids, sucrose, citrulline, and phenolic compounds have also been analyzed in a similar nondestructive manner in excised root nodules of *Alnus glutineas* to examine their pattern of accumulation and evaluate the effect of the nutritional state on the biochemistry of symbiosis.²⁹

2. ¹³C Isotopic Enrichment Studies

As we have seen from the above, natural abundance ¹³C NMR spectra are useful for the study of highly concentrated storage compounds. However, one cannot examine the less concentrated metabolites with this methodology. Labeled ¹³C-enriched compounds can be used to investigate the products of various metabolic pathways and yield information regarding relative fluxes through these pathways. Typically, a ¹³C NMR spectrum can be obtained from a low intracellular concentration (approximately 1 μmol) of a ¹³C-enriched metabolite (minimum 30%) within a few minutes.

While ³¹P NMR can examine some cellular processes, it has two important limitations: (1) a large number of metabolic processes do not directly involve significant changes in the concentration of key phosphorylated species and (2) ³¹P's high natural abundance precludes its use to trace the fate of a particular ³¹P metabolite. Thus, the only way to measure the turnover of phosphorylated metabolites *in vivo* is by saturation transfer and that is only possible if the rate of the process is fast enough and the relaxation time, T_1 , is of the order of the exchange rates (see Section A.2 above on saturation transfer). ¹³C NMR studies with ¹³C-enriched compounds can directly monitor the rates of incorporation or degradation of a label, the level of its steady-state incorporation or exchange, and the specific position of the label in the metabolite. In addition, the pH-sensitive shift can be used to report the intracellular pH of compartment cells. A survey by Avison et al.⁹ has reviewed the recent literature of *in vivo* ¹³C NMR studies of animals, humans, and perfused organs and tissues which include brain, heart, kidney, and skeletal muscle.

The use of ¹³C enrichment has dominated the voluminous numbers of reports describing carbon fluxes in microorganisms.^{2,132} This methodology has not yet attained widespread applications in the area of *in vivo* plant studies although a number of reports on algae and fungi has recently appeared and been reviewed.²⁹ Stidham et al.¹³³ have successfully used the ¹³C signal from malate in intact *Kalanchoe tubiflora* leaves (introduced by exposure to ¹³CO₂) to follow the decarboxylation of malate of this Crassulacean acid metabolism (CAM) plant in the light. After a period of darkness in air, a resynthesis was observed in which all four carbons of malate were found to be labeled with ¹³C. The position of the ¹³C resonance was also useful for determining the pH of the vacuole during light and dark periods. Since the malate was only found in the vacuole, the change in chemical shift of the four carbons was used to evaluate the change in vacuolar pH under light and dark conditions. In contrast to the Pi resonance, the four ¹³C resonances of malate are excellent pH indicators for acidic compartments such as the vacuole since their pK_as are of the order of 4.5 (see Figure 27) as opposed to 6.8 for Pi. Following a dark period, the pH of the vacuole was 4.0; however, it rose to 6.0 after 6 h of light.

In a most elegant study Holtum et al.¹³⁴ were able to directly evaluate the activity of an enzyme in the dark synthesis of malate in CAM and other plant leaves. By observing the ¹⁸O-labeled malate indirectly via the isotopic shift and J coupling of its ¹³C-carbonyl resonance (see Figure 28), the authors were able to determine if dark CO₂ fixation required the intervention of carbonic anhydrase. If malate synthesis in the dark did require high carbonic anhydrase activities, then oxygen exchange between CO₂ and cellular water (not enriched in ¹⁸O) would occur more rapidly than carboxylation and the ¹³C-malate formed would contain little more than the natural abundance level of ¹⁸O. Following the ¹³C-¹⁸O₂ exposure, the leaves were harvested and the ¹³C spectrum of the extracts were recorded. From the relative area of the ¹³C-¹⁸O shifted resonance of the malic acid carbonyl group, it was demonstrated that only minor ¹⁸O labeling of malate had occurred, proving that CAM leaves do have a substantial carbonic anhydrase activity.

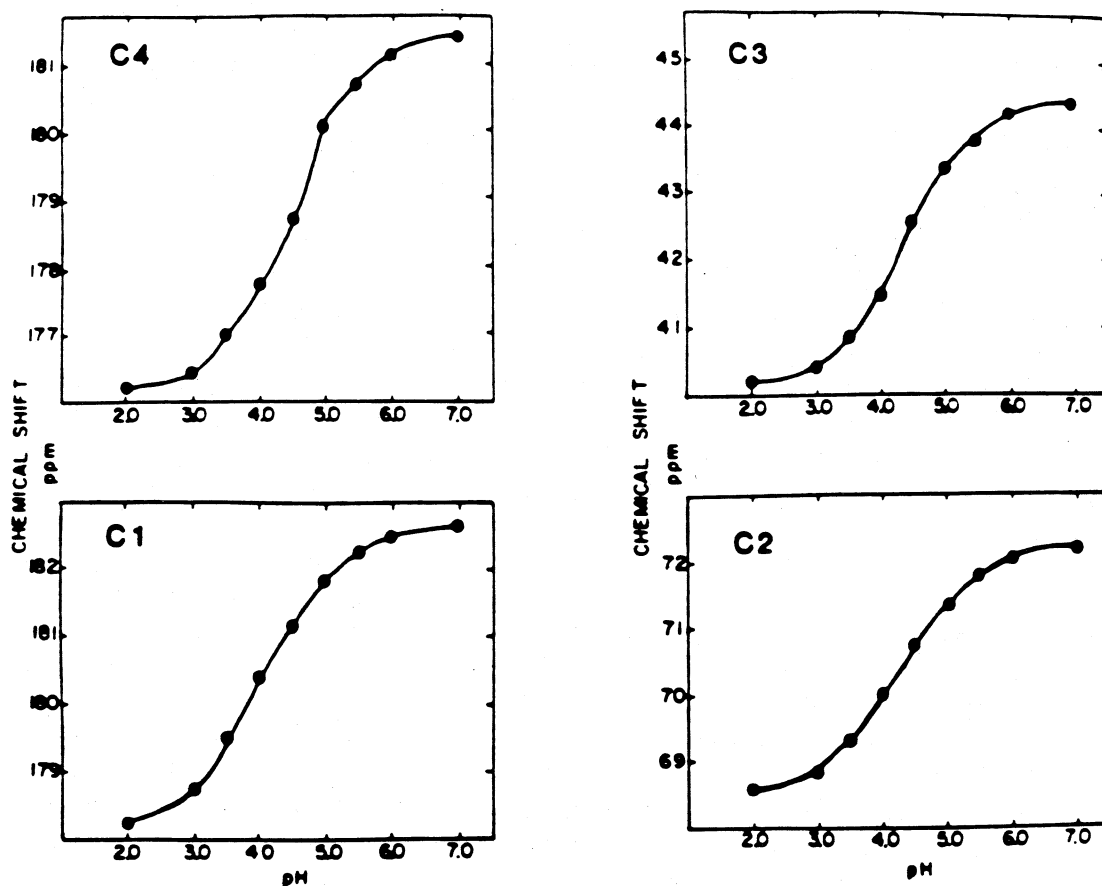


FIGURE 27. pH dependence of the chemical shifts of the ^{13}C NMR signals of malic acid. Malic acid (0.5 M) was prepared and adjusted to the appropriate pH with 5 N KOH. A 5-mm coaxial insert containing D_2O and a 0.5-mm capillary containing acetone was used in a 10-mm tube containing the malic acid. In other trials, 0.1 M malic acid was used with different references and lock compounds, and identical results were obtained. (From Coombe, B. G. and Jones, G. P., *Phytochemistry*, 22, 2185, 1983. With permission.)

Ashworth and Mettler¹³² have carried out metabolic studies in both cultured tobacco and corn cells to establish intracellular glycine and serine pool sizes. These workers utilized 2- ^{13}C -glycine and observed signals from 2- ^{13}C -glycine, 2- ^{13}C -serine, 3- ^{13}C -serine and 2,3- ^{13}C serine *in vivo*. Assignments were verified by ^{13}C homonuclear two-dimensional COSY experiments. The results of these studies suggest that serine formation from glycine is the result of a tight coupling between glycine decarboxylase and serine hydroxymethyl transferase. The metabolism of 1- ^{13}C -glucose has also been followed in the elaboration of cell wall polysaccharide biosynthesis in protoplasts from cell suspensions of millet.¹³⁵ In these studies the plant cells were grown in the NMR tube with the 1- ^{13}C -glucose substrate so the production of β -glucan could be measured directly in real time. Roberts et al.¹³⁶ has utilized 1- ^{13}C -glucose feeding with excised maize root tips to visualize the production of lactate, ethanol, and alanine under hypoxia. The quantity of each compound was determined by measuring the area of each corresponding methyl resonance.

Martin and Canet¹³⁷ have studied the accumulation of free amino acids in the presence of ammonium ion in nitrogen-starved mycelia of the ectomycorrhizal ascomycete *Cenococcum geophilum*. ^{13}C -NMR spectroscopy of extracts from cells grown on 1- ^{13}C -glucose were used to examine the biosynthesis of amino acids. Incorporation of the ^{13}C label resulted in the formation of 3- ^{13}C -alanine and glutamine, glutamate, γ -aminobutyrate, and arginine labeled at the C2, C3, and C4 positions (see Figure 29). These results indicate that labeled pyruvate enters the alanine pool via alanine aminotransferase and the Krebs cycle through both pyruvate carboxylase (and/or phosphoenolpyruvate carboxykinase) and pyruvate dehydrogenase activities. The pyruvate and acetate metabolism has been studied in cell cultures of *Zea mays* by *in vivo* ^{13}C -NMR.¹³⁵ This

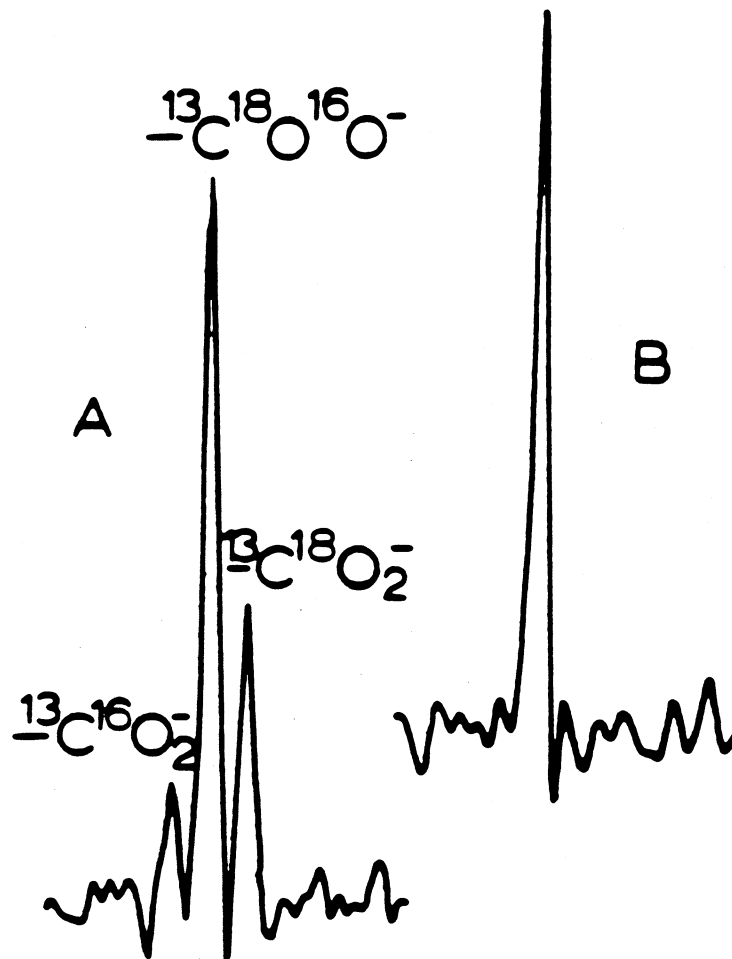


FIGURE 28. ^{13}C NMR spectra of the carboxyl region of malic acid produced by reaction of P-enolpyruvate and P-enolpyruvate carboxylase in the presence of $^{13}\text{C}^{18}\text{O}_2$. A, in the absence of carbonic anhydrase. B, in the presence of carbonic anhydrase. The single resonance seen in B represents only $^{13}\text{C}^{18}\text{O}^{-}$. (From Holtum, J. A., Summons, R., Roeska, C. A., Comins, H. N., and O'Leary, M., *J. Biol. Chem.*, 259, 6870, 1984. With permission.)

work demonstrated that growth of the corn cells in the presence of 2 mM $[2-^{13}\text{C}]$ acetate produced primarily labeled glutamate and malate. Further metabolism of these intermediates resulted in labeled glutamine, aspartate, and alanine. With $[1-^{13}\text{C}]$ acetate, little incorporation was observed due to the loss of label as $^{13}\text{CO}_2$. The uptake of $[3-^{13}\text{C}]$ pyruvate gave similar labeling patterns to the $[2-^{13}\text{C}]$ acetate but was considerably slower. Ito and co-workers¹³⁹ examined the environmental factors such as NO_2 and O_3 pollution on photosynthetic $^{13}\text{CO}_2$ assimilation in kidney bean primary leaves. NO_2 and, to a greater extent, O_3 inhibited the production of ^{13}C -labeled sucrose and fructose from photosynthetic pathways as evidenced by the lack of these compounds in the ^{13}C spectra of leaf tissue extracts. This result implies that carbon flow through the glycolate pathway (nonphotosynthetic) is stimulated in leaves exposed to NO_2 and/or O_3 . In their studies of *Staphylococcus aureus* cells, Ezra et al.¹⁴⁰ have examined the intra- and extracellular ^{13}C resonances of lactate to measure the distribution and transport of this metabolite. Due to the fact that the interior of the cells contained manganese, these workers observed a downfield shift and broadening of the intracellular ^{13}C resonances of lactate relative to that of the exterior (see Figure 30). Thus, ^{13}C -NMR was used to monitor the internal and external lactate independently. The ratio of the two resonances, external (L^e) and internal lactate (L^i), was correlated with lactate uptake in the presence of oxygen and a rapid efflux as the cells

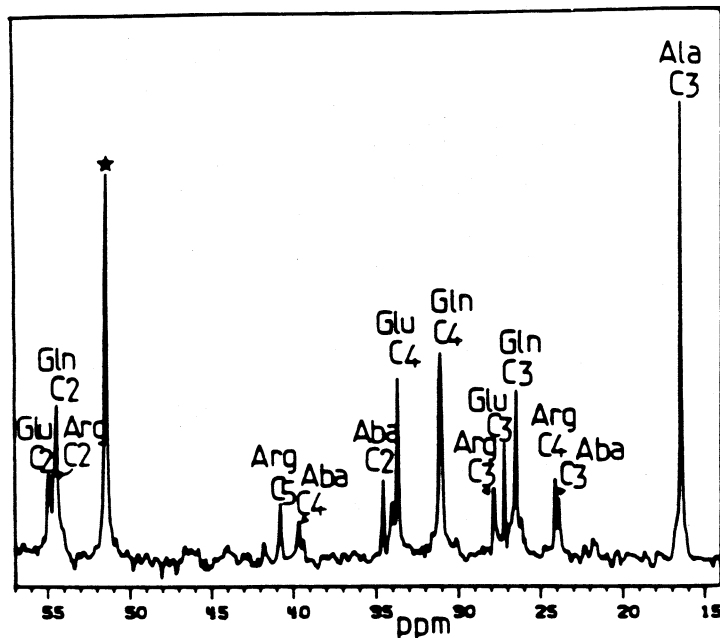


FIGURE 29. ^{13}C NMR (50.4 MHz) of an aqueous mycelial extract taken 5 h after addition of 20 mM $[1-^{13}\text{C}]$ glucose to a suspension of *Cenococcum geophilum*. The region between 15 and 60 ppm, which contains most of the amino acid peaks is shown. The spectrum is a Fourier transform of the accumulation of 1000 radio frequency pulses of 90° free induction decays, with 2-s recovery time between pulses. Samples were dissolved in 50 mM ethylenediaminetetraacetate solution (pH 7.0) containing 20% D_2O . Identified are signals from alanine, arginine, γ -aminobutyrate (Aba), glutamate, glutamine, and ethylenediaminetetraacetate (*). (From Martin, F. and Canet, D., *Physiol. Veg.*, 24, 209, 1986. With permission.)

reverted to an anaerobic state. Treatment with fatty acid antimicrobial agents lowered the transmembrane pH gradient and showed a loss of lactate from the cells during glycolysis. In addition, the uptake of lactate under these conditions in the presence of oxygen was completely inhibited.

C. Other Nuclei

1. ^{14}N and ^{15}N

Natural abundance ^{14}N NMR has found very limited application in *in vivo* studies for the reasons outlined in Section III.A. In spite of these drawbacks, Belton and co-workers¹⁴¹ examined the intracellular uptake of nitrate and ammonium ion in maize, barley, and pea root tips. Both NO_3^- and NH_4^+ gave rise to relatively sharp resonances ($\delta_{1/2} = 15$ Hz), while the amide and amino nitrogen resonances were broad and featureless ($\delta_{1/2} = 600$ Hz). Figure 31 shows the ^{14}N spectra observed for both NH_4^+ - and NO_3^- -grown barley and pea roots. The assignments are as follows: 0.0 δ , NO_3^- ; -200.0 δ , amide nitrogen; -335.0 δ , amino nitrogen; and 355.0 δ , NH_4^+ . The spin-lattice relaxation times were very short for the ^{14}N resonances associated with the large proteins (<10 ms) while the small nitrate and ammonium molecules had T_1 values of 0.1 and 0.5 s, respectively. Since the average nitrate concentration in nitrate-grown barley roots was as high as 87 mmol dm^{-3} tissue, satisfactory spectra could be obtained in as little as 5 min. The change in internal nitrate concentration followed a single exponential and was rationalized in terms of nitrate exchange and reduction. Only one pool of nitrate ion was observed and assigned to the vacuolar compartment. In contrast, the ammonium resonance showed diphasic behavior indicative of some form of compartmentation in the tissue.

Despite the need for isotopic enrichment, ^{15}N is generally the nitrogen nucleus of choice for

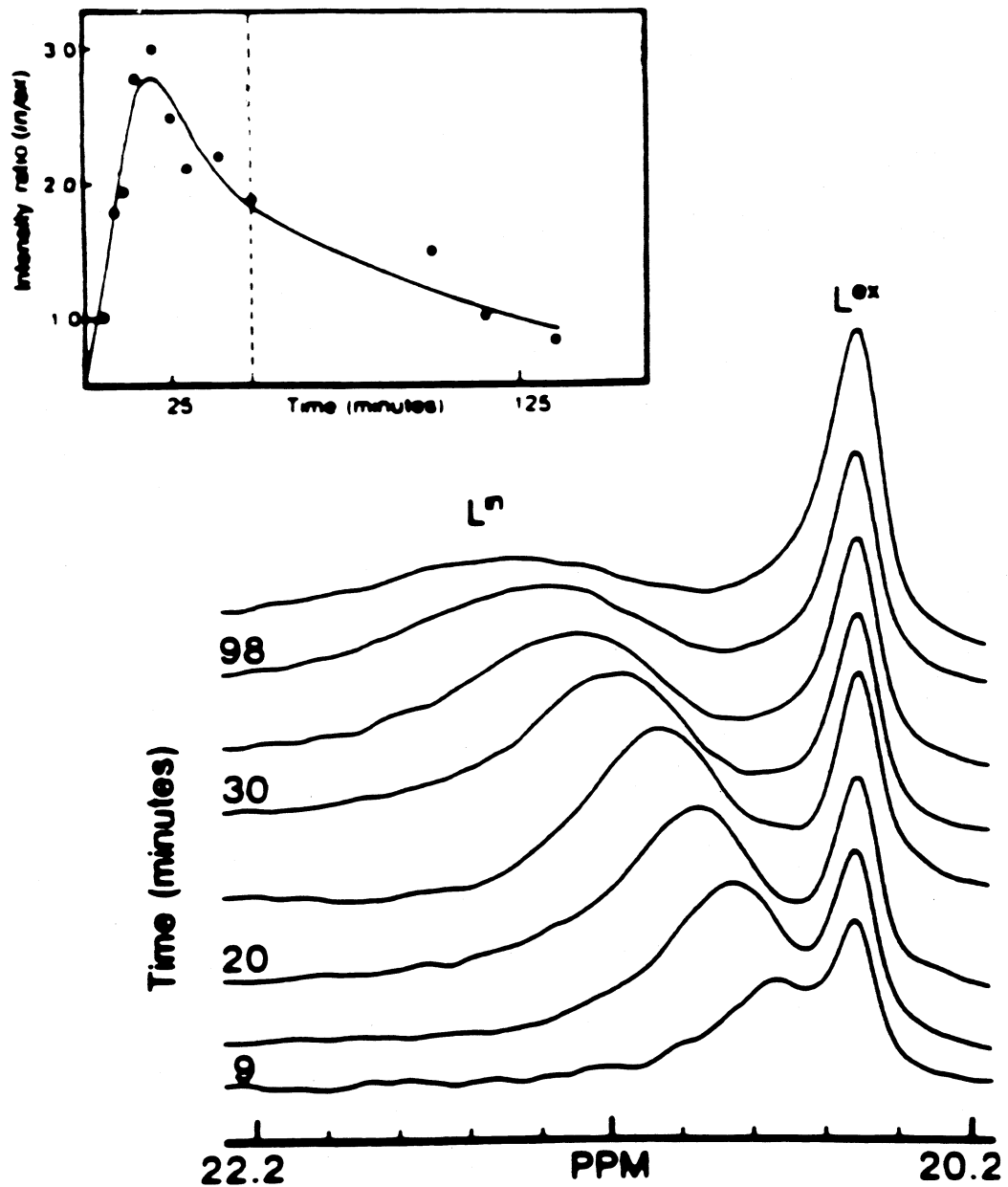


FIGURE 30. Lactate region (20.2 to 22.2 ppm) of the proton-decoupled ^{13}C NMR spectra of glycolyzing *S. aureus* cells as a function of time. The insert shows the time course of the intracellular/extracellular lactate integrated intensity ratio. Glucose consumption is completed at ~50 min (vertical dashed line). L^i , intracellular lactate and L^o , extracellular lactate. (From Ezra, F., Lucas, D. S., Mustacich, V., and Russel, A. F., *Biochemistry*, 22, 3841, 1983. With permission.)

most *in vivo* applications for the reasons mentioned in Section III.A. Kanamori et al.¹⁴² capitalized on the dipolar relaxation of intracellular ^{15}N -labeled glutamine, alanine, and arginine to establish that the viscosity of the cytoplasm of *Neurospora crassa* is substantially less than its vacuole due to polyanion interactions in the latter. ^{15}N has also been used as an intracellular pH probe for *N. crassa* mycelia. Line widths as well as chemical shifts correlated with the pH environment of ^{15}N -labeled amino acids, histidine, arginine, alanine, and proline used in the study. The pH dependence of the chemical shift of N_α of histidine was found to be most sensitive in the pH range 5 to 7 (characteristic of the vacuole), whereas P_i whose pK is closer to 6.8 is relatively insensitive for reporting the relatively acidic compartment.

Both cytosolic amino acids such as glutamine and alanine and vacuolar amino acids such as

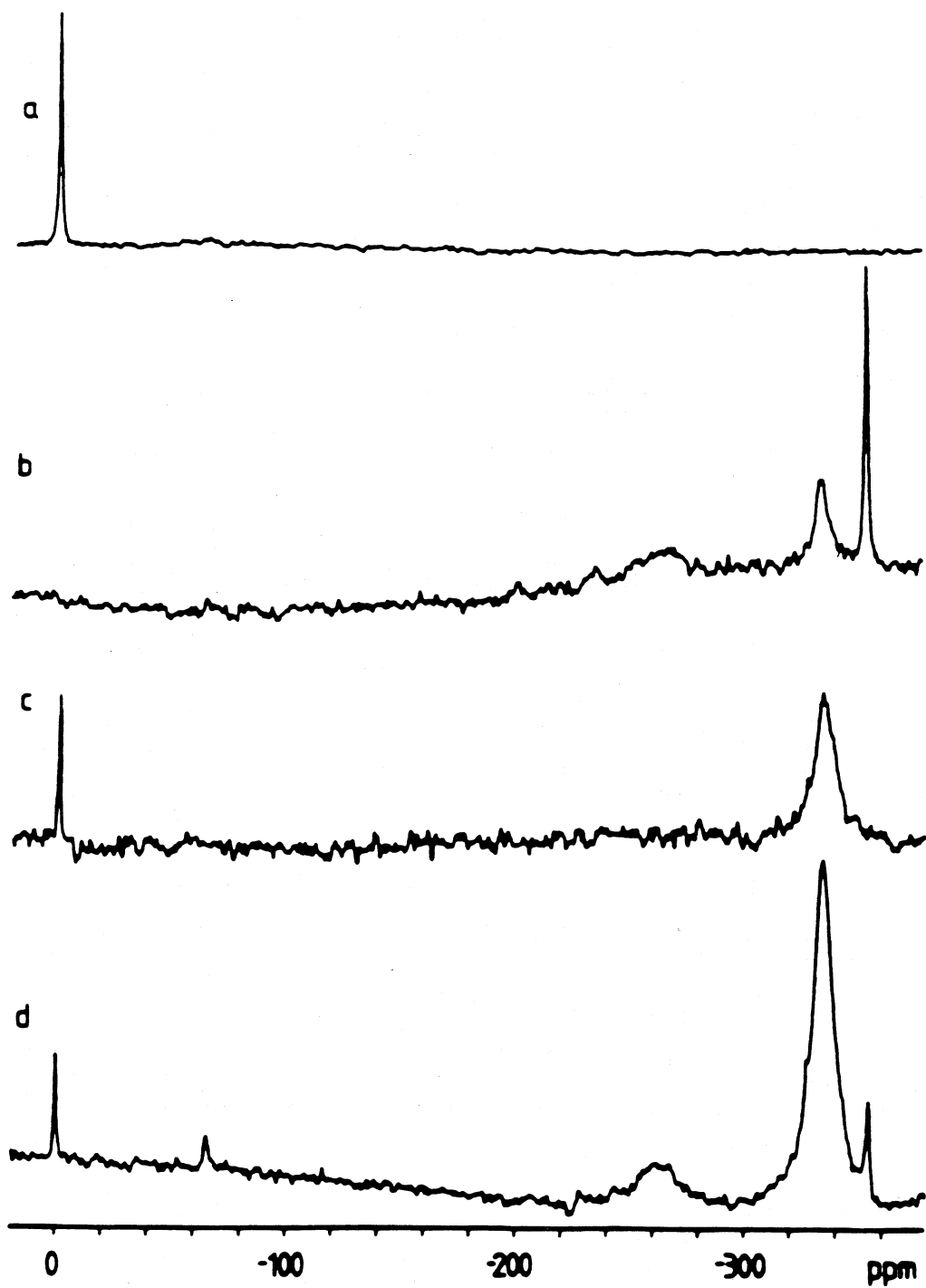


FIGURE 31. The 21.68-MHz ^{14}N spectra of (a) 11-d-old barley roots grown on 5.0 mol m^{-3} nitrate; (b) 11-d-old barley roots grown on 5.0 mol m^{-3} ammonium; (c) 5.0-mm root tips from 10-d-old pea roots grown on 5.0 mol m^{-3} nitrate; and (d) 5.0-mm root tips from 10-d-old pea roots grown on 1.0 mol m^{-3} nitrate, supplemented with 5.0 mol m^{-3} ammonium for the 12 h before excision. The spectra were accumulated (a) in 20 min with a 65° pulse and a 0.25-s recycle; (b) in 40 min with a 65° pulse and a 1-s recycle; (c) as (a); (d) in 1 h with a 90° pulse and a 0.2-s recycle. The approximate spin-lattice relaxation times for the tissue resonances are amide/amino, $<10 \text{ ms}$; nitrate, $\sim 0.1 \text{ s}$; and ammonium, $>0.5 \text{ s}$. It follows that the optimum acquisition conditions, both for qualitative and quantitative spectra, differ widely for the various resonances. The resonance assignments are discussed in the text. (From Belton, P. S., Lee, R. B., and Ratcliffe, G., *J. Exp. Bot.*, 36, 190, 1985. With permission.)

arginine and lysine gave excellent ^{15}N spectra in metabolic studies of *N. crassa* mycelia and *Saccharomyces cerevisiae* cells incubated with ^{15}N -labeled substrate.^{142,143} Martin¹⁴⁴ investigated ^{15}N -labeled metabolites in ectomycorrhizal fungi mycelia and cell-free extracts. These spectra are shown in Figure 32. A time course of incorporation of $^{15}\text{NH}_4^+$ (kinetic labeling) demonstrated glutamine synthetase activity because the glutamine amide-N was the most highly labeled component over the 1st h. The failure to observe the arginine $\text{N}_{\omega,\omega}$ resonance in the intact mycelia while it is present in the extracts (see Figure 32B) suggests that the positively charged guanidino group of arginine may be associated with negatively charged PP in the fungal vacuole. This observation is in accord with the observation of Kanamori et al.¹⁴² that PPs decrease the T_1 of the arginine $^{15}\text{N}_{\omega,\omega}$ resonance.

By feeding [guanidino- ^{15}N] arginine to detached shoots of beech (*Fagus sylvatica*), Martin²⁹ was able to demonstrate with *in vivo* ^{15}N NMR that the ammonium nitrogen produced by arginine catabolism is reassimilated via glutamine synthetase.

The pathway of NH_4^+ assimilation in *Lemna gibba*, a floating aquatic angiosperm, has recently been elucidated with labeled ^{15}N NH_4^+ .¹⁴⁵ In this instance, the $^{15}\text{NH}_4\text{Cl}$ was taken up by the floating plant for 24 h. Following this period, ^{15}N NMR analysis of the aqueous extracts of the plant tissue revealed ^{15}N incorporation into glutamine and glutamic acid with no detectable free ammonium ion. When the tissue was exposed to methionine sulfoximine, an inhibitor of glutamine synthetase, no incorporation of ^{15}N was observed. In the presence of azaserine, a glutamate synthase inhibitor, only ^{15}N incorporation was seen in the amide group of glutamate. These results indicate glutamine synthetase and glutamate synthase are major pathways for the assimilation of ammonium ions.¹⁴⁵

2. ^1H and ^{19}F

A great number of ^1H NMR studies of heterogeneous tissues has been carried out solely through the examination of the characteristic water resonance. The reason is partly because of the complexity of the ^1H spectrum due to its high sensitivity and small chemical shift range and partly because of the sheer dominance of the water resonance over everything else in the spectrum. By examining the water resonance, one can obtain important information concerning the tissue, i.e., the water content and the relaxation properties (T_1 and T_2 and thereby the mobility and interaction with paramagnetic centers). A number of T_1 and T_2 relaxation rates of water in plant tissues and their relationship to frost hardiness have been thoroughly reviewed by Loughman and Ratcliffe.⁴ These relaxation properties were also exploited to measure the exchange between the water in the cortical cells and extracellular space in maize roots in the presence of Mn-EDTA (a nontoxic form of Mn^{2+}).¹⁴⁶ In addition, the water-free space of the root and viscosity of the cell cytoplasm were also estimated. The proton water relaxation properties were used to monitor the translocation of the paramagnetic ion directly, since these properties measure the relaxation of the tissue water affected by the paramagnetic ions (assuming the enhancement of water relaxation is proportional to the intracellular ion concentration).¹⁴⁶ This same principle is presently being exploited to increase the resolution of proton magnetic resonance imaging (MRI) in plant and other agricultural materials (see Chapter 15 for full details).

High-resolution ^1H studies of heterogeneous tissues requires special spectroscopic techniques as mentioned above. First, one must suppress the dominant water resonance to begin to observe other components. Second, it is necessary to reduce the broad resonances due to proteins and relatively immobile lipids. Along with the new instrumentation, computers, and software, which have proliferated in the past years, has come a variety of pulse sequences capable of making ^1H NMR a practical tool for studying *in vivo* metabolism. The pioneering work of Campbell and co-workers^{147,148} on the application of spin-echo techniques in the study of erythrocytes laid the groundwork for most of the work that is continuing today.

The broad ^1H resonances of protein and immobile lipids can be eliminated by exploiting their

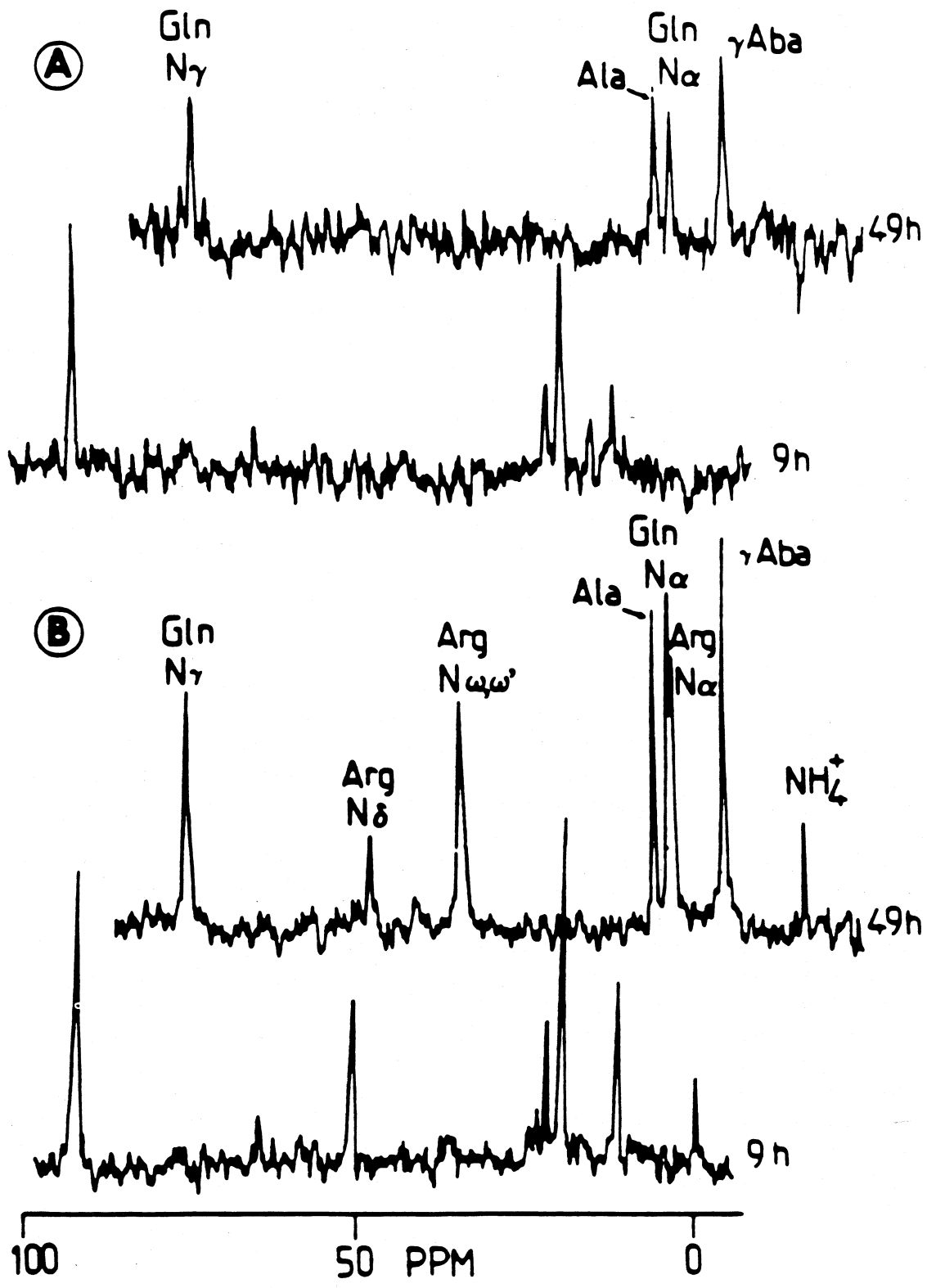


FIGURE 32. The ^{15}N spectra of ^{15}N amino acids in living mycelia (A) and cell-free extract (B) of *Cenococcum graniforme*. The fungus was fed 5 mM ($^{15}\text{NH}_4$) $_2\text{SO}_4$ (50 atom percent excess) at time zero. Each spectrum (40.5 MHz) consists of 1000 (A) or 2500 (B) scans of 2-s pulse intervals. The first peaks to appear are due to glutamine; these are followed by alanine, γ -aminobutyrate, and arginine nitrogen signals. (From Martin, F., *Physiol. Veg.*, 4, 463, 1985. With permission.)

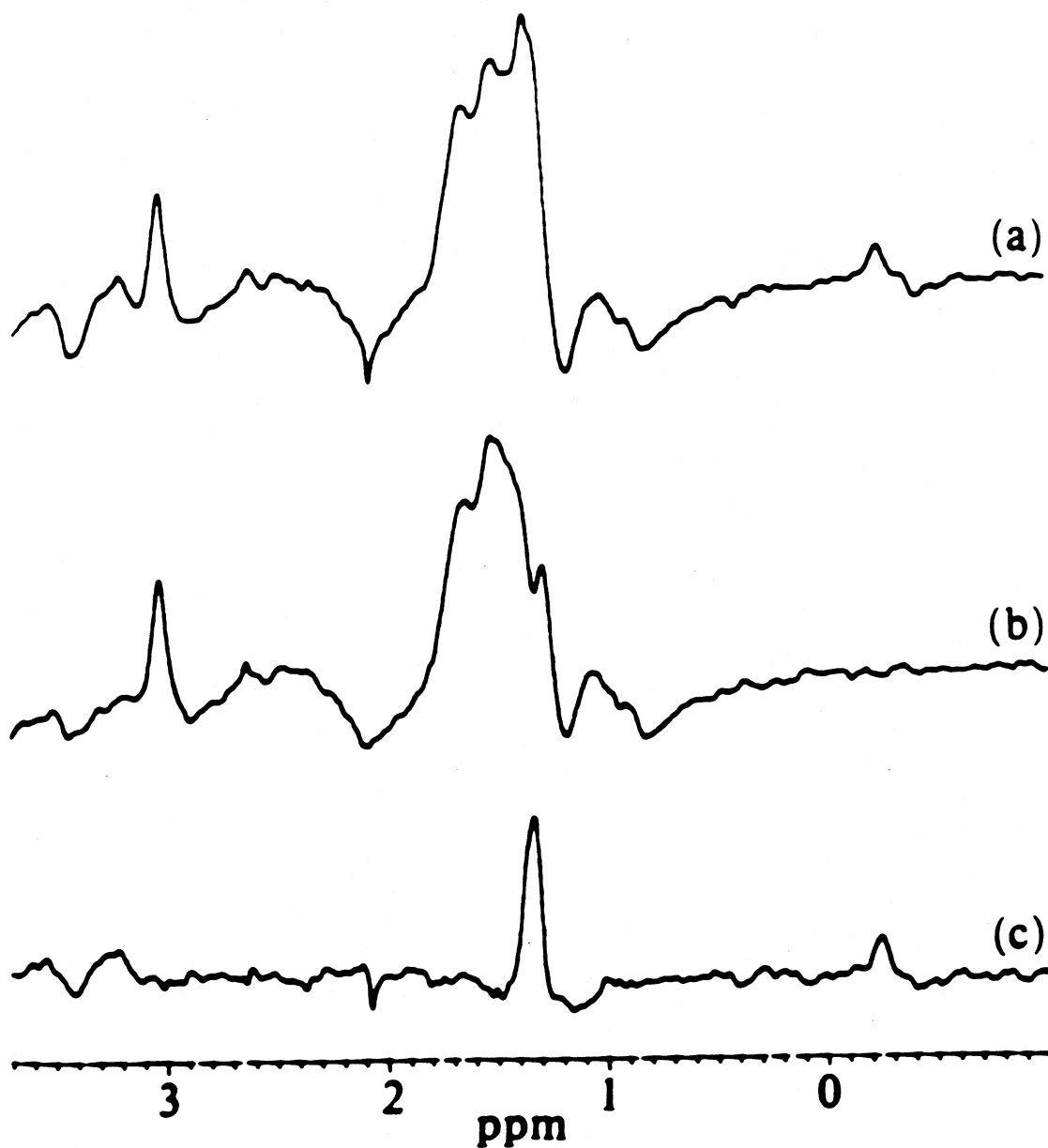


FIGURE 33. The ^1H NMR spectra obtained from the rat leg *in vivo* about 1 h after applying a ligation around the upper part of the leg. The spectra were obtained using the Hahn spin-echo sequence (90° - τ - 180° - τ -observe), and the phase of the 180° pulse relative to the 90° pulse was shifted by $+90^\circ$ and -90° on alternate scans. (a) Accumulation of 32 scans at intervals of 1.9 s using a 68-ms delay between the 90° and 180° pulses. Homonuclear decoupling ($\gamma B_1 = 50$ Hz) was applied at 4.11 ppm during the 136 ms (2τ) echo delay period. The lactate signal is obscured by the large fat peak. (b) As for (a) except that the irradiation during the echo delay was switched to the opposite side of the lactate CH_1 signal, i.e., to -1.47 ppm. (c) The difference spectrum (a) to (b), showing the lactate signal at 1.32 ppm. (From Williams, S. R., Gadian, D. G., Proctor, E., Sprague, D. B., and Talbot, D. F., *J. Magn. Reson.*, 63, 406, 1985. With permission.)

relatively short T_2 s, using a variety of the spin-echo sequence.¹⁴⁸ In addition, the large H_2O resonance can be suppressed significantly by a number of different methods including single frequency irradiation,¹⁴⁹ a Dante saturation pulse sequence,¹⁵⁰ and spin-echo sequences composed of frequency-selective Dante pulse trains.¹⁵¹ Using this methodology, ^1H NMR has been used to evaluate lactic acid formation in various tissues under different metabolic stresses.^{152,153} Figure 33 demonstrates the spectral resolution of the lactate resonance that can be achieved from the *in vivo* ^1H spectrum of a rat leg using a Hahn spin-echo sequence with selective proton decoupling.¹⁵⁴ As we have seen in Section II. A, two-dimensional (2-D) COSY methodology can

be used to help resolve a complex ^1H spectrum of plant tissue in a superfused state²¹ (see Figure 11). In this particular example, the one-dimensional (1-D) water-suppressed ^1H spectrum of carrot root tissue was of sufficiently good quality, i.e., line widths were relatively narrow, that molecular connectivities and dipolar coupling could be determined with the 2-D experiment *in vivo*. As we have seen in Figure 11 and Table 3, the spectrum is dominated by mobile, low molecular weight sugars, organic acids, amino acids, and ethanol.²¹ In addition, T_1 values and the chemical shift position of the B-protons of malate in carrot roots suggest that malate is located in a relatively viscous and acidic compartment.²¹

Another technique has recently been developed to exploit the sensitivity of the proton resonance in combination with the greater shift dispersion of the ^{13}C spectrum to observe metabolites that could not be resolved previously.¹⁵⁵ Observation of the ^{13}C -coupled protons during the specific decoupling of the attached ^{13}C nuclei and subsequently subtraction of the non- ^{13}C -decoupled proton spectrum yields an ^1H spectrum of the ^{13}C -labeled metabolite without the broad ^1H background resonances of the cell.¹⁵⁵ This method of indirect ^1H detection of ^{13}C NMR signals has one major drawback. Because of the overlap in resonance frequencies, one cannot single-frequency decouple unless the chemical shift difference between the ^{13}C resonances is much greater than the proton-carbon coupling constant. Figure 34 shows the ^1H difference spectra of *Saccharomyces cerevisiae* following incubation with ^{13}C -enriched acetate at ($\delta = 1.9$). Note that in the initial spectrum only the ^{13}C acetate ^1H resonance was present, but as ^{13}C acetate was consumed the ^{13}C -associated ^1H resonances of the subsequently labeled amino acids appeared. This technique is particularly useful for examining systems where rapid metabolic processes require that the NMR time constant for data acquisition be very short.

^{19}F NMR has seen limited application to *in vivo* studies because there are no naturally occurring fluorinated metabolites of sufficient concentration in plant or animal tissues to detect. There are, however, some fluorinated drugs in current use whose uptake has been examined by ^{19}F NMR. For example, some have been recently used for the study of malignant tumors.¹⁵⁶ Fluorinated anesthetics have also been studied in various tissues,¹⁵⁷ e.g., halothane and isoflurane, which have been utilized to differentiate normal and tumor tissue.¹⁵⁸

Fluorine compounds such as mono-, di- and trifluoromethylamine whose pKas are 8.5, 7.3, and 5.9, respectively, have been found to be effective spy molecules for assessing cytoplasmic pH.¹⁵⁹ All three can be loaded simultaneously into cells as methyl esters which permeate the plasma membrane easily. Once inside the cell, they are enzymatically hydrolyzed to the fluoroamino acids which are stable and noncytotoxic.¹⁶⁰ In combination, these pH indicators can determine intracellular vs. extracellular pH profiles over a wide range (>2 pH units) of extracellular pH.¹⁵⁷ Dimethylfluoroalanine is very useful as an internal pH indicator since its proton-decoupled spectrum is a doublet whose splitting is pH dependent.¹⁶¹ This is convenient since no other signal in the spectrum is required as a reference to measure the intracellular pH.

Symmetrically substituted difluoro derivatives of 1,2-bis-(*O*-aminophenoxy)-ethane-*N,N,N',N'*, primes tetraacetic acid (nFBAPTA) can be used as ^{19}F NMR probes for divalent cations.¹⁶² In particular, 4FBAPTA and 5FBAPTA show large ^{19}F NMR chemical shifts on chelating Ca^{2+} and since the two complexes show fast and slow exchange behavior, respectively, they can be used to determine the free intracellular Ca^{2+} concentrations. This measurement is unaffected by free Mg^{2+} concentrations <10 mM, by pH to 8, or by other contaminating ions such as Zn^{2+} , Fe^{2+} , or Mn^{2+} .¹⁶² As in the previous studies, these chelators are loaded as their corresponding methyl esters and are hydrolyzed within the cells. Since the 5FBAPTA derivatives display two ^{19}F shifts in the presence of Ca^{2+} (one for free and one for bound Ca^{2+}), it is easy to follow the change in intracellular Ca^{2+} concentration as a function of the area of these two resonances. Figure 35 shows the change in internal Ca^{2+} concentration after treatment of mouse thymocytes with succinyl Con A and A23187, which allows extracellular Ca^{2+} to flood the cells. In addition to the Ca^{2+} -binding affinities of 5FBAPTA, this molecule also has a ^{19}F pH-sensitive

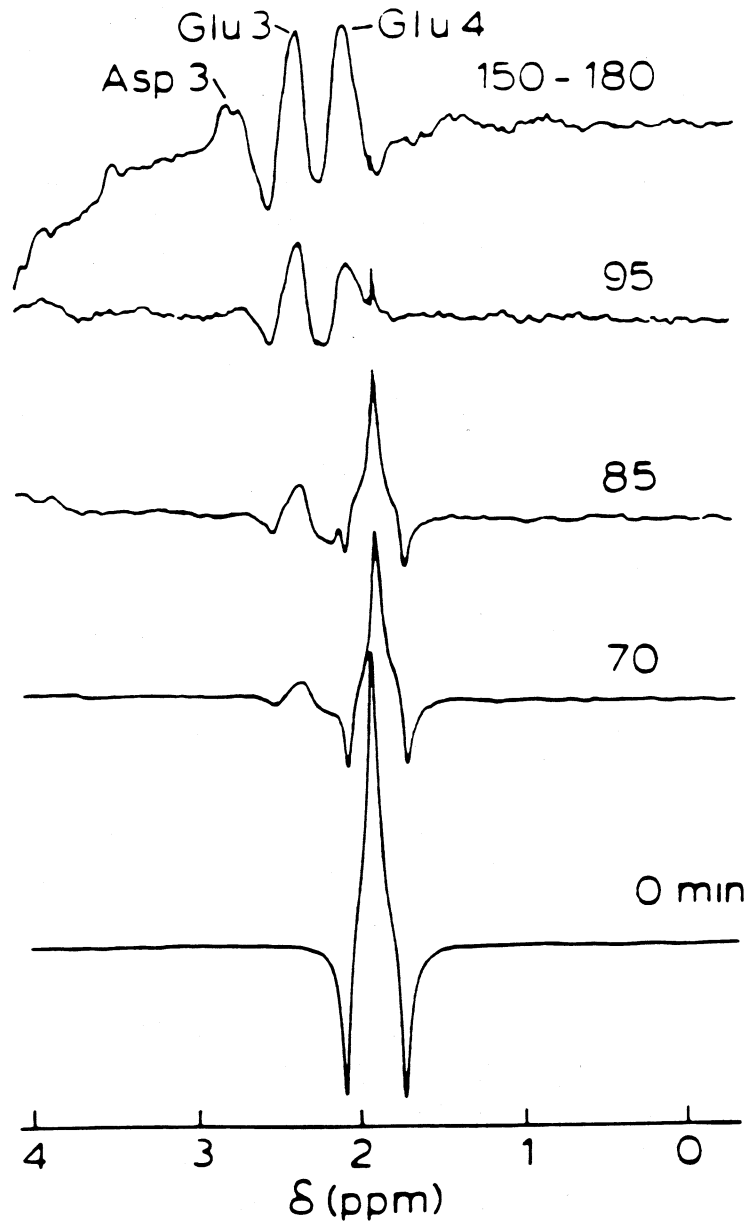


FIGURE 34. Time course of changes after oxygenation in the difference spectra obtained from the *S. cerevisiae* sample under conditions of broadband ^{13}C decoupling. Identified are signals arising from glutamate C_α , C_β , aspartate C_α , and acetate C_α with ^{13}C coupling to the observed ^1H resonances at 2.12 ppm (Glu H_α), 2.33 ppm (Glu H_β), and 2.87 ppm (Asp H_α). (From Sillerud, L. O., Alger, J. R., and Shulman, R. G., *J. Magn. Reson.*, 45, 142, 1981. With permission.)

shift (pKa 5.7) that can be useful for determining intracellular pH. Furthermore, both 4FBAPTA and 5FBAPTA can be used for studies with opaque cell suspensions and tissues that cannot be examined by fluorescence measurements. Present applications include lymphocytes, thymocytes, tumor cells, and rat hearts.¹⁶³ Unfortunately, problems of diffusing these chelators into plant cells has made this methodology thus far inapplicable to plant tissues,¹⁶⁴ presumably because of the presence of the cell wall. However, studies of plant cell protoplasts may prove more successful.

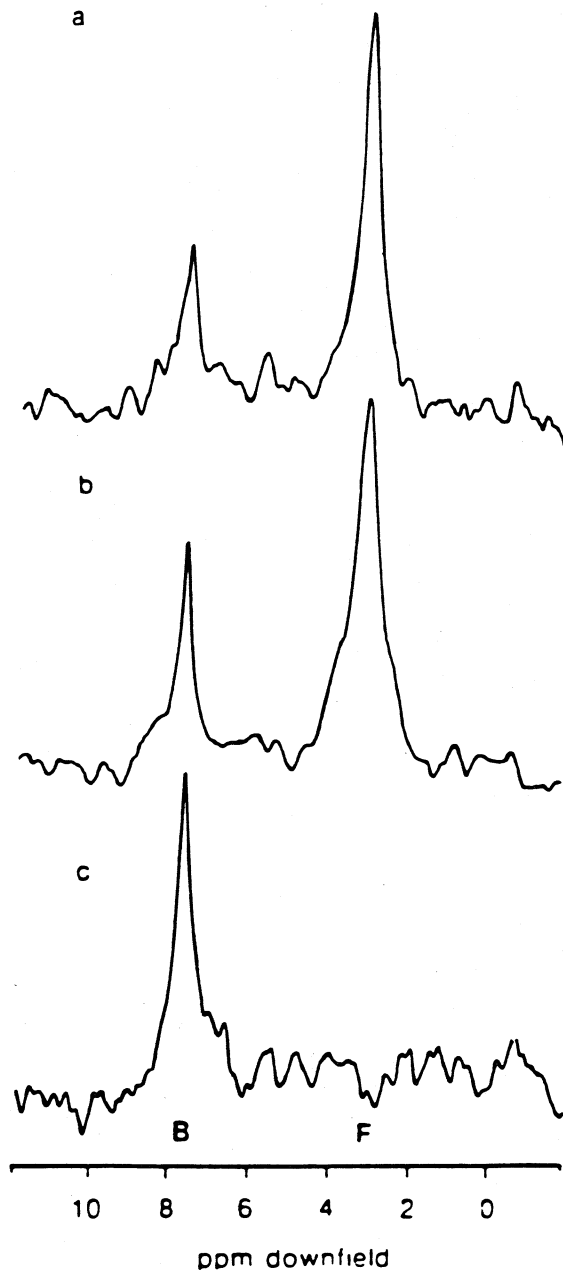


FIGURE 35. (a) ^{19}F spectrum at 37°C and 188.3 MHz of $[^1\text{H}]\text{5FBAPTA}$ in BALB/c mouse thymocytes accumulated in 20 min at 37°C . (b) Effect of addition of succinyl Con A at $100\ \mu\text{g}/\text{ml}$. (c) Effect of addition of $50\ \mu\text{M}$ A23187 to the same cell preparation. The intracellular 5FBAPTA is saturated with Ca^{2+} (B) and a single resonance at the Ca-5FBAPTA position is observed. F, resonance of 5FBAPTA without Ca^{2+} . (From Smith, G. A., Hesketh, R. T., Metcalfe, J. C., Feeney, J., and Morris, P. G., *Proc. Natl. Acad. Sci. U.S.A.*, 80, 7178, 1983. With permission.)

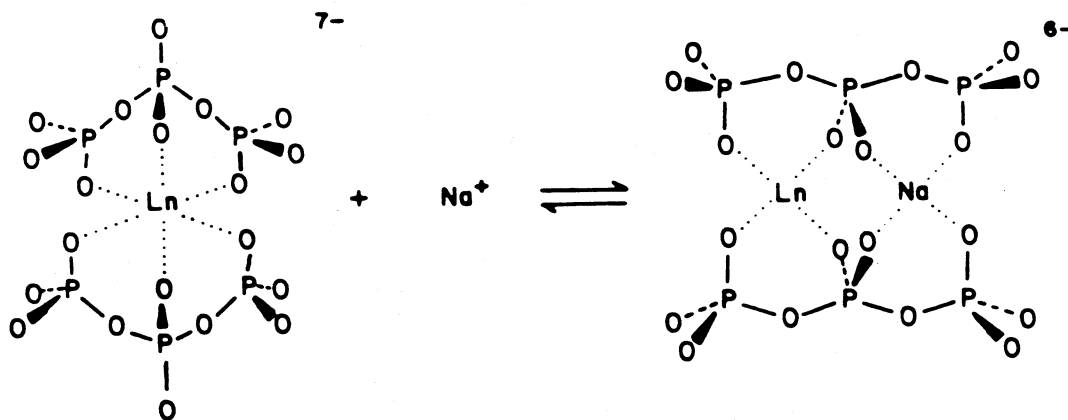


FIGURE 36. Hypothetical structures for $\text{Ln}(\text{PPP})_2^{7-}$ and $\text{Na}^+\cdot\text{Ln}(\text{PPP})_2^{6-}$. (From Chu, S. C., Pike, N. M., Fossel, E. T., Smith, T. W., Balschi, J. A., and Springer, C. S., Jr., *J. Magn. Reson.*, 56, 33, 1984. With permission.)

3. ^{23}Na and ^{39}K

In the past, the lack of spectral resolution has limited the utility of NMR to the study of intracellular Na^+ ions. The relatively small internal ^{23}Na resonance and the overwhelming extracellular ^{23}Na resonance occur at the same frequency in the spectra of intact cells, living tissues, organelles, and cell suspensions. Highly anionic hyperfine shift reagents such as bis(tripolyphosphate)dysprosium(III) $\text{Dy}(\text{PPP})_2^{7-}$ provide a convenient means whereby this problem can be circumvented, and separate NMR signals from intra- and extracellular sodium or potassium can be detected.¹⁶⁵⁻¹⁶⁸

Chu et al.¹⁶⁹ have published a hypothetical structure (shown in Figure 36) which portrays the possible type of interaction which alkali metal ions can undergo with lanthanide shift reagents. The ability to detect these separate resonances from internal and external sodium and potassium ions depends on the fact that a hyperfine shift in frequency will only be induced on the resonances of the sodium or potassium ions which are accessible to the shift reagent. Because of its very high ionic charge and subsequent inability (under most circumstances) to penetrate a cell membrane during the time course of typical NMR measurements, the agent remains outside of the cells. Therefore, only the extracellular sodium or potassium ions are affected and undergo a resonance shift.

The cytosolic enzymes of many plants are inhibited by high intracellular concentrations of sodium ion.¹⁷⁰ The manner in which various plant hybrids deal with sodium, especially its exclusion, represents a key feature in their ability to survive in saline environments. Salinity can increase drastically during periods of prolonged irrigation due to the salts which accumulate in the aqueous environment. The observation of ^{23}Na resonances provides a rapid, noninvasive method for the determination of sodium ion concentrations and distributions in cells. The data can essentially be acquired within seconds to a minute. Furthermore, the living tissue is not disturbed, extracted, or disrupted. Finally, influx and efflux rates can be monitored *in vivo* in the case of plants, plant tissues, and single cells. Minimally one can measure as little as 1.0 mM sodium ion concentrations with typical S/N ratios on the order of 10:1.

The external and internal sodium signals in corn roots were distinguished by means of a shift reagent, 3.0 mM $\text{Dy}(\text{PPP})_2^{7-}$.¹⁶⁶⁻¹⁶⁸ We see in Figure 37 that the two signals from the internal and the external sodium are well resolved. The uptake of sodium by the corn root is also readily apparent in the same figure as the intensity of the internal resonance increases with time of exposure to the salt.¹⁶⁸

The rates of Na^+ uptake can easily be monitored under conditions where respiration and/or metabolism are perturbed. In Figure 38 the relative rates of Na^+ influx are depicted for the same corn root system under a variety of metabolic states.¹⁶⁸ Na^+ ion influx is seen to decrease upon

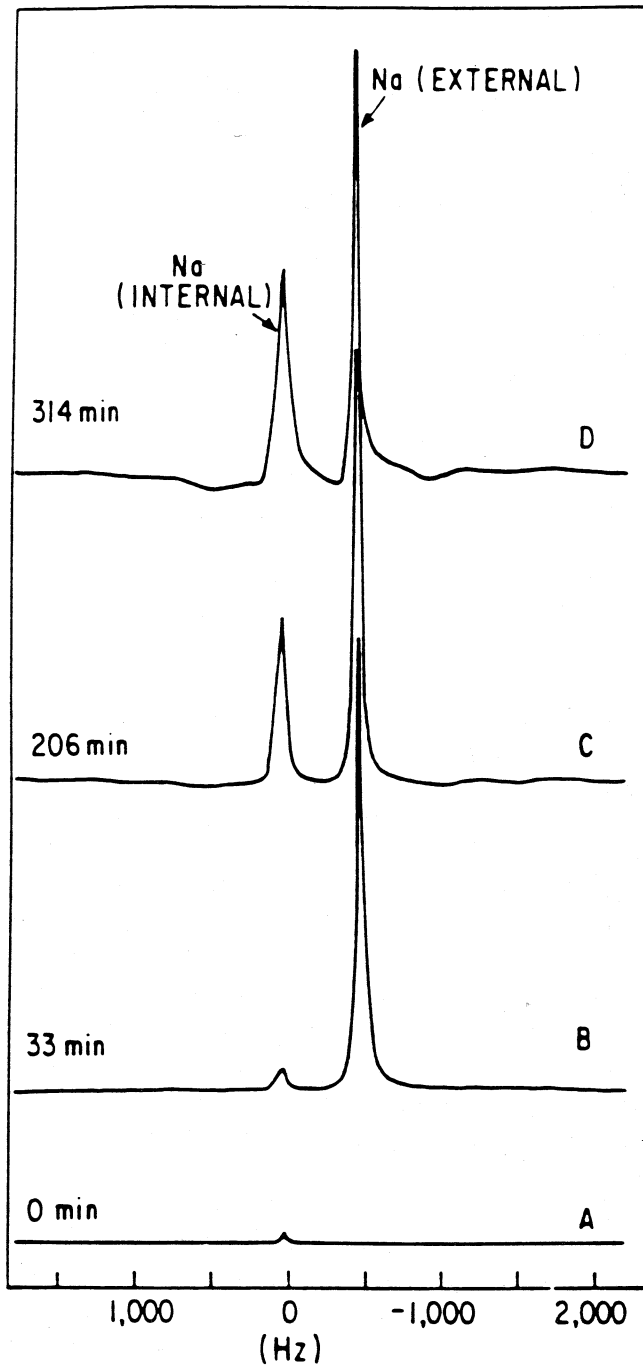


FIGURE 37. Sodium influx into aerobic root tissue. A total of 3.0 mM of $\text{Dy}(\text{PPP})_3$ was added along with the appropriate amount of NaCl to keep the concentration of Na^+ at 160 mM. Spectrum (A) represents the endogenous Na^+ concentration. Spectra (B), (C), and (D) represent the distribution of Na^+ between cellular and external spaces at the indicated time after the addition of shift reagent and NaCl. Each spectrum was time averaged for 10.83 min. Other experimental conditions used were frequency range 8 KHz; 16 K data points zero filled to 16 K; 548 transients per spectrum; repetition time 1.124 s; 28.5 ms (90° pulse); and zero broadening factor. (From Gerasimowicz, W. V., Tu, S., and Pfeffer, P. E., *Plant Physiol.*, 81, 925, 1986. With permission.)

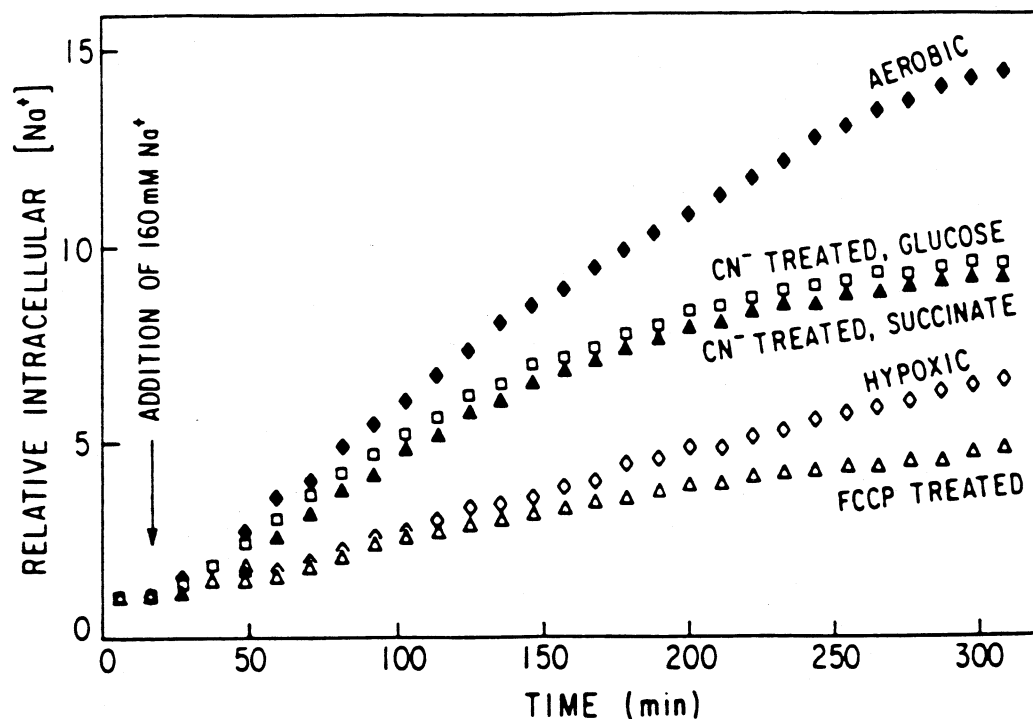


FIGURE 38. Relative rates of Na^+ influx under different conditions. The plant tissue was first treated as mentioned in Figure 37 except, in indicated cases, glucose was replaced by 25 mM Tris-succinate. Modifications during perfusion are as indicated in the figure. The intensities of the intracellular sodium resonances were normalized to the ^{23}Na signal observed for the roots prior to any addition of external Na^+ to the perfusion medium. The normalized intensities were plotted at the middle time of each spectral acquisition. (From Gerasimowicz, W. V., Tu, S., and Pfeffer, P. E., *Plant Physiol.*, 81, 925, 1986. With permission.)

treatment with CN^- and upon depression of ATP under the influence of hypoxia. Furthermore, when the roots are subjected to FCCP treatment, the uptake rate is even slower than that observed under anaerobic conditions.

Sillerud has studied the uptake and efflux of sodium ion in NaCl-adapted and -nonadapted millet (*Panicum miliaceum*) suspensions.¹⁷¹ Figure 39 shows the time dependence of the intracellular sodium concentration in suspensions of cultured millet cells as monitored by means of natural-abundance sodium-23 NMR. The efflux curve was explained on the basis of a biexponential fit. The implication inherent in this finding is the presence of two sodium compartments in the system. One compartment equilibrates rapidly with the medium, whereas the intracellular compartment equilibrates at a slower rate.¹⁷¹

Sillerud et al.¹³⁵ have studied sodium transport in roots from intact *Distichlis spicata*. This particular plant has the ability to thrive in highly saline environments such as salt marshes. However, the ability of such species to adapt to high, constant levels of sodium ion is not well characterized. When plants grown in 130 mM NaCl-containing medium were subjected to conditions where no sodium was available, the efflux curve shown in Figure 40 was obtained.¹³⁵ Once again biphasic kinetics were seen. Upon completion of the efflux experiments, the authors place the roots into media containing $\text{Dy}(\text{PPP})_2$ and NaCl in order to ascertain the dynamics of ion influx. Figure 41 shows the result. Therefore, one can readily begin to correlate plant saline stress adaptability with the measured ion transport and translocation rate data.

In a very unique study, simultaneous ^{23}Na and ^{31}P NMR spectra were acquired for a number of yeast suspensions.¹⁷² Before all of the NMR experiments were performed, the cells were preloaded with sodium. These particular yeast cells were also distinguished by the fact that no PP species were evident indicating that the cells were somewhat deficient in phosphorus. These cells were suspended in media which were low in sodium but contained inorganic phosphorus.

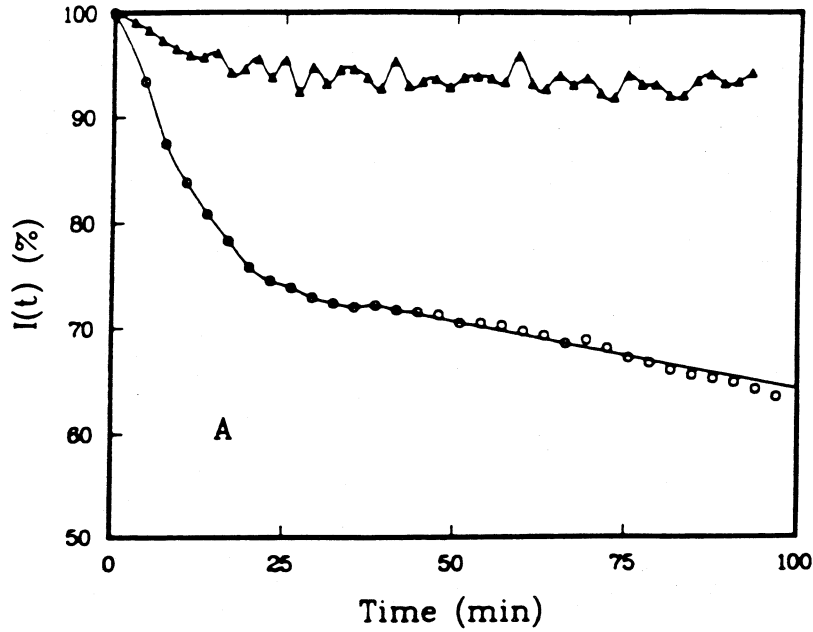


FIGURE 39. Net efflux of ^{23}Na in the presence of DyTp at pH 6.9 in the external medium. The percent change in integrals $I(t)(\%)$ of internal ^{23}Na peak vs. time is shown. For efflux the NaCl-adapted cells (O) were grown for 3 weeks on 130 mM NaCl and had resumed normal growth, while nonadapted cells (s) were preloaded for 5 d. (From Sillerud, L. O. and Heyser, J. W., *Plant Physiol.*, 75, 269, 2984. With permission.)

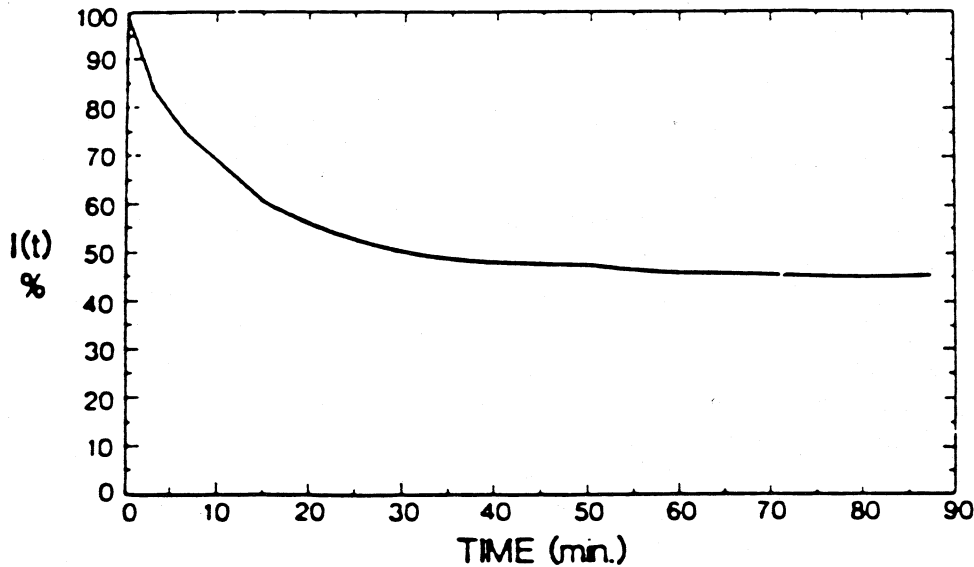


FIGURE 40. Time dependence of the intracellular sodium-23 NMR signal for *Distichlis spicata*. Seen here is sodium efflux from the roots of this whole plant after the roots were placed into a medium containing 0 mM NaCl and 5 mM DyTP. In this and the following figure, the plants were grown hydroponically on 130 mM NaCl and either washed extensively with sodium-free medium for the influx experiments, or placed directly into the NMR tube in sodium-free medium for the efflux runs. (From Sillerud, L. O., Heyser, J. W., Han, C. H., and Bitensky, M. W., *NMR in Living Systems*, Axenrod, T. and Ceccarelli, G., Eds., D. Reidel, New York, 1986. With permission.)

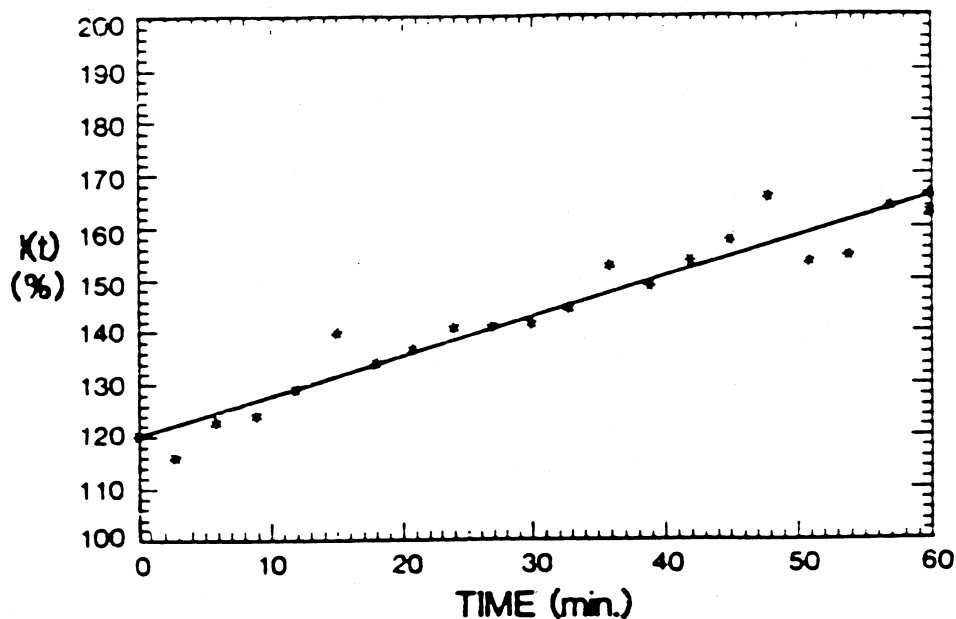


FIGURE 41. Influx of sodium into the roots of a salt-adapted whole plant, *Distichlis spicata*, as monitored with the aid of real-time sodium-23 NMR. (From Sillerud, L. O., Heyser, J. W., Han, C. H., and Bitensky, M. W., *NMR in Living Systems*, Axenrod, T. and Ceccarelli, G., Eds., D. Reidel, New York, 1986. With permission.)

The spectra obtained in these studies indicated that a net efflux of sodium occurred in all cases with a concomitant uptake of P_i . Such dual observation NMR experiments cannot be performed on standard NMR equipment typically available from vendors. The authors modified their instruments to include two entirely separate NMR transmitters, receiver channels, as well as pulse programmers and computers in order to observe and acquire data on the two nuclei simultaneously.¹⁷²

Several recent reports on sodium transport in bacteria have appeared.^{45,173,174} Shulman's group found that while extracellular sodium was completely visible in *Escherichia coli* by NMR, only 45% of the intracellular sodium could be accounted for in this fashion.⁴⁵ Internal sodium concentrations were found to be correlated with the development and maintenance of proton-driven Na^+/H^+ exchange mechanisms and/or intracellular pH condition.⁴⁵ Packer et al.¹⁷³ studied the effects of salt stress on the freshwater cyanobacterium *Synechococcus* 6311. Their findings indicated that when the bacteria were subjected to elevated levels of salt (0.5 M NaCl), NTP concentrations decreased while P_i and cytoplasmic pH both increased. The cell suspensions were illuminated during the spectral acquisition. The authors claim they can monitor light and dark reactions in such systems. However, an examination of the ^{23}Na spectra brings into question even qualitative interpretations of the data presented due to its relatively poor quality, i.e., extremely low intensity for the sodium and the unresolved nature of the internal and external sodium peaks in their spectra.¹⁷³

One cautionary note should also be sounded at this point. Martin et al.¹⁷⁴ recently studied the intracellular sodium ion concentration in amoeba from the slime mold *Dictyostelium discoideum*. Two distinct peaks could be distinguished in these systems with the use of shift reagents. Cells which had been starved of Na^+ could easily be reloaded. However, the most interesting observation made by the authors was that $Dy(PPP)_2^{-7}$ was being degraded during the NMR experiments. They concluded that an acid phosphatase produced by the amoeba was responsible for this degradation. In all such experiments with living systems, one must ascertain the toxicity (if any) of the shift reagent on the system and establish the stability of the reagents being employed.

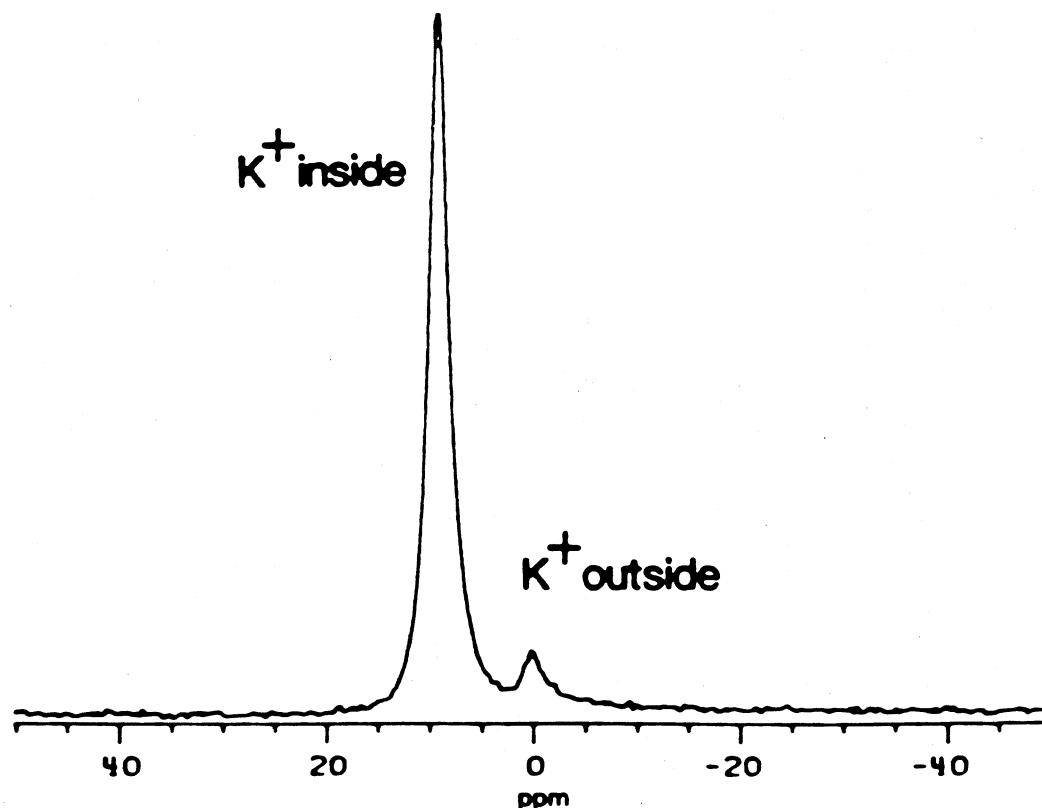


FIGURE 42. ^{39}K NMR spectrum at 16.9 MHz, 25°C in the same solution as above. A total of 35,000 pulses were collected with an acquisition time of 0.15. (Spectra courtesy of Peter Lundberg and Hans J. Vogel.) (From Braunlin, W. H., Drakenberg, T., and Forsén, S., *Current Topics in Bioenergetics*, Vol. 14, Academic Press, New York, 1985, 97. With permission.)

Intracellular ^{39}K concentrations (if visible) can also be studied by the same shift reagent methods described above. However, the ^{39}K nucleus presents more severe problems to the NMR spectroscopist than does ^{23}Na . The receptivity of potassium is lower than any other alkali metal in terms of the NMR experiment. On the other hand, the concentration of potassium in most cell types is generally an order of magnitude greater than that of sodium. Therefore, some compensation is apparent. We show an example of the separation of intracellular and extracellular ^{39}K signals in the presence of shift reagent which is possible from the spectrum of human erythrocytes in Figure 42.⁴⁴ Very little has been done to exploit ^{39}K NMR in agriculture. Some studies are being carried out in the medical areas.¹⁷⁵ If one can correct for losses in signal intensities, a vast potential exists for this technique in all areas of agricultural science (analogous to the work ongoing in the medical areas). At the time of this writing no literature exists on ^{39}K NMR in areas of whole plants, plant tissues, and plant metabolism.

REFERENCES

1. Moon, R. B. and Richards, J. H., Determination of intracellular pH by ^{31}P nuclear magnetic resonance, *J. Biol. Chem.*, 248, 7276, 1973.
2. Baxter, R. L., Microbiological applications of NMR spectroscopy. I, *Microbiol. Sci.*, 2, 203, 1985; Baxter, R. L. and Baxter, R. L., Microbiological applications of NMR spectroscopy. II, *Microbiol. Sci.*, 2, 340, 1985.

3. Shulman, R. G., Brown, T. R., Ugurbil, K., Ogawa, S., and Cohen, S. M., Cellular application of ^{31}P and ^{13}C nuclear magnetic resonance. *Science*, 205, 160, 1979.
4. Loughman, B. C. and Ratcliffe, R. G., Nuclear magnetic resonance and the study of plants, in *Advances in Plant Nutrition*, Vol. 1, Praeger, New York, 1984; Roberts, J. K. M., Study of plant metabolism *in vivo* using NMR spectroscopy. *Annu. Rev. Plant Physiol.*, 35, 375, 1984.
5. Degane, H., Laughlin, M., Campbell, S., and Shulman, R. G., Kinetics of creatine kinase in heart: ^{31}P NMR saturation- and inversion-transfer study. *Biochemistry*, 24, 5510, 1985.
6. Alger, J. R., Behar, K. L., Rothman, D., and Shulman, R. G., *J. Magn. Reson.*, 56, 334, 1984.
7. Roberts, J. K. M. and Jardetzky, O., Monitoring of cellular metabolism by NMR. *Biochim. Biophys. Acta*, 639, 53, 1981.
8. Gadian, D. G., *Nuclear Magnetic Resonance and Its Applications to Living Systems*. Clarendon Press, Oxford, 1982.
9. Avison, M. J., Hetherington, H. P., and Shulman, R. G., Applications of NMR to studies of tissue metabolism. *Annu. Rev. Biophys. Chem.*, 15, 337, 1986.
10. Becker, E. D., High resolution NMR, *Theory and Chemical Applications*. Academic Press, New York, 1980.
11. Shaw, D., *Fourier Transform NMR Spectroscopy*. Elsevier, Amsterdam, 1979.
12. Sanders, J. K. M. and Hunter, B. K., *Modern NMR Spectroscopy a Guide for the Chemist*. Oxford University Press, Oxford, 1987.
13. Roberts, J. K. M., Ray, P. M., Jardetzky, N. W., and Jardetzky, O., Estimation of cytoplasmic and vacuolar pH in higher plants cells by ^{31}P NMR. *Nature*, 283, 870, 1980.
14. Pfeffer, P. E., Tu, S.-I., Gerasimowicz, W. V., and Cavanaugh, J. R., *In vivo* ^{31}P NMR studies of corn root tissue and its uptake of toxic metals. *Plant Physiol.*, 80, 77, 1986.
15. Gard, J. K. and Ackerman, J. H., A ^{31}P NMR external reference for intact biological systems. *J. Magn. Reson.*, 51, 124, 1983.
16. Pfeffer, P. E., Tu, S.-I., Gerasimowicz, W. V., and Boswell, R. T., Effects of aluminum on the release and/or immobilization of soluble phosphate in corn root tissues. *Planta*, 172, 200, 1987.
17. Batley, M. and Redmond, J. W., ^{31}P NMR reference standards for aqueous samples. *J. Magn. Reson.*, 49, 172, 1982.
18. Ratcliffe, R. G., NMR and the inorganic composition of plants. *Inorg. Biochem.*, 28, 347, 1986.
19. Lee, R. B. and Ratcliffe, R. G., Development of an aerobic system for use in plant tissue NMR experiments. *Exp. Bot.*, 34, 1213, 1983.
20. Roby, C., Martin, J. B., Bligny, R., and Douce, R., Biochemical changes during sucrose deprivation in higher plant cells. II. Phosphorus-31 nuclear magnetic resonance studies. *J. Biol. Chem.*, 262, 5000, 1987.
21. Fan, W.-M. T., Higashi, R. M., and Lane, A., Monitoring hypoxic metabolism in superfused plant tissue by *in vivo* ^1H NMR. *Arch. Biochem. Biophys.*, 251, 674, 1986.
22. den Hollander, J. A., Ugurbil, R., Brown, T. R., and Shulman, R. G., Phosphorus-31 nuclear magnetic resonance studies of the effect of oxygen upon glycolysis in yeast. *Biochemistry*, 20, 5871, 1981.
23. Boulanger, Y., Vinay, D., Phan Viet, M. T., Guardo, R., and Desroches, M., An improved perfusion system for NMR study of living cells. *Magn. Reson. Med.*, 2, 495, 1985.
24. Geoffrion, Y., Lareau, S., Deslauriers, R., Butler, K., Pass, M., and Smith, I. C. P., A versatile perfusion technique for metabolic studies by NMR. *Magn. Res. Med.*, 2, 65, 1985.
25. Balaban, R. S., Kantor, H. L., and Ferretti, J. A., *In vivo* flux between phosphocreatine and adenosine triphosphate determined by two-dimensional phosphorus NMR. *Biol. Chem.*, 21, 12787, 1983.
26. Chance, B., Clark, B. J., Nioka, S., Subramanian, H., Maris, J. M., Argov, Z., and Bode, H., Phosphorus nuclear magnetic resonance spectroscopy *in vivo*. *Circulation*, 72 (4), 103, 1985.
27. Martin, J. B., Bligny, R., Rebeille, F., Douce, R., Leguay, J. J., Mathiew, Y., and Guern, J., ^{31}P nuclear magnetic resonance study of intracellular pH of plant cells cultivated in liquid medium. *Plant Physiol.*, 70, 1156, 1982.
28. Stothers, J. B., *Carbon-13 NMR Spectroscopy*. Academic Press, New York, 1972.
29. Martin, F., Monitoring plant metabolism by ^{13}C , ^{15}N and ^{14}N nuclear magnetic resonance spectroscopy. A review of the applications to algae, fungi and higher plants. *Physiol. Veg.*, 4, 463, 1985.
30. Reinhard, B. and Gunther, H., Modern pulse methods in high-resolution NMR spectroscopy. *Angew. Chem. Int. Ed. Engl.*, 22, 350, 1983.
31. Walker, T. E., Han, C. H., Kollman, V. H., London, R. E., and Matwiyoff, N. A., ^{13}C NMR studies of the biosyntheses by microbacterium ammoniaphilum of L-glutamate selectively enriched with carbon-13. *J. Biol. Chem.*, 257, 1189, 1982.
32. Ashworth, D. J. and Mettler, I. J., Direct observation of glycine metabolism in tobacco suspension cells by carbon-13 NMR spectroscopy. *Biochemistry*, 23, 2252, 1984.
33. Stinson, E. E., Wise, W. B., Moreau, R. A., Jurewicz, A. J., and Pfeffer, P. E., Alternariol: evidence for biosynthesis via norlichexanthone. *Can. J. Chem.*, 64, 1590, 1986.
34. Martin, F., Nitrogen-15 NMR studies of nitrogen assimilation and amino acid biosynthesis in the ectomycorrhizal fungus *cenococcum graniforme*. *FEBS Lett.*, 182, 350, 1985.

35. Mason, J., Nitrogen NMR spectroscopy in inorganic, organometallic and bio-inorganic chemistry, *Chem. Rev.*, 81, 205, 1981.
36. Belton, P. S., Lee, R. B., and Ratcliffe, R. G., A ^{14}N NMR study of inorganic nitrogen metabolism in barley, maize and pea roots, *J. Exp. Bot.*, 36, 190, 1985.
37. Brown, F., Campbell, I. D., and Kuchel, P. W., Human erythrocyte metabolism studies by ^1H spin echo NMR, *FEBS Lett.*, 82, 12, 1977.
38. Kime, M. J., Ratcliffe, R. G., and Williams, R. J. P., The application of ^{31}P nuclear magnetic resonance to higher plants, *J. Exp. Bot.*, 33, 656, 1982.
39. Schleich, T., Willis, J. A., and Matson, G. B., Longitudinal (T_1) relaxation times and phosphorus metabolites in bovine and rabbit lens, *Exp. Eye Res.*, 39, 455, 1984.
40. Lee, R. B. and Ratcliffe, R. G., Phosphorus nutrition and the intracellular distribution of inorganic phosphate in pea root tips. A quantitative study using ^{31}P -NMR, *J. Exp. Bot.*, 34, 1222, 1983.
41. Reid, R. J., Loughman, B. C., and Ratcliffe, R. G., ^{31}P NMR measurements of cytoplasmic pH changes in maize root tips, *J. Exp. Bot.*, 36, 889, 1985.
42. Kanamori, K., Legerton, T. L., Weiss, R. L., and Roberts, J. D., Nitrogen-15 spin-lattice relaxation times of amino acids in *Neurospora crassa* as a probe for intracellular environment, *Biochemistry*, 21, 4916, 1982.
43. Kanamori, K. and Roberts, J. D., ^{15}N NMR studies of biological systems, *Acc. Chem. Res.*, 16, 35, 1983.
44. Braunlin, W. H., Drakenberg, T., and Forsén, S., Metal in NMR: application to biological systems, in *Current Topics in Bioenergetics*, Vol. 14, Academic Press, New York, 1985, 97.
45. Castle, A. M., Macnab, R. M., and Shulman, R. G., Measurement of intracellular sodium concentration and sodium transport in *Escherichia coli* by ^{23}Na NMR, *J. Biol. Chem.*, 261, 3288, 1986.
46. Gupta, R. K., NMR spectroscopy of intracellular sodium ions in living cells, in *NMR in Living Systems*, Axenrod, T. and Ceccurelli, G., Eds., D. Reidel, New York, 1986, 291.
47. Rooney, W. D., Barbara, T. M., and Springer, C. S., Jr., Two-dimensional double-quantum NMR spectroscopy of isolated spin 3/2 systems, *J. Am. Chem. Soc.*, 110, 674, 1988.
48. Ratcliffe, R. G., The application of NMR methods to plant tissues, *Methods Enzymol.*, 148, 683, 1986.
49. Navone, G., Shulman, R. G., Yamane, T., Eccleshall, T. R., Lam, K.-B., Baronsky, J. J., and Murmur, J., P-31 NMR studies of wild-type and glycolytic pathway mutants of *Saccharomyces cerevisiae*, *Biochemistry*, 21, 4487, 1979.
50. Boyd, R. K., DeFreitas, A. S. W., Hoyle, J., McCulloch, A. W., McInnes, A. G., Rogerson, A., and Walter, J. A., Glycerol 1, 2-cyclic phosphate in centric diatoms, *J. Biol. Chem.*, 262, 12406, 1987.
51. Batley, M., Redmond, J. W., Djordjevic, S. P., and Rolfe, B. C., Characterization of glycerophosphorylated cyclic β -1,2-glucans from fast-growing Rhizobium species, *Biochim. Biophys. Acta*, 901, 119, 1987.
52. Turner, J. F. and Turner, D. H., The regulation of glycolysis and the pentose phosphate pathway, in *The Biochemistry of Plants*, Vol. 2, Davies, D. D., Ed., Academic Press, New York, 1980, 279.
53. Scarpa, A., in *Membrane Transport in Biology*, Giebish, G., Tosteson, D. C., and Ussing, H. H., Eds., Springer-Verlag, Berlin, 1979, 263.
54. Preiss, J. and Levi, C., in *Proc. 4th Int. Congr. Photosynthesis*, Hall, D. O., Coombs, J., and Goodwin, T. W., Eds., The Biochemical Society, London, 1982, 457.
55. Rebeillé, F., Bligny, R., and Douce, R., Regulation of Pi uptake by *Acer pseudoplatanus* cells, *Arch. Biochem. Biophys.*, 219, 371, 1982.
56. Jacob, G. S., Schaefer, J., Stejskal, E. O., and McKay, R. A., Solid state NMR determination of glyphosate metabolism in a *Pseudomonas* sp., *J. Biol. Chem.*, 260, 5899, 1985.
57. Slonczewski, J. L., Rosen, B. P., Alger, J. R., and Macnab, R. M., pH homeostasis in *Escherichia coli*: measurement by ^{31}P NMR of methylphosphonate and phosphate, *Proc. Natl. Acad. Sci. U.S.A.*, 78, 6271, 1981.
58. Kushmerick, M. J. and Meyer, R. A., *Am. J. Physiol.*, 248, C542, 1985.
59. Roberts, J. K. M., Jardetzky, N. W., and Jardetzky, O., Intracellular pH measurements by ^{31}P NMR. Influence of factors other than pH on ^{31}P chemical shifts, *Biochemistry*, 20, 5389, 1981.
60. Ogawa, S., Rottenberg, H., Brown, T. R., Shulman, R. G., Castillo, C. L., and Glynn, P., *Proc. Natl. Acad. Sci. U.S.A.*, 75, 1796, 1978.
61. Gupta, R. K., Gupta, P., Yushok, W. D., and Rose, Z., On the non-invasive measurement of intracellular free magnesium by ^{31}P NMR spectroscopy. High-resolution phosphorus-31 nuclear magnetic resonance study of rat liver mitochondria, *Physiol. Chem. Phys. Med. NMR*, 15, 265, 1983.
62. Sondheimer, G. M., Kuhn, W., and Kalbitzer, H. R., Observation of Mg^{2+} -ATP and uncomplexed ATP in slow exchange by ^{31}P -NMR at high magnetic fields, *Biochem. Biophys. Res. Commun.*, 134, 1379, 1986.
63. Cohen, S. M., Ogawa, S., Rothenberg, H., Glynn, P., and Yamane, T., *Nature*, 273, 554, 1978.
64. Mahler, H. R. and Cordes, E. H., *Biological Chemistry*, Harper & Row, New York, 1966, 420.
65. Pfeffer, P. E., Tu, S.-I., Gerasimowicz, W. V., and Boswell, R. T., Role of the vacuole in metal ion trapping as studied by *in vivo* ^{31}P NMR spectroscopy, in *Plant Vacuoles*, Marin, B., Ed., Plenum Press, New York, 1987, 349.
66. Samofus, B. and Schwimmer, S., Phytic acid as a phosphorus reservoir in the developing potato tuber, *Nature*, 194, 578, 1962.

67. McCain, D. C., ³¹P-NMR study of turnip seed germination and sprout growth inhibition by peroxydisulfate ion, *Biochim. Biophys. Acta.* 783, 231, 1983.
68. Defini, M., Angeline, R., Bruno, F., Conti, F., Dicocco, M. E., Guildiani, A. M., and Manes, F., Phosphate metabolites in germinating lettuce seeds observed by ³¹P NMR spectroscopy, *Cell. Mol. Biol.*, 31, 385, 1985.
69. Hendrix, D. L., Radin, J. W., and Nieman, R. A., Intracellular pH of cotton embryos and seed coats during fruit development determined by ³¹P NMR spectroscopy, *Plant Physiol.*, 85, 588, 1987.
70. Busa, W. B., Cellular dormancy and the scope of pH mediated metabolic regulation, in *Intracellular pH: Measurement and Regulation*. Alan R. Liss, New York, 1982, 64.
71. Aducci, P., Federico, R., Carpinelli, G., and Podo, F., Temperature dependence of intracellular pH in higher plant cells, *Planta*, 156, 579, 1982.
72. Roberts, J. K. M., Wemmer, D., Ray, P. N., and Jardetzky, O., Regulation of cytoplasmic and vacuolar pH in maize root tips under different experimental conditions, *Plant Physiol.*, 69, 1344, 1982.
73. Reid, R. J., Loughman, B. C., and Ratcliffe, R. G., ³¹P NMR measurements of cytoplasmic pH changes in maize root tips, *J. Exp. Bot.*, 36, 889, 1985.
74. Reid, R. J., Field, L. D., and Pitman, M. G., Effects of external pH, fusicoccin and butyrate on the cytoplasmic pH in barley root tips measured by ³¹P-NMR spectroscopy, *Planta*, 166, 341, 1985.
75. Wofender, J. and Wellburn, A. R., Cellular readjustment of barley seedlings to simulated acid rain, *New Phytol.*, 104, 97, 1986.
76. Jackson, P. C., Pfeffer, P. E., and Gerasimowicz, W. V., Use of ³¹P NMR to assess effects of DNP on ATP levels *in vivo* in barley roots, *Plant Physiol.*, 81, 1130, 1986.
77. Torimitsu, K., Hayashi, M., Ohta, E., and Sakata, M., Effect of K⁺ and H⁺ stress and role of Ca²⁺ in the regulation of intracellular K⁺ concentration in mung bean, *Physiol. Plant.*, 63, 247, 1985.
78. Hughes, W. A., Bociek, S. M., Barrett, J. N., and Ratcliffe, R. G., An investigation of the growth characteristics of oil-palm (*Elaeis guineensis*) suspension cultures using ³¹P NMR, *Biosci. Rep.*, 3, 1141, 1983.
79. Guern, J., Mathieu, Y., Pean, M., Corinne, P., Beloeil, J.-C., and Lallemand, J.-Y., Cytoplasmic pH regulation in *Acer pseudoplatanus* cells, *Plant Physiol.*, 82, 840, 1986.
80. Ojalva, J., Roken, J. S., Navon, G., and Goldberg, I., ³¹P NMR study of elicitor treated *Phaseolus velgans* cell suspension cultures, *Plant Physiol.*, 85, 716, 1987.
81. Mitsumori, F., Yoneyama, T., and Ito, O., Phosphorus-31 NMR studies on higher plant tissue, *Plant Sci.*, 38, 87, 1985.
82. Menegus, F. and Fronza, G., Modulation of glycerophosphorylcholine and glycerophosphorylethanolamine in rice shoots by the environment oxygen level, *FEBS Lett.*, 187, 151, 1985.
83. Roberts, J. K. M., Lane, A. N., Clark, R. A., and Nieman, R. H., Relationship between the rate of synthesis of ATP and the concentration of reactants and products of ATP hydrolysis in maize root tips, determined by ³¹P NMR, *Arch. Biochem. Biophys.*, 240, 712, 1985.
84. Alger, J. R. and Shulman, R. G., *Q. Rev. Biophys.*, 17, 83, 1984.
85. Roberts, J. K. M., Wemmer, D., and Jardetzky, O., Measurement of mitochondrial ATPase activity in maize root tips by saturation transfer ³¹P NMR, *Plant Physiol.*, 74, 632, 1984.
86. Shoubridge, E. A., Briggs, R. W., and Radda, G. K., ³¹P NMR saturation transfer measurements of the steady state rates of creatine kinase and ATP synthetase in rat brain, *FEBS Lett.*, 140, 288, 1982.
87. Dawson, M. J. and Gadian, D. G., Studies of the biochemistry of contracting and relaxing muscle by the use of P-31 NMR in conjunction with other techniques, *Philos. Trans. R. Soc. B.*, 289, 445, 1980.
88. Hanson, J. B., Bertagnoli, B. L., and Shepard, W. D., Phosphate-induced stimulation of acceptorless respiration in corn mitochondria, *Plant Physiol.*, 50, 347, 1972.
89. Rebeille, F., Bligny, R., Martin, J. B., and Douce, R., Effect of sucrose starvation on sycamore (*Acer pseudoplatanus*) cell carbohydrates and Pi status, *Biochem. J.*, 226, 679, 1985.
90. Roby, C., Martin, J. B., Bligny, R., and Douce, R., Biochemical changes during sucrose deprivation in higher plant cells. II. Phosphorus-31 NMR studies, *J. Biol. Chem.*, 262, 5000, 1987.
91. Dorne, A. J., Bligny, R., Rebeille, F., Roby, C., and Douce, R., Fatty acid disappearance and phosphorylcholine accumulation in higher plant cells after a long period of sucrose deprivation, *Plant Physiol Biochem.*, 25, 589, 1987.
92. Brodelius, P. and Vogel, H. J., A phosphorus-31 NMR study of phosphate uptake and storage in cultured *Catharanthus roseus* and *Daucus carota* plant cells, *J. Biol. Chem.*, 260, 3556, 1985.
93. Nicolay, K., Scheffers, W. A., Bruinenberg, P. M., and Kaptein, R., *In vivo* ³¹P NMR studies of the role of the vacuole in phosphate metabolism of yeasts, *Arch. Microbiol.*, 134, 270, 1983.
94. Greenfield, N. J., Hussain, M., and Lenard, J., Effects of growth state and amines on cytoplasmic and vacuolar pH, phosphate and polyphosphate levels in *Saccharomyces cerevisiae*: a ³¹P-NMR study, *Biochim. Biophys. Acta.* 926, 205, 1987.
95. Cassone, A., Carpinelli, G., Angiolella, L., Maddaluno, G., and Podo, F., ³¹P NMR study of growth and dimorphic transition in *Candida albicans*, *J. Gen. Microbiol.*, 129, 1569, 1983.
96. Roberts, J. K. M., Linker, C. S., Benoit, A. G., Jardetzky, O., and Nieman, R. H., Salt stimulation of phosphate uptake in maize root tips studied by ³¹P NMR, *Plant Physiol.*, 74, 947, 1984.

97. **Ben-Hayyim, G. and Navon, G.**, Phosphorus-31 NMR studies of wild-type and NaCl-tolerant citrus cells. *J. Exp. Bot.*, 36, 1877, 1985.
98. **Foy, C. D., Chaney, R. L., and White, M. C.**, The physiology of metal toxicity in plants. *Annu. Rev. Plant Physiol.*, 29, 511, 1978.
99. **Foy, C. D.**, The physiology of plant adaptation to mineral stress. *Iowa State J. Res.*, 57, 355, 1983.
100. **Maas, E. V.**, Calcium uptake by excised maize roots and interactions with alkali cations. *Plant Physiol.*, 44, 985, 1969.
101. **Hussain, F., Overstreet, R., and Jacobson, L.**, The influence of hydrogen ion concentration on cation absorption by barley roots. *Plant Physiol.*, 29, 234, 1954.
102. **Loughman, B. C.**, The application of *in vivo* techniques in the study of metabolic aspects of ion absorption in crop plants. *Plant Soil*, 99, 63, 1987.
103. **Haug, A.**, Molecular aspects of aluminium toxicity. *Crit. Rev. Plant Sci.*, 1, 345, 1984.
104. **Sirkar, S. and Amin, J. V.**, Influence of auxin on respiration of manganese toxic cotton plants. *Indian J. Exp. Biol.*, 17, 618, 1979.
105. **Dwek, R. A.**, *NMR in Biochemistry*. Clarendon Press, Oxford, 1973.
106. **Kime, M. J., Loughman, B. C., and Ratcliffe, R. G.**, The application of ³¹P NMR to higher plant tissue. II. Detection of intracellular changes. *J. Exp. Bot.*, 33, 670, 1982.
107. **Roberts, J. K. M., Callis, J., Jardetzky, O., Walbot, U., and Freeling, M.**, Cytoplasmic acidosis as a determinant of flooding intolerance in plants. *Proc. Natl. Acad. Sci. U.S.A.*, 81, 6029, 1984.
108. **Kopp, S. J., Prentice, R. C., Glonek, T., Feliksik, J. M., and Tow, J. P.**, Cadmium interaction with sarcoplasmic inorganic phosphate detected in the intact isolated heart. in *Trace Substances in Environmental Health, Part XVII*. Hemphill, D. D., Ed., University of Missouri Press, Columbia, MO, 1982, 25.
109. **Racker, E.**, Transport of ions. *Chem. Rev.*, 12, 338, 1979.
110. **Roby, C., Bligny, R., Douce, R., Tu, S.-I., and Pfeffer, P. E.**, Facilitated transport of Mn^{2+} in sycamore (*Acer pseudoplatanus*) cells and excised maize root tips. A comparative *in vivo* ³¹P study. *Biochem. J.*, 252, 401, 1988.
111. **Kallas, T. and Dahlquist, F. W.**, Phosphorus-31 NMR analysis of internal pH during photosynthesis in the *Cyanobacterium synechococcus*. *Biochemistry*, 20, 5900, 1981.
112. **Foyer, C., Walker, D., Spencer, C., and Mann, B.**, Observations on the phosphate status and intracellular pH of intact cell, protoplasts and chloroplasts from photosynthetic tissue using phosphorus-31 NMR. *Biochem. J.*, 202, 429, 1982.
113. **Waterton, J. C., Bridges, I. G., and Irving, M. P.**, Intracellular compartmentation detected by ³¹P-NMR in intact photosynthetic wheat-leaf tissue. *Biochim. Biophys. Acta*, 763, 315, 1983.
114. **Foyer, C. and Spencer, C.**, Observations on the phosphorus status of photosynthetic tissue using phosphorus-31 NMR. *Agric. Res. Council. Rep. Photosynth. Group*, 24, 1982.
115. **Foyer, C. and Spencer, C.**, The relationship between phosphate status and photosynthesis in leaves. *Planta*, 167, 369, 1986.
116. **Mitsumori, F. and Osamu, I.**, Phosphorus-31 NMR studies of photosynthesizing *Chlorella*. *FEBS Lett.*, 174, 248, 1984; **Sianoudis, J., Kusel, A. C., Meyer, A., Grimme, L. H., and Leibfritz, D.**, The cytoplasmic pH in photosynthesizing cells of the green alga *Chlorella fusca*. measured by P-31 NMR spectroscopy. *Arch. Microbiol.*, 147, 25, 1987.
117. **Kuchitsu, K., Oh-hama, T., Tsuzuki, M., and Miyachi, S.**, Detection and characterization of acidic compartments (vacuoles) in *Chlorella vulgaris* 11h cells by ³¹P-*in vivo* NMR spectroscopy and cytochemical techniques. *Arch. Microbiol.*, 148, 83, 1987.
118. **Enami, I., Akutsu, H., and Kyogoku, Y.**, Intracellular pH regulation in an acidophilic unicellular alga, *Cyanidium caldarium*. ³¹P-NMR determination of intracellular pH. *Plant Cell Physiol.*, 27, 1351, 1986; **Ginzburg, M., Ratcliffe, R. G., and Southon, T. E.**, Phosphorus metabolism and intracellular pH in the halotolerant alga *Dunaliella parva* studied by ³¹P-NMR. *Biochim. Biophys. Acta*, in press.
119. **Martin, F., Canet, D., Rolin, D., Marchal, J. P., and Larher, F.**, Phosphorus-31 NMR study of polyphosphate metabolism in intact ectomycorrhizal fungi. *Plant Soil*, 71, 469, 1983.
120. **Martin, F., Marchal, J. P., Timinska, A., and Canet, D.**, The metabolism and physical state of polyphosphates in ectomycorrhizal fungi. A ³¹P NMR study. *New Phytol.*, 101, 275, 1985.
121. **Pfeffer, P. E., Rolin, D. B., Gerasimowicz, W. V., Tu, S.-I., Boswell, R. T., and Sloger, C.**, Legume-rhizobium symbiosis as examined by *in vivo* ³¹P NMR spectroscopy. in 14th Annu. Meet. Fed. Analytical Chemistry and Spectroscopy Societies, Detroit, October 1987, 69.
122. **Martin, F., Canet, D., and Marchal, J. P.**, *In vivo* natural abundance ¹³C NMR studies of the carbohydrate storage in ectomycorrhizal fungi. *Physiol. Veg.*, 22, 733, 1984.
123. **MacKay, M. A., Norton, R. S., and Borowitzka, L. J.**, Marine blue-green algae have a unique osmoregulatory system. *Mar. Biol.*, 73, 301, 1983.
124. **Norton, R. S., MacKay, M. A., and Borowitzka, L. J.**, The physical state of osmoregulatory solutes in unicellular algae. A natural-abundance carbon-13 NMR relaxation study. *Biochem. J.*, 202, 699, 1982.

125. **Martin, F., Marchal, J. P., and Brondeau, J.,** *In vivo* natural abundance ^{13}C NMR studies of living ectomycorrhizal fungi. Observation of fatty acid in *Cenococcum graniforme* and *Helelona crustuliniforme*. *Plant Physiol.*, 75, 151, 1984.
126. **Hocking, A. D. and Norton, R. S.,** Natural abundance ^{13}C NMR studies on the internal solutes of xerophilic fungi. *J. Gen. Microbiol.*, 129, 2915, 1983.
127. **Kainosho, M. and Konishi, H.,** ^{13}C NMR spectrum of dried star anise fruits and its histological implications. *Tetrahedron Lett.*, 51, 4757, 1976.
128. **Kainosho, M. and Ajisaka, K.,** Carbon-13 NMR spectra of gross plant tissues containing starch. *Tetrahedron Lett.*, 18, 1563, 1978.
129. **Pfeffer, P. E., Osman, S. F., and Vincendon, M.,** unpublished results.
130. **Coombe, B. G. and Jones, G. P.,** Measurement of the changes in the composition of developing undetached grape berries by using ^{13}C NMR techniques. *Phytochemistry*, 22, 2185, 1983.
131. **Thomas, T. H. and Ratcliffe, R. G.,** ^{13}C NMR determination of sugar levels in storage roots of carrot (*Daucus carota*). *Physiol. Plant.*, 63, 284, 1985.
132. **den Hollander, J. A. and Shulman, R. G.,** ^{13}C studies of *in vivo* kinetic rates of metabolic processes. *Tetrahedron Lett.*, 39, 3529, 1983.
133. **Stidham, M. A., Moreland, D. E., and Siedow, J. N.,** ^{13}C NMR studies of Crassulacean acid metabolism in intact leaves of *Kalanchoe tubiflora*. *Plant Physiol.*, 73, 517, 1983.
134. **Holtum, J. A., Summons, R., Roeska, C. A., Comins, H. N., and O'Leary, M.,** Oxygen-18 incorporation into malic acid during nocturnal carbon dioxide fixation in crassulacean acid metabolism plants. A new approach to estimating *in vivo* carbonic anhydrase activity. *J. Biol. Chem.*, 259, 6870, 1984.
135. **Sillerud, L. O., Heyser, J. W., Han, C. H., and Bitensky, M. W.,** Applications of carbon-13 and sodium-23 NMR in the study of plants, animals and human cells, in *NMR in Living Systems*, Axenrod, T. and Ceccarelli, G., Eds., D. Reidel, New York, 1986, 309.
136. **Roberts, J. K. M., Callis, J., Wemmer, D., Walbot, V., and Jardetzky, O.,** The mechanism of cytoplasmic pH regulation in hypoxic maize root tips and its role in survival under hypoxia. *Proc. Natl. Acad. Sci. U.S.A.*, 81, 3379, 1984.
137. **Martin, F. and Canet, D.,** Biosynthesis of amino acids during ^{13}C glucose utilization by the ectomycorrhizal ascomycete *Cenococcum geophilium* monitored by ^{13}C NMR. *Physiol. Veg.*, 24, 209, 1986.
138. **Ashworth, D. J., Lee, R. Y., and Adams, D. O.,** Characterization of acetate and pyruvate metabolism in suspension cultures of *Zea mays* by ^{13}C NMR spectroscopy. *Plant Physiol.*, 85, 463, 1987.
139. **Ito, O., Mitsumori, F., and Totsuka, T.,** Effects of NO_2 and O_3 alone or in combination on kidney bean plants. III. Photosynthetic $^{13}\text{CO}_2$ assimilation observed by ^{13}C NMR. *Res. Rep. Natl. Inst. Environ. Stud. Jpn.*, 66, 27, 1984.
140. **Ezra, F., Lucas, D. S., Mustacich, V., and Russel, A. F.,** Phosphorus-31 and carbon-13 NMR studies of anaerobic glucose metabolism and lactate transport in *Staphylococcus aureus* cells. *Biochemistry*, 22, 3841, 1983.
141. **Belton, P. S., Lee, R. B., and Ratcliffe, G.,** A ^{14}N NMR study of inorganic nitrogen metabolism in barley, maize and pea roots. *J. Exp. Bot.*, 36, 190, 1985.
142. **Kanamori, K., Legerton, T. L., Weiss, R. L., and Roberts, J. D.,** Effect of nitrogen source on glutamine and alanine biosynthesis in *Neurospora crassa*. An *in vivo* ^{14}N NMR study. *J. Biol. Chem.*, 257, 14168, 1982.
143. **Rüterjan, H. and Juretschke, H. P.,** NMR study of cells and tissues, in *Proc. 4th Int. Sym. Rapid Methods and Automation in Microbiology and Immunology*, Springer-Verlag, Berlin, 1985, 1.
144. **Martin, F.,** ^{14}N -NMR studies of nitrogen assimilation and amino acid biosynthesis in ectomycorrhizal fungus *Cenococcum graniforme*. *FEBS Lett.*, 182, 350, 1985.
145. **Monselesse, E. B.-I., Kost, D., Porath, D., and Tal, M.,** ^{14}N NMR of ammonium ion assimilation by *Lemna gibba* L. *New Phytol.*, 107, 341, 1987.
146. **Bacic, G. and Ratkovic, S.,** Water exchange in plant tissue studied by proton NMR in the presence of paramagnetic centers. *Biophys. J.*, 45, 767, 1984.
147. **Campbell, I. D. and Dobson, C. M.,** Spin-echo double resonance: a novel method for detecting decoupling in Fourier transform NMR. *J. Chem. Soc. Commun.*, 18, 750, 1975.
148. **Brown, F. F., Campbell, I. D., Kuchel, P., and Rabenstein, D. L.,** Human erythrocyte metabolism studies by ^1H spin-echo NMR. *FEBS Lett.*, 82, 12, 1977.
149. **Rabenstein, D. L. and Isab, A. A.,** Water elimination by T_2 relaxation in ^1H spin-echo FT NMR studies of intact human erythrocytes and protein solutions. *J. Magn. Reson.*, 36, 281, 1979.
150. **Ugurbil, K., Petein, M., Maiden, R., Michurski, S., Cohen, J. N., and From, A. H.,** High resolution NMR studies of perfused hearts. *FEBS Lett.*, 167, 73, 1984.
151. **Jue, T., Arias-Mendoza, F., Gonnella, N. C., Shulman, G. I., and Shulman, R. G.,** A ^1H technique for observing metabolite signals in the spectrum of perfused liver. *Proc. Natl. Acad. Sci.*, 82, 4246, 1985.

152. Behar, K. L., Rothman, D. L., Shulman, R. G., Petroff, O. A. C., and Prichard, J. W., Detection of cerebral lactate *in vivo* during hypoxemia by ^1H NMR at relatively low field strengths (1.9T). *Proc. Natl. Acad. Sci. U.S.A.*, 81, 2517, 1984.
153. Schnall, M. D., Subramanian, V. H., Leigh, J. S., Gyalai, A., McLaughlin, A., and Chance, B., A technique for simultaneous ^1H and ^{31}P NMR at 2.2T *in vivo*. *J. Magn. Reson.*, 63, 401, 1985.
154. Williams, S. R., Gadian, D. G., Proctor, E., Sprague, D. B., and Talbot, D. F., Proton NMR studies of muscle metabolites *in vivo*. *J. Magn. Reson.*, 63, 406, 1985.
155. Sillerud, L. O., Alger, J. R., and Shulman, R. G., High resolution proton NMR studies of intracellular metabolites in yeast using ^{13}C decoupling. *J. Magn. Reson.*, 45, 142, 1981.
156. Stevens, A. N., Morris, P. G., Iles, R. A., Sheldon, P. W., and Griffiths, J. R., *Br. J. Cancer*, 50, 113, 1984.
157. Wyrwicz, A. M., Bzenny, M. H., Schofield, J. C., Tillman, P. C., Gordon, R. E., and Martin, P. A., *Science*, 222, 428, 1983.
158. Burt, C. T., Moore, R. R., Roberts, M. F., and Brady, T. J., The fluorinated anesthetic halothane as a potential NMR biologic probe. *Biochim. Biophys. Acta*, 805, 375, 1984.
159. Taylor, J. S. and Deutsch, C., Fluorinated α -methylamino acids as indicators of intracellular pH. *Biophys. J.*, 43, 261, 1983.
160. Deutsch, C. J. and Taylor, J. S., Use of ^{19}F NMR in the measurement of intracellular pH, in *NMR Spectroscopy of Cells and Organisms*. Gupta, R. K., Ed., CRC Press, Boca Raton, FL, 1987, 55.
161. Deutsch, C. J., Kashiwagura, T., Taylor, J., Wilson, D. F., and Erecinska, M., The effect of glucagon and adrenergic agonists on intracellular pH of isolated rat hepatocytes. *J. Biol. Chem.*, 260, 6808, 1985.
162. Smith, G. A., Hesketh, R. T., Metcalfe, J. C., Feeney, J., and Morris, P. G., Intracellular calcium measurements by ^{19}F NMR of fluorine-labelled chelators. *Proc. Natl. Acad. Sci. U.S.A.*, 80, 7178, 1983.
163. Metcalf, J. C., Hesketh, T. R., and Smith, G. A., Free cytosolic Ca^{2+} measurements with fluorine labelled indicators using ^{19}F NMR. *Cell Calcium*, 6, 183, 1985.
164. Cook, R. J., *Plant Cell Environ.*, 9, 157, 1986.
165. Gupta, R. K. and Gupta, P., Direct observation of resolved resonances from intra- and extracellular sodium-23 ions in NMR studies of intact cells and tissues using dysprosium (III) tripolyphosphate as a paramagnetic shift reagent. *J. Magn. Reson.*, 47, 344, 1982.
166. Gupta, R. K., Kostellow, A. B., and Morrill, G. A., NMR studies of intracellular ^{23}Na in amphibian oocytes, ovulated eggs, and early embryos. *Biophys. J.*, 41, 128a, 1983.
167. Balshi, J. A., Cirillo, V. P., and Springer, C. S., Direct high resolution nuclear magnetic resonance studies of cation transport *in vivo*. *Biophys. J.*, 38, 323, 1982.
168. Gerasimowicz, W. V., Tu, S., and Pfeffer, P. E., Energy facilitated Na^+ uptake in excised corn roots via ^{31}P and ^{23}Na NMR. *Plant Physiol.*, 81, 925, 1986.
169. Chu, S. C., Pike, N. M., Fossel, E. T., Smith, T. W., Balschi, J. A., and Springer, C. S., Jr., Aqueous shift reagents for high-resolution cationic nuclear magnetic resonance. III. $\text{Dy}(\text{TTHA})^{3+}$, $\text{Tm}(\text{TTHA})^{3+}$, and $\text{Tm}(\text{PPP})^{3+}$. *J. Magn. Reson.*, 56, 33, 1984.
170. Greenway, H. and Munns, R., Mechanisms of salt tolerance in nonhalophytes. *Annu. Rev. Plant Physiol.*, 31, 149, 1980.
171. Sillerud, L. O. and Heyser, J. W., Use of ^{23}Na -nuclear magnetic resonance to follow sodium uptake and efflux in NaCl-adapted and nonadapted millet (*Panicum miliaceum*) suspensions. *Plant Physiol.*, 75, 269, 1984.
172. Höfeler, H., Jensen, D., Pike, M. M., Delayre, J. L., Cirillo, V. P., Springer, C. S., Fossel, E. T., and Balschi, J. A., Sodium transport and phosphorus metabolism in sodium-loaded yeast: simultaneous observation with sodium-23 and phosphorus-31 NMR spectroscopy *in vivo*. *Biochemistry*, 26, 4953, 1987.
173. Packer, L., Spathy S., Martin, J. P., Roby, C., and Bligny, R., ^{23}Na and ^{31}P NMR studies of the effects of salt stress on the fresh water *Cyromobacterium synecococcus* 6311. *Arch. Biochem. Biophys.*, 256, 354, 1987.
174. Martin, J. B., Klein, G., and Satre, M., ^{23}Na NMR study of intracellular sodium ions in *Dictyostelium discoideum* amoeba. *Arch. Biochem. Biophys.*, 254, 559, 1987.
175. Adam, W. R., Koretsky, A. P., and Wiener, M. W., Measurement of tissue potassium *in vivo* using potassium-39 NMR. *Biophys. J.*, 51, 265, 1987.